Analysis of Reinforced Concrete Columns under Blast Load

Politecnico di Milano

Faculty of Building Engineering

Department of Structural Engineering

In Partial Fulfillment of the Requirements for the Degree of

Master of Science in Building Engineering

Thesis Supervisor: Dr. Eng. Prof. Sergio Tattoni

Angelo Perini

Milan, December 2014

Table of Contents

Chapter 3: Conceptual Approach and Calculation of Blast Load on Structures

Chapter 4: Materials

Chapter 5: F.E.M. Models and Relative Discussion of Analysis

Chapter 6: Dynamics of Structures and SDOF Method Approach

List of Figures

Chapter 1

Chapter 2

Chapter 3

Chapter 4

Chapter 5

Chapter 6

List of Tables

Chapter 1

Chapter 3

Chapter 5

Chapter 6

Abstract

Quando una struttura viene sottoposta ad un carico esplosiovo, la sua risposta sarà del tutto differente da quella che si ottiene da un carico di tipo statico. Generalmente nel campo dell' ingegneria si sviluppa una progettazione legata al solo utilizzo di carichi statici, ma la commune conoscenza della progettazione di edifice soggetti ad esplosioni è molto limitata. Si possono trovare nei manuali e normative alcune linee guida sulla progettazione di edifice a rischio di esplosioni attraverso l'utilizzo di metodi semplificati, ma in generale risultano in parte superate, nonchè la generale spiegazione del fenomeno. Questa Tesi di Laurea Specialistica raccoglie alcune di queste importanti linee guida e ne sviluppa la teoria che porta alla formulazione di tali approcci tecnici. Si deve inoltre aggiungere che per meglio comprendere la risposta strutturale è necessario conoscere la teoria di base legata al campo delle esplosioni, i diversi comportamenti materiali e le dinamiche di base , anch'essi argomento di tesi .

In generale la struttura, e più nel dettaglio il singolo element pilastro, verrà semplificata attraverso la trasformazione ad un solo grado di sistema libertà (SDOF Method), la cui affidabilità sarà oggetto di questa tesi, presentando un confront tra i risultati di calcolo con il metodo SDOF e quelli derivanti da un'analisi FEM con software Midas Gen.

Il grado di libertà del sistema è dato considerando il punto di massimo spostamento del sistema, ed in seguito confrontato con calcoli a mano per i massimi valori di spostamento e con analisi agli elementi finiti non lineari. Si considerano quindi metodi semplificati di calcolo ed approcci più tecnici per lo studio della risposta strutturale delle colonne soggette ad un carico esplosivo, considerando come element principe elementi presso-inflessi in cemento armato.

Abstract

When a structure is subjected to an explosion, it will have a response that differs from the one that arises from a static load. Engineers are used to design for static loads but the common knowledge of how to design for explosions is weak. There are guidelines for how to design for explosions with simplified methods but they are partly outdated and the explanation of how they are derived is vague. This Master thesis compiles some of the most important guidelines and explains the underlying theory. In order to understand the structural response one must first study basic theory of explosions, different material behaviours and basic dynamics, which are also presented in the thesis.

A structure can be simplified by transformation into a single degree of freedom- system (SDOF-system), and the reliability of such an SDOF-system is evaluated within this thesis and result of SDOF Calculation are compared with the one obtain from F.E.M Analysis with software Midas Gen. Indeed the SDOF-system is created by using a system point where the maximum displacement will occur, and it is compared to hand calculations for the maximum values and to non-linear finite element analyses. The SDOF-model assumes a specific deflection shape which is taken into account by using certain transformation factors. The simplified methods of calculating the structural response are presented in general, but the examples are made for reinforced concrete columns.

Chapter

1

Introduction and Conceptual Approach to the Blast Effects on Structures

1. Introduction

On the last century, the importance of considering the effects on structures, caused by explosions, induced a lot of structural engineers to analyzed this phenomenon and research solutions to optimize the buildings design projects. The reasons, that bring engineers to start studying blast effects on structures, were tied by Second World War, occurs in the middle of the 20th century, because, for the first time in the history, weapons used by armies had a really destructive effects on cities, especially on buildings. Moreover, from that time, new technologies and the insertion of new weapons by armies, create a different way to engage war. At last, the beginning of the 21th century was affected by a lot of terrorism attacks, with the goal to strike down the enemies, from inside. Many of bombing attacks, occurs on main buildings of the most important cities around the world, caused irreversible damages, besides the death of many people.

It is also important to remember that many explosions occurred on buildings, are not only caused by the use of weapons, as we saw considering damages produced by wars, but many times blast effects were create, and not only in the past, by emissions of gases or problems with plant systems, occurring inside the building, or moreover, caused by dust, participating during the industrial cycle process.

The aim of this work is to analyze the different kind of explosions, the reasons that cause this phenomenon, and their effects of building's structures. So, the author will try to list and explain these events and their effects on constructions, integrating the text with some theoretical information that can help to better understand blast situations. Therefore, create a general reference frame of these kinds of phenomenon, occurring in civil engineering, overall could help for the first approach on these themes.

2. Types of Explosions

In general, impact and impulsive loadings are mostly extreme loading cases with a very low probability of occurrence during the lifetime of a structure, and the impulsive one represents very well the kind of dynamic load involving a structure subjected to an explosion. So, in the design of structures to resist the effects of blast loading or other severe dynamic loads, it is important to have large energy absorbing capabilities, and structural elements with a large plastic deformation capacities, are therefore desirable. Structures need to be designed for ductile response in order to prevent partial or total collapse due to locally failed elements. Afterwards, for a correct analysis of this type of effects on structures, it is important to considered the material's behavior, cause of the mechanical necessity for energy absorption in failure situations, and it is also important, to well known the theory of elastic and plastic impact, considered the nonlinear behavior of material (constitutive laws with strain rate effects included), and in many cases also the geometric nonlinearities. In order to explain effects on structures, at the beginning, it is important to analyze the different types of explosions, the causes and their effects.

Explosions could be natural or artificial, simply defined as a sudden release of energy. Generally, this phenomenon can be categorized on the basis of their nature, nuclear or chemical events. In physical explosions energy may be released from the catastrophic failure of a cylinder of compressed gas, volcanic eruptions or even mixing of two liquids at different temperatures. In a nuclear explosion, energy is released from the formation of different atomic nuclei by the redistribution of the protons and neutrons, within the interacting nuclei, whereas the rapid oxidation of fuel elements (carbon and hydrogen atoms) is the main source of energy, in the case of chemical explosions. Furthermore, explosive materials can be classified according to their physical state of solid, liquid or gas. Solid explosives are mainly high for which blast effects are best known. They can be classified on the basis of their sensitivity to ignition as secondary or primary explosive. The latter is the one that can be easily detonated by simple ignition from a spark, flame or impact. Materials such as mercury fulminate and lead acid are primary explosive. Secondary explosives, when detonated, create blast (shock) waves, which can result in widespread damage to the surroundings. Examples include trinitrotoluene (TNT) and Ammonium nitrate fuel oil (ANFO).

In general, every kind of explosion produces an energy release, creating a sudden acceleration of air particles that strike against the structure surface. This release of energy created by explosion, is accompanied by large changes of pressure, typically with a flash or loud noise,

which is called the expansion. Explosions cause pressure waves in the local medium in which they occur. These pressure waves are called deflagrations, if they are subsonic, while are called detonations when the event occurs with a supersonic velocity. An example would be gunpowder in a firearm or fuel in an internal combustion engine. Deflagrations are easier to control than detonations, when the goal is to move an object (a bullet in a gun, or a piston in an engine) with the force of the expanding gas. To be more precise, detonation involves a supersonic exothermic front, accelerating through a medium that eventually drives a shock front propagating directly in front of it, in reverse of deflagration, that describes a subsonic combustion propagating through a heat transfer. This categorization represents the two big sets that included all types of blast events.

Overall, the goal of this booklet is to supply fundamentals about four different types of explosions, caused by the contribution of dust, liquid, gas or high explosive sources. Each one produces various effects involving the structural elements, relate if occur deflagrations and detonations in presence of one of these sources.

2.1 Dust Explosion

A dust explosion is the fast combustion of dust particles suspended in the air in an enclosed location. During the history, this kind of explosions occur many time and generally inside on industries or mines. The first one, in the history, dates back on 14th December 1785 in Turin when an explosion occurred inside a flours warehouse. Others examples are the explosions, in 1982, of a sugar industry in Boiry-Sainte-Rictrude (France), or in 1999, inside an industry plant of Ford Motor Company in Michigan, produced by the effects of coal (it was registered the death of 6 persons and 36 more were injured). The last dust explosion occurred on November 2010, by the effect of aluminum's dust in a motorcycle industry. So, looking the examples, it is possible to list some of typical dust productions that could be dangerous and generate explosive events:

- Production of organic materials, with natural origin, like sugar, flour or wood;
- Production of organic materials, with synthetic origin, like plastic or pesticide;
- Production of coal or peat;
- Production of metals, like aluminum, magnesium or zinc;

Generally, the majorities of dust (organic or inorganic) are combustible and generate blazes or explosions according to the external situations, when the combustion process occurs. When a mass of solid flammable material is heated, it burns away slowly, owing to the limited surface area exposed to the oxygen of the air. The energy produced is liberated gradually and harmlessly, because it is dissipated as quickly as it is released. The result is quite different if the same mass of material is ground to a fine powder and intimately mixed with air in the form of a dust cloud. In these conditions, the surface area exposed to the air is very great and, if the ignition occurs, the whole of the material burn with great rapidity; the energy which in the case of the mass was liberated gradually and harmlessly, is released suddenly with the evolution of large quantities of heat and, as a rule, gaseous reaction products. Although, mixture of dust and air, within the flammable range, are capable of explosion, they will not explode unless they are ignited in some way. Once a source of ignition is presented to the flammable mixture, flame will propagate throughout the cloud. The mode of ignition of a dust cloud is typically a hot source, an electrical spark or a mechanically generated frictional spark. The minimum condition necessary to initiate a dust explosion, with certain mode of ignition, can be measured, with experimental procedures. Following, it is proposed a table, showing the principal properties of most important dust material, to better understand what it will be explained below.

MATERIAL	Ignition Temperature [°C]	Min. Ignition Energy [MJ]	Lower Explosive Limit [g/m^3]	P_{MAX} [bar]	K_{ST} [bar
Aluminum	560	< 1	60	11,2	515
Magnesium	760	> 1000	30	17,5	508
Zinc	250	300	250	6,7	125
Cellulose Acetate	520	-	30	9,8	180
Methyl Cellulose	-	-	-	-	-
Methyl Acrylamide	500	100	30	8,7	97
Phenolic Resin	460	-	-	9,3	73
Polyamide	460	> 1000	125	6,9	38
Polystyrene	450	100	400	5,4	14
Urea	520	100	125	9,7	119
Cocoa (dust)	-	-	60	7,6	75
Coffee	470	> 1000	60	9,0	90
Cornstarch	400	10	30	8,2	117
Grain (dust)	510	-	125	9,2	131
Potato (flour)	480	-	125	9,1	69
Sugar	480	10	100	8,5	138
Adipic Acid	580	-	60	8,0	97
Coal	540	> 1000	60	8,5	117
Sewage Sludge	450	100	250	6,5	79
Sulphur	280	< 1	280	6,8	151
Yeast	450	100	60	6,2	40

Table 1 – Dust Explosion General Conditions

Usually, when in an industrial plant, a dust explosion occurs, it is possible to identify two different events happening subsequently, called primary and secondary explosion. The primary explosion start inside an industrial gear, that they are generally not rather hard to resist to the generated pressure. After the structural yielding, pressure produces a disruption of the air, wasting dusts in the medium and generating the secondary explosion. During the second event, participate a bigger quantity of dusts than the first one. This is why, secondary explosions are always more destructive than primary explosions.

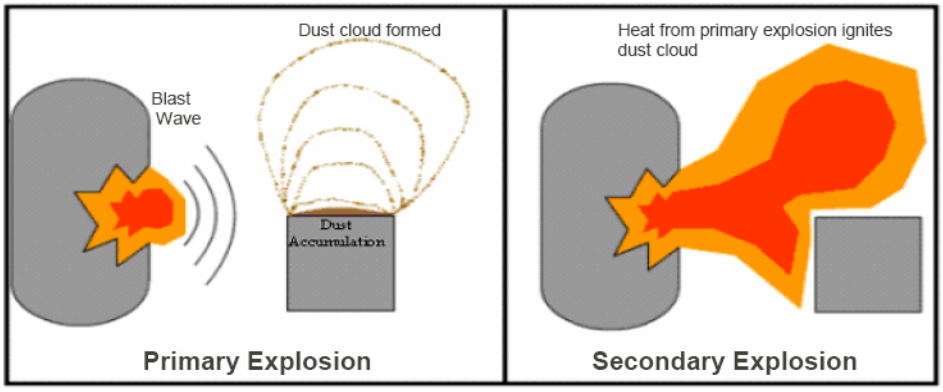

Figure 1 – Dust Explosion Phases

So, a dust explosion is a process, where the increase of pressure and temperature, and the production of a blast wave, are generated by the rapid combustion of a mixture of dusts and air, or combustible and others oxidant sources. So as a dust explosion occurs, it is important to respect five conditions:

- The participation of an oxidant - the combustive agent usually is the oxygen present in the air;
- The participation of a matter or a blend of gases, fumes or dusts;
- It must be present a spring, that satisfy the energetic condition, necessary to get the reaction;
- It must be present on the atmosphere, a blend of gases with a concentration included on a range between two limits, called limits of flammability. When the mix dust-air has lesser concentrations than the lower bound, it is not possible that any explosive events occur. The same thing happens when concentrations of mixture are higher than the upper limit;
- The flammable blend must be restrain in a finite volume; it can be an industrial gear or a closed space.

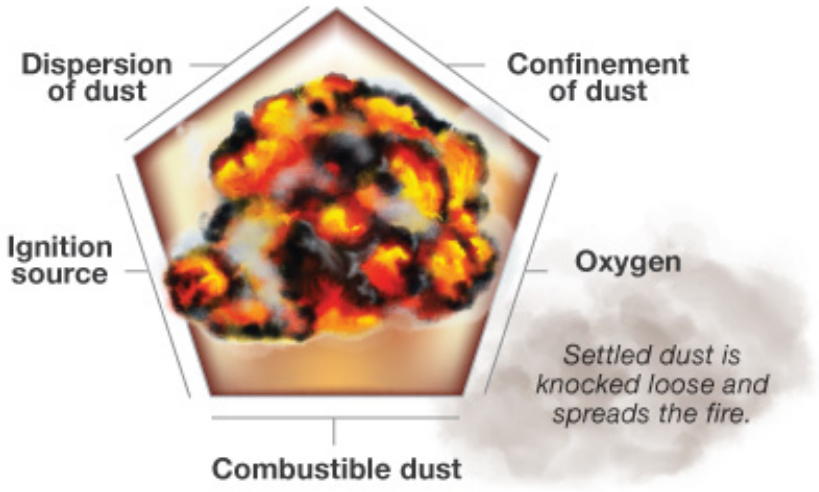

Figure 2 – Dust Explosion Process

2.1.1 Explosive Properties of Dust Source

As above-mentioned, dust is in fact a combustible source. Any "Material that will burn in air" in a solid form, can be explosive when in a finely divided form. Combustible dust is defined by NFPA 654 as: "any finely divided solid material that is 420 microns or smaller in diameter and presents a fire or explosion hazard when dispersed or ignited in the air". Different dusts of the same chemical material will have different ignitability and explosibility characteristics, depending upon many variables, such as particle size, shape and moisture content. Additionally, these variables can change while the material is passing through process equipment. For these reasons, once explained general mechanisms of dust sources explosions, it is important to list and analyzed principal properties that characterized this phenomenon. In the following table principal properties are resumed.

EXPLOSIVE PROPERTIES	Norms
Minimum Ignition Energy (MIE)	UNI EN 13821:2004
Maximum Explosion Overpressure	UNI EN 14034-1:2005
Explosion Pressure Development	UNI EN 14034-2:2006
Specific Characteristic of Explosibility	UNI EN 14034-2:2006
Lower Flammability Limit (LFL)	UNI EN 14034-3:2006
Limiting Oxygen Concentration (LOC)	UNI EN 14034-4:2005
Minimum Ignition Temperature of Dust Clouds	CEI EN 50281-2-1:1999
Minimum Ignition Temperature of Dust Layer	CEI EN 50281-2-1:1999

Table 2 – Explosive Properties

MINIMUM IGNITION ENERGY

The Minimum Ignition Energy (MIE) specifies the ignition sensibility of the combustible dust and it is defined as the lowest energy able to generate a primer of the combustible dust cloud wasted in the air. MIE values depend on the chemical nature of the dusts, their particles size, uniformity of the cloud and its turbulence. So, as defined in the norms, the Minimum Ignition Energy of a dust cloud is the lowest energy value of a high-voltage capacitor discharge required to ignite the most readily ignitable dust/air mixture at atmospheric pressure and room temperature. The dust concentration and the ignition delay are systematically varied until a minimum value of the ignition energy is found. The tested energy levels are generally 1000, 300, 100, 30, 10 and 1 [MJ].

It is well known that, explosive dust cloud might be ignites by electric sparks and arcs that occur in switches and motors, and in short-circuiting caused by damaged cables. In addition,

some categories of electrostatic discharges may initiate dust explosions in industry. For an assessment of the hazard situation in dust-processing installations, knowledge of the MIE is indispensable. This value can possibly determine the extent and hence the cost of protective measures.

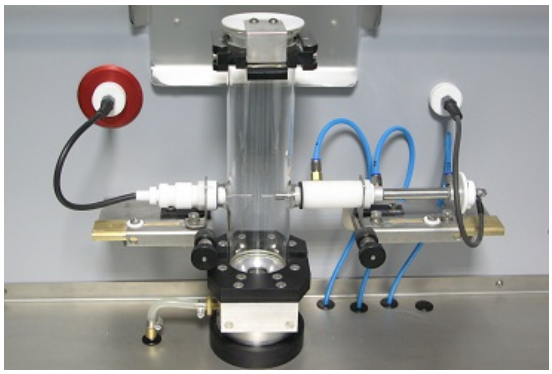

Figure 3 – Ignition Energy Machine Test

MAXIMUM EXPLOSION OVERPRESSURE-EXPLOSION PRESSURE DEVELOPMENT AND SPECIFIC CHARACTERISTIC OF EXPLODIBILITY

Actually, dusts are categorized by experimental explosion tests conduct using bombs with constant volume (Vessel test). The results of these tests registered the development of the pressure according to the time, and the gain is shows by the identification of fundamental parameters indicate as maximum overpressure and bend slope. Referring to the latter, maximum overpressure (P_{MAX}), measures the highest pressure occurred during the explosion, explain with the law:

$$P_{MAX} = P_{fin} - P_0$$

where P_0 represents the atmospheric pressure.

Blend slope, *dP/dt*, indicate the rapidity of the combustion event. Its knowledge allows the classification of dusts with the K_{ST} parameter, representing the explosibility of the dust. These two values are connected with the "Cubic Law", banding together volume and maximum growth of pressure. So, the blend slope says that the product between the maximum tangent to the pressure-time blend and the cubic root of volume are constant and independent from the test's volume, considering an initial concentration and turbulence.

$$\left(\frac{dP}{dt}\right)_{MAX} * \sqrt[3]{V} = K_{ST} = Cost$$

Cause K_{ST} is a constant quantity, depending exclusively on the mixture of dust-air, its classification is a function of this value.

EXPLODIBILITY CLASS	K_{ST} [bar m/sec]	TYPE OF MIXTURE	EXAMPLES
St.0	0	Not Explosive	Not Combustible Dusts
St.1	$0 \leq K_{ST} \leq 200$	Weakly Explosive	Organic Dusts, Wood
St.2	$200 \leq K_{ST} \leq 300$	Explosive	Organic Pigments
St.3	$K_{ST} > 300$	Extremely Explosive	Metallic Dusts

Table 3 – Explodibility Class and Values of Dust Explosion

The maximum overpressure values and blend slope are conditioned by powder diameter and the oxygen content.

FLAMMABILITY BOUNDS OF A DUST-AIR MIXTURE

As saw, the ignition and propagation of flame in a dust cloud depend on a number of factors, such as dust concentration, the composition of the dust and moisture content, particle size and shape, and at last turbulence in the system. These factors not only determine the severity of the explosion but also influence the type and degree of precautions, which it may be practicable to take.

Mixtures of dispersed combustible materials (such as gaseous or vaporized fuels, and some dusts) and air will burn only if fuel concentration lies within well-defined lower and upper bounds, determined experimentally, referred to as flammability limits or explosive limits. Combustion can range in violence from deflagration, through detonation, to explosion. Limits vary with temperature and pressure, but are normally expressed in terms of volume percentage at 25,0 [°C] and atmospheric pressure. These limits are relevant both to producing and optimizing explosion or combustion, as in an engine, or to preventing it, as in uncontrolled explosions of build-ups of combustible gas or dust. Attaining the best combustible or explosive mixture of fuel and air, it is important in internal combustion engines, such as gasoline or diesel engine. In order to have combustion of a flammable mixture, it is important to have a precise quantity of combustible. So, as previously said, the dust concentration in the air must be included between defined limits:

- Lower Flammability Limit (LFL): is the lowest concentration of powder that is able to give combustion, after the primer. If participate lower concentration, the distance between particles prevent the propagation of the combustion.
- Upper Flammability Limit (UFL): is the highest concentration of dust able to

generate the combustion, after the primer. When the concentration exceeds this value, the density of particles prevents the presence of oxygen, essential for the combustion. It is difficult to calculate this limit, because it is required that particles waste uniformly in the cloud, during the test. Generally it is rare that a dust cloud could maintain higher concentration than the upper limit, inside a medium. Only for some mixture it was possible to determine this value experimentally and it was included between 2,0 and 6,0 [g/l].

Defined the two limits, it is possible to note that dust concentrations determine the general characteristic of the event. To better understand the real meaning of the fixed boundaries, it is necessary to explain the concept of dust concentration. The maximum pressures and rates of pressure rise with the influence and severity of a dust explosion, vary with the chemical constitution and certain physical properties of the dust. Some metal powder, like aluminum, magnesium and alloys of aluminum and magnesium, can generate maximum pressures of 12 [bar] and maximum rates of pressure rise in excess of 500 [bar m/sec]. Organics materials typically produce maximum explosion pressures up to 10 [bar] and rates of pressure rise below 200 [bar m/sec]. Flammable materials that form dust clouds may be a mixture of two or more substances. Generally one of these is an incombustible matter in the form of inert material, non-flammable volatile components or moisture, and tends to reduce the flammability of the dust both by chemical inhibition and by the cooling effect of the particles. High concentrations of moisture in the dust may also impede the formation of a dust cloud. Below are reported two charts that present the relationship between combustible concentrations and their effects on pressure development.

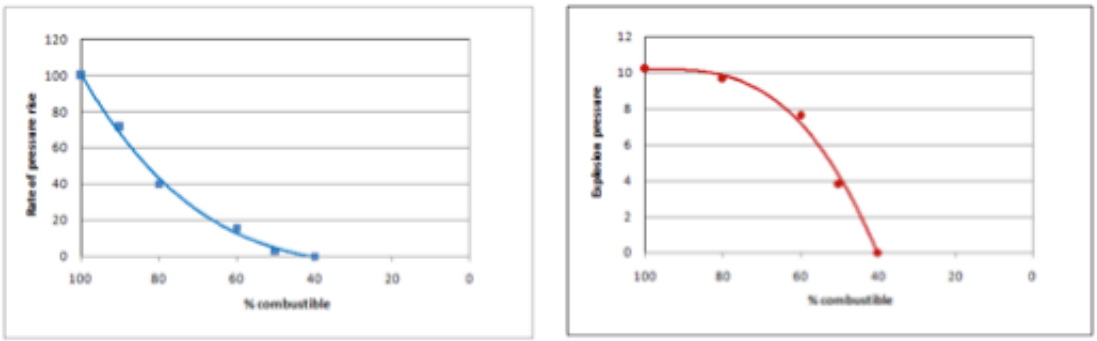

Figure 4 –Combustible concentration and effect on pressure

LIMITING OXYGEN CONCENTRATION (LOC)

The limit of the oxygen concentration is defined as the highest value of concentration of dust-air mixture, able to avoid the explosion. When the oxygen present in the atmosphere assumed values lower that the LOC, on of the explosion condition is not verify and the event does not occur. A common way to reach this result is to make the atmosphere inert, replacing the oxygen with other gas, like nitrogen.

To calculate the LOC, it is needed a test, performed using a 20 [l] sphere apparatus. Powder or dust samples of various sizes are dispersed in the vessel and attempts are made to ignite the resulting dust cloud with an energetic ignition source (2,0 [kJ]). Trials are repeated at decreasing oxygen concentrations until the LOC is determined. It should be emphasized that the LOC test is inert gas type dependent, because of the different capacities of these inert gases. The norm that explain this type of analysis is EN 14034-4: "Determination of explosion characteristics of dust clouds – Part 4: determination of the limiting oxygen concentration LOC of dust clouds". An example of the result of this test is show on the chart below.

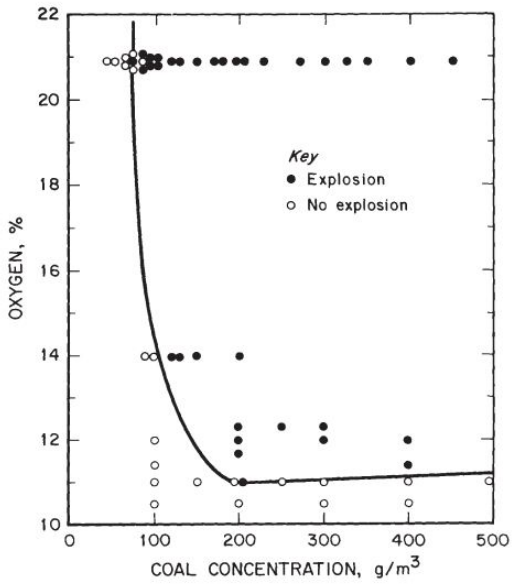

Figure 5 – LOC Dust Cloud Test Results

Full spheres represent the occurred explosion, while the empty spheres, the explosion that does not occurred. The blend represented the boundaries between oxygen concentrations that are supporting or not the combustions, is the set of the LOC values of dust-air mixture.

MINIMUM IGNITION TEMPERATURE OF A DUST CLOUD OR LAYER

Hot surface capable of igniting dust clouds exist in a number of situations in industry, such as in furnaces and burners, and dryers of various kind. In addition, hot surface can be generated accidentally by overheating of bearings and other mechanical parts. If an explosive dust cloud is generated on some uncontrolled way in the proximity of a hot surface of temperature above the actual minimum ignition temperature, the result can be a dust explosion. It is important, therefore to know the actual minimum ignition temperature and to take adequate precautions to ensure that temperatures of hot surfaces in areas where explosive dust cloud can occur. However, the minimum ignition temperature is not a true constant for a given dust cloud, but depends on the geometry of the hot surface and the dynamics of the cloud.

The minimum ignition temperature of a dust cloud (T_{CL}) is define as the lowest temperature which a hot surface, in contact with a dust explosive mixture and air, can generate the primer of the explosion.

The minimum ignition temperature of dust layer (T_{5mm}), conventionally fixed in 5 [mm], is the lowest temperature of the hot surface that could generate the ignition of the dust layer. The values are generally lower than the minimum ignition temperature of a dust cloud, and they are included in a range between 300,0 [°C] and 400,0 [°C].

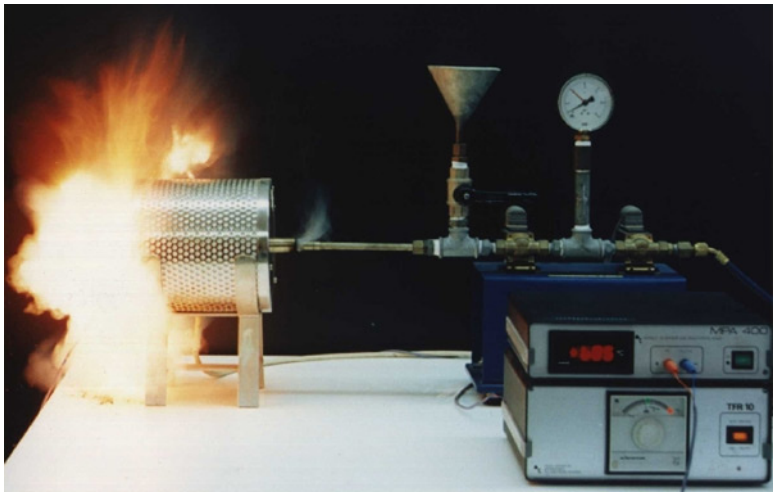

Figure 6 – Minimum Ignition Test

2.2 Gas or Liquid Explosions

An explosion produced by gas is characterized by a rapidly combustion of a cloud, composed with a blend of air and fuel, that generate an increase of pressure, temperature and shock waves. As dust explosions, this type of event occurs generally with the same properties. Indeed it is possible to say that explosive conditions explained previously, are working also for gases explosions. One of the first examples of gas explosion in the history occurs on March 1937 in Texas, when a natural gas leak caused an explosion, destroying the New London School, causing the death of 300 students and teachers.

In general, a flammable gas may be an element, such as hydrogen, which can be made to react with oxygen with very little additional energy. Flammable gases are often compounds of carbon and hydrogen. These gases and vapors require only small amounts of energy to react with atmospheric oxygen. A vapor is the proportion of a liquid – if talking about the explosion protection of flammable liquid – which has evaporated into the surrounding air as the result of the vapor pressure above the surface of the liquid, around a jet of that liquid or around droplets of liquids. Mist is a special type, which because of its explosion behavior could be included with the vapors, for the purposes of fulfillment of safety considerations.

Flammable liquids are often hydrocarbon compounds such as ether, acetone or petroleum spirit. Even at room temperature, sufficient quantities of these can change into the vapor phase so that an explosive atmosphere forms near their surface. Other liquids form such an atmosphere near their surface only at increased temperatures. Under atmospheric conditions this process is strongly influenced by the temperature of the liquid. For this reason the flash point, or rather the flash point temperature is an important factor when dealing with flammable liquids. The flash point relates as for dust sources, to the lowest temperature at which a flammable liquid will form, under certain conditions, a sufficient quantity of vapor on its surface to enable an effective ignition source to ignite the vapor air mixture. The flash point is important for the classification of potentially explosive atmosphere. Flammable liquid with a high flash point is less dangerous than those with a flash point at room temperature or below. When spraying a flammable liquid, a mist can form consisting of very small droplets with a very large overall surface area, as is well known from spray cans or from car spraying stations. Such a mist can explode. In this case the flash point is of lesser importance. Fro a fine mist made from a flammable liquid, the behavior relevant to safety can be roughly derived from the known behavior of the vapor.

So, as explained for dust explosions, gases detonation occurs, if it will be verified five conditions:

- The participation of an oxidant - the combustive agent usually is the oxygen present in the air;
- The participation of a matter or a blend of gases, fumes;
- It must be present a spring, that satisfy the energetic condition, necessary to get the reaction;
- It must be present on the atmosphere, a blend of gases with a concentration included on a range between two limits, called limits of flammability.

The flammable blend must be restrain in a finite volume (for example an industrial gear or a closed space).

In these cases, deflagration is certainly the most common type of explosion (considering that it is possible to called deflagration every kind of explosion characterized by presence of flame). During deflagration, it occurs a flame's front propagating with sub-sonic velocity, compared with the unburned cloud, and the process reach pressure's values included between 1 and 10 [barg2].

In general, it is possible to find two different types of front's flame propagation, according to the state, that occur with different velocity:

- Laminar flow propagation;
- Turbulent propagation.

When gasses cloud are activated by weary source and unburned gas, it proceeds with laminar flow motion and the propagation way of the flame is characterized with heat and mass molecular diffusion. If the fluid-dynamics conditions of unburned gasses on the front's flame maintain laminar properties, flame motion is characterized by laminar flow propagation, subjected by chemical and physical properties of blend. In reverse, if flame runs into obstacles (frequent aspect occurs on the analysis of industrial and civil structures), it generates acceleration and it changes into turbulent deflagration. In this situation, unburned gases have turbulent motion with vortex, producing pleated front's flame, increasing the contact surface with unburned gasses. A turbulent deflagration produced also a growth of velocity. During the explosion of gases blend, the chemical reactions generate an increasing of volume. This expansion produced air compression with consequent generation of blast wave, moving away from the source with very high velocity.

2.2.1 Explosive Properties of Gas and Liquid Sources

There are such important properties to consider in this type of events that generally differ from dust explosion analysis. These characteristics are listed below.

SIZE PROPERTIES OF EXPLOSIBILITY FOR AIR-GAS MIXTURE

The first one is called stoichiometric composition of a mixture and referred to the specific composition where the quantity of the combustible and oxygen is balanced in order to have in terms of reactions none exceed of combustible and oxygen. Usually, the mixture concentration of gases can be defined by the ratio between volume of gas and volume of air-gas mixture.

$$C = \frac{V_{gas}}{V_{air} + V_{gas}} * 100$$

$$C = \frac{n_{gas}}{n_{air} + n_{gas}} * 100$$

Determined volume and number of air moles, containing oxygen needed to complete gas combustion, using formulas proposed before, it is possible to calculate the stoichiometric composition.

Other important property is the equivalence relation, defined as the ratio between the mixture and its stoichiometric composition.

$$\emptyset = \frac{\frac{air}{gas}}{(\frac{air}{gas})_{Stoic}}$$

Notice that, in case of mixture with stoichiometric composition the value of the equivalence relation is unitary.

FLAMMABILITY BOUNDS OF A GAS-AIR MIXTURE

The general concept of this property is totally similar to the analysis of flammability bounds of a dust-air mixture. What really change are values of different types of gases.

In order to have the combustion of a flammable mixture, it is needed that the compound is made with correct quantities of combustible. Below is presented a table with different values of flammability bounds, referred to a gas-air mixture.

SOURCE	CHEMICAL COMPOSITION	LFL (%)	UFL (%)
Methane	CH_4	5	15
Ethane	C_2H_6	3	13,4
Propane	C_3H_8	2,1	9,5
Butane	C_4H_{10}	1,8	8,5
Benzene	C_6H_6	1,3	7,9
Acetylene	C_2H_2	2,5	100

Table 4 – LFL and UFL value for different sources

FLASH POINT ANALYSIS

The flash point of a combustible is an index of volatility of a mixture, representing tendency to dry off, characteristic of a liquid. So the flash point is defined as the lowest temperature that the liquid produces with vaporization, needed quantity of vapor to create an air mixture, with composition higher than LFL limit, when an ignition occurs.

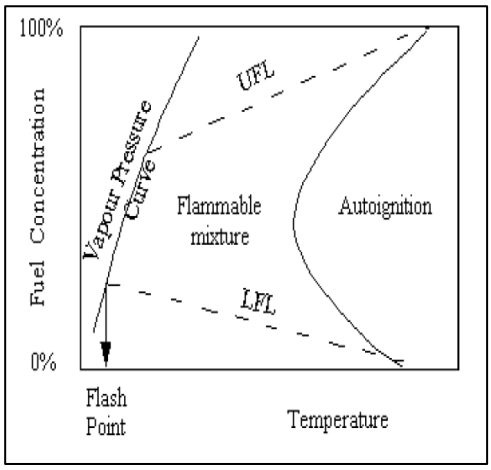

Figure 7 – Flash Point Chart

Analyzing the safety, it is important to know the flash point values because permit to define blaze and explosion risks for a particular situation and location. As known, liquid that as a lower value of flash point must be considered as the dangerous one, considering temperature lower than 50 [°C].

Below principal flash point values are listed in a table.

SOURCE	FLASH POINT [°C]
Methane	-188
Ethane	-104
Propane	-19
Butane	12
Benzene	45
Acetylene	> 55

Table 5 – Flash Point Temperature

AUTO-IGNITION TEMPERATURE (AIT)

Auto-ignition temperature is defined as the index of reactivity for a mixture. It is the lowest value of temperature needed in order to generate the spontaneous burning of the mixture, without primer, occurring in presence of the oxygen. In this case, the high temperature could be considered the primer of the combustion.

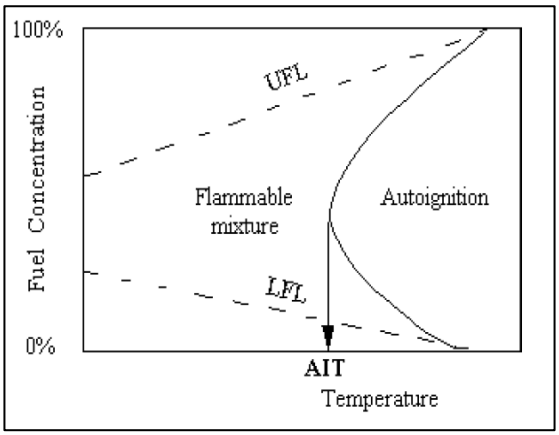

Figure 8 – Auto-Ignition Temperature Charts

VELOCITY OF THE LAMINAR FLOW COMBUSTION

The velocity of the laminar flow combustion S_{CL} is defined as the velocity, which the combustion occurs, or the velocity of front flame relate to an integral system with the reagents. Some velocity, relate to the laminar flow combustion are reported below.

SOURCE	S_{CL} [m/sec]
Methane	0,37
Ethane	0,44
Propane	0,42
Butane	0,42
Benzene	0,45
Acetylene	1,70

Table 6 – Velocity of Laminar Flow Values

3. High Explosive Source

In this section, the analysis is related to detonation events, occurring in presence of high explosive source, while deflagrations, that generally are referred to the dust, gases or liquid explosions. High explosive sources are, for example, the different types of explosives used for demolition or, as explained on the introduction, weapons used for bombing attacks. Talking about detonation means that the "explosive shock front" occurs and passes through the explosive faster than the speed of sound. Velocity rates generally range from 3000 to 9000 [m/sec].

High explosives, strictly speaking, fall under two classes:

- Primary high explosives;
- Secondary high explosives.

Primary high explosives are sensitive explosive substances used for detonating usually higher quantities of secondary high explosives. Applications include detonator assemblies for blasting, primers, "detonation cord" and other such initiating compounds. Primary explosives may be sensitive to impact, heat, electromagnetic radiation, friction and static electricity. Some extremely sensitive substances are even sensitive to tiny amounts of air movement or temperature changes. In reverse, secondary high explosive are usually employed in most demolition, mining and military applications. This type of explosive source is less sensitive explosive substances and required much more energy to detonate than primary explosives. Velocity, sensitivity, reliability and general safety in use varies, greatly depending on the type of explosive.

So generally, the high explosives detonate under the influence of the shock of the explosion of a suitable primary explosive (sometimes called as initiator – it explode or detonate when they are heated or subjected to shock). The high explosive do not function by burning; in fact, not all of them are combustible, but most of them can be ignited by a flame and in small amount generally burn tranquilly and can be extinguished easily. Another property of high explosives is that if they are heated to a high temperature by external heat or by their own combustion, they sometimes explode.

PROPAGATION OF EXPLOSION

As explained for other types of explosive, like for example black powder, its activation with fire, create a chemical reaction, which results in the productions of hot gases. The gas, tending to expand in all directions from the place where it is produced, warms the next portion of the black powder to the kindling temperature. So in general it is possible to say that, this phenomenon is dependent upon the transmission of heat.

The explosion of a primary explosive or a high explosive, on the other hand, is believed to be a phenomenon which is dependent upon transmission of pressure or, perhaps more properly, upon the transmission of shock. Fire, friction, or shock, acting upon, say, fulminate, in the first instance cause it to undergo a rapid chemical transformation which produces hot gas, and the transformation is so rapid that advancing front of the mass of hot gas amounts to a wave of pressure capable of initiating by its shock the explosion of the next portion of fulminate. This explodes to furnish additional shock, which explodes the next adjacent portion of fulminate, and so on, the explosion advancing through the mass with incredible quickness. For example, in a standard blasting cap the explosion proceeds with a velocity of about 3500 [m/sec].

In general, when high explosive detonation occurs, it exerts a mechanical effect upon whatever is near them, whether they are confined or not. Example are dynamite, trinitrotoluene, tetryl, picric acid, nitrocellulose, nitroglycerin, liquid oxygen mixed with wood pulp, fuming nitric acid mixed with nitrobenzene, compressed acetylene and cyanogen, ammonium nitrate and perchlorate, nitroguanidine.

VELOCITY OF DETONATION

If the quantity of the primary explosive used to initiate the explosion of a high explosive is increased beyond the minimum necessary for that result, the velocity with which the resulting explosion propagates itself through the high explosive is correspondingly increased, until a certain optimum is reached, depending upon the physical state of the explosive, whether cast of powdered, whether compressed much or little, upon the width of the column and the strength of the material which confines it and of course upon the particular explosive used. To determine the effects caused by a high explosive substance, as the goal of this dissertation, at first, its physical properties must be known. So causes produced by explosion could be fully understood only knowing properties and factors affecting explosive source. Some important characteristics of explosive source are listed below.

DYNAMITE

This type of explosive material made of sawdust or diatomaceous earth as an absorbent and nitroglycerin as the explosive agent. It commonly sold in the shape of sticks and used with line of fuse, with primary explosive at the end acting as its charge, called a "blasting cap".

Dynamite is classified as a high explosive and it was firstly used in the First World War. It has a highly and lethal effects. Nobel becomes notorious for his invention of dynamite. The properties of dynamite are primarily three parts: nitroglycerin, which acts as its explosive agent, an absorbent, mostly one part of diatomaceous earth and a small amount of sodium carbonate.

AMMONIUM NITRATE AND FUEL OIL (ANFO)

This type of explosive mixture was invented by Melvin Cook's, in December of 1956. The safety and efficiency of this new mixture (composed by ammonium nitrate, aliminium powder and water) was revolutionary.

The ANFO (or AN/FO, for ammonium nitrate / fuel oil) is a widely used explosive mixture. This kind of source, under certain conditions, is considered an high explosive; it decomposes through detonation rather than deflagration and with a high velocity. It is an explosive consisting of distinct fuel and oxidizer phases and requires confinement for efficient detonation and brisance. Its sensitivity is relatively low. It generally requires a booster (one or two sticks of dynamite, as historically used, or, in more recent times, Tovex) to ensure reliable detonation. The explosive efficiency associated with ANFO is approximately 80% of TNT, also stated as TNT equivalence, as it will be presented later.

The basic chemistry of ANFO detonation is the reaction of ammonium nitrate (NH_4NO_3) with a long chain hydrocarbon (C_nH_{2n}+2) to form nitrogen, carbon dioxide and water. In an ideal stoichiometric balanced reaction, ANFO is generally composed of approximately 94% of AN and 6% of FO by weight.

TNT SOURCE

Trinitrotoluene, most commonly shortened to TNT, is a solid yellow-colored chemical compound. It is used as a reagent in chemical synthesis and as explosive material. Most often

confused as being similar to dynamite, TNT is a chemical compound, while dynamite, as explained before, is a mixture of nitroglycerin and absorbent agent such as sawdust.

TNT is a comparatively insensitive explosive, which enabled it to be poured while in liquid form into shell cases. The earliest use of this source as a military explosive was during 1902, when Germans used it as a filling for artillery shells. These TNT-filled shells would explode after penetrating the armor of the target. TNT is still widely used by the arms and by various construction companies worldwide. It is valued for general use because of its safety and stability. TNT is also insensitive to shock as well as friction, which allows it to be transported and used without much risk for accidental detonation. Other property referred to this type of explosive is its water resistance, which allows it to be used in wet environments. In demolition and for clearing away large debris in building foundations, TNT generally is used.

TNT is synthesized in a three-step process. First, toluene is nitrated with a mixture of sulfuric and nitric acid to produce mono-nitrotoluene or MNT. The MNT is then nitrated to dinitrotoluene or DNT. In the final step, the DNT is nitrated to trinitrotoluene or TNT. In the picture below is presented the chemical formulas referred to this production process.

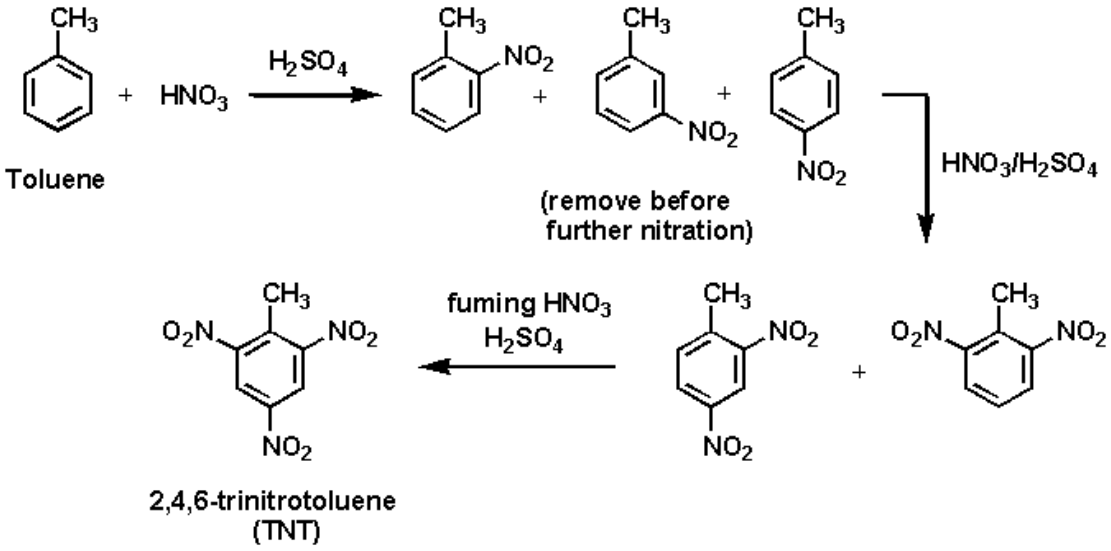

Figure 9 – TNT Chemical Formula

Upon detonation, TNT decomposes as follows:

$$2C_7H_5N_3O_6 \rightarrow 3N_2 + 5H_2O + 7CO + 7C$$

3.1 The Importance of TNT

The majorities of explosives, despite the fact that have different chemical and physical properties, when activated, they react with detonation form that well approximate the ideal blast phenomenon. An easy way to predict the effects of this kind of explosion consists on the assumption of a theoretical explosive with ideal properties that equals the energy released on a specific real explosion and its behavior. This assumption permits to covert the blast shock of a certain quantity of explosive with an equivalent quantity of TNT source, referring on the energy release during the phenomenon. In case of high explosives, the energetic equivalence permits to evaluate the weight of TNT equivalent, multiplying the weight of the source with a certain coefficient, used for the conversion. As an example, below is presented a table that resumes some values used for the conversion of sources with the TNT equivalent method.

SOURCE	COEFFICIENT	SOURCE	COEFFICIENT
TNT	1	RDX	1,25
Torpex	1,23	HMX	1,27
Gelatins-Dynamite	0,8	Pentrite	1,3
C 4	1,2	Nitroglycerin-dynamite	0,9
Amatol 50/50	0,97	Fulminate Mercury	0,39
Compound B	1,15	Pentolite	1,3

Table 7 – TNT equivalent Values

The TNT method could be used also in case of VCE explosion, rounding up the effects of deflagration with an ideal detonation approach using solid source. Indeed, though these two phenomena have different properties and way to evolve, just knowing that 1 [kg] of TNT release 4520 [KJ/kg], it is possible to convert the blast effects of a certain explosive source with the TNT equivalence method. To better understand the phenomenon and the meaning of the TNT equivalence, below it is analyze this method, and the applications for the different types of explosion. Below the author will present a general approach to the analysis for the TNT equivalence, that will be better formulate into the chapter 3, where the blast load function parameters are calculate.

TNT EQUIVALENCE

Generally, the TNT equivalent represents the mass of TNT that would result in an explosion of the same energy level as the unit weight of the explosive under consideration. Specifically, the TNT equivalent is defined as the ratio of the mass of TNT to the mass of the explosive that results in the same magnitude of blast wave (or impulsive pressure) at the same radial distance for each charge.

The primary reason for choosing TNT as an explosive reference is that, there is a large amount of experimental data regarding the characteristics of blast waves associated with this explosive. There are several methods for determining the explosive characteristics of different explosives, but they do not yield the same values for the TNT equivalent. These values depend on the characteristic parameter of the blast wave, the geometry of the load and the distance from the explosive charge, while the mechanism of energy release during the detonation process varies depending on the nature of the explosive. It is possible to distinguish between approaches based on the pressure, impulse, explosion yield and the conventional methods of the Health and Safety Executive.

Pressure-based concept

It is based of the equivalence of the incident pressure as the mass ratio of TNT to the considered explosives that cause the peak pressure at the same radial distance of each load. The equivalent mass of an explosive pressure is then:

$$E_P - TNT = \frac{M_{TNT}}{M} = \left(\frac{Z}{Z_{TNT}}\right)_P^3$$

Where Z is the reduced distance. During 2002, Ohashi and Kleine described a procedure to calculate the TNT equivalent, based on knowledge of the shock radius – time of arrival diagram of the shock wave for the explosive under consideration. These data are used to calculate the Mach number of the shock and the peak overpressure as a function of distance. The TNT equivalent pressure is between 0,4 and 0,6 for a stoichiometric propane-oxygen charge of 19281 [kg].

Impulse-based concept

A similar approach is used to obtain the equivalent mass of impulse:

$$E_I - TNT = \frac{M_{TNT}}{M} = \left(\frac{Z}{Z_{TNT}}\right)_I^3$$

However, the impulses are reported as the cube root of the mass, and the equivalent impulse is obtained by moving the curves along the diagonal.

Explosion yield-based concept

Lannoy, during 1984, conducted an analysis of 150 incidents that resulted in accidents and fires in the gas, oil and chemical industries. The results are representative of 23 accidents for which the data are sufficient to yield a calculation of the explosion. The database relies on the same pressure-based approach. The TNT equivalent of an explosive or explosive gas mixture is the mass of TNT that causes an explosion with the same pressure field as 1 [kg] of the explosive. The energy equivalence is defined by the following ratio:

$$\frac{Heat\ of\ combustion\ of\ the\ Hydrocarbon}{Calorific\ poqer\ of\ TNT}\ where\ \frac{46900\ [\frac{kJ}{kg}]}{4690\ [\frac{kJ}{kg}]}$$

Thus, it is possible to define the theoretical equivalence energy as 10 [kg] of TNT for 1 [kg] of hydrocarbon; however, the validity of this value should be determined. To determine the validity, Lannoy suggested a total return of explosion to establish a comparison with the analysis of the 23 accidents. The explosion yield is defined by the ratio:

$$\frac{TNT\ mass\ equivalent\ energy\ of\ combustion}{Energy\ of\ combustion\ of\ the\ liberated\ product\ mass}$$

$$E - TNT = \frac{mass\ of\ TNT\ equivalent * 4690\ [\frac{kJ}{kg}]}{mass\ of\ the\ released\ product * Q\ [\frac{kJ}{kg}]}$$

Where Q represents the energy released by the complete combustion in air of a unit mass of the product under consideration. Below is presented a table that shows a severity scale for explosions, referred to this method of calculation.

RANGE PERFORMANCE %	VALUE %	TNT EQUIVALENCE	FREQUENCY
0 < E-TNT < 6,0	4	2	0,80
6,0 < E-TNT < 12,0	10	5	0,97
12,0 < E-TNT < 18,0	16	8	1,00

Table 8 – TNT Equivalence Ranges performance

So, if an accidental explosion occurs, then the resulting damage can be determined by using a TNT equivalence of 2 for a mass of hydrocarbon within the flammability limits.

Conventional TNT equivalence methods from HSE (1986)

The conventional TNT equivalent method recommended by the Health and Safety Executive (HSE) applies to the case of liquid fuel spilled on the ground of the environment. The mass of the TNT equivalent charge is related to the total quantity of fuel in the cloud, which is determined by the following procedure:

- **1st step**: determination of the fraction of fuel F. The fraction F of liquid fuel released is calculated by using the following equation:

$$F = 1 - exp\left(-\frac{c_P * \Delta T}{L_V}\right)$$

  Where c_p is the mean specific heat [$kJ.kg^{-1}.K^{-1}$], ΔT is the temperature difference between vessel temperature and the boiling temperature at ambient pressure, and L_V is the latent heat of vaporization.

- **2nd step**: mass of fuel w_f in the cloud. The mass of fuel in the cloud is equal to the fraction of fuel multiplied by the quantity of fuel released. To report the charge in free-air without ground effects, a factor of 2 is applied as:

$$w_f = 2F * m_f$$

  Where mf is the total quantity of fuel released.

- **3rd step**: mass of the charge of TNT equivalent calculates using the following formula:

$$W_{TNT} = \eta_e \frac{w_f * H_f}{H_{TNT}}$$

Where W_{TNT} is the mass equivalent of TNT [kg], w_f is the mass of fuel in the cloud [kg], H_f is the heat of combustion of the fuel [$MJ.kg^{-1}$], H_{TNT} is the detonation energy of TNT [4,68 $MJ.kg^{-1}$] and the η_e is the efficiency factor for TNT (generally equal to 0,03).

- **4th step**: overpressure of blast wave. If the equivalent mass of TNT is known, then the overpressure of the blast wave following the detonation of the charge gas can be determined. The peak overpressure produced by the detonation of the TNT charge is plotted against the scale distance $\underline{R}$ from the load.

$$\underline{R} = \frac{R}{W_{TNT}^{1/3}}$$

Where $\underline{R}$ is the reduced distance [$m.kg^{-1/3}$], W_{TNT} is the mass equivalent of TNT [kg] and R the actual distance of the load [m].

4. General Blast Effects on Structures

A blast wave can be classified into two different types:

- Shock wave;
- Pressure wave.

The shock wave is typical on detonations and occurs in case of explosions produced by weapons. The pressure wave evolves during deflagrations and it is characterize by a pressure-time diagram. Since this phenomenon is slowly, the pressure growth gradually and rarely occurs a negative phase, with values of pressure shorter than atmosphere. As we saw, both detonation and deflagration are characterized respectively by a shock and pressure waves. In general the blast wave spreads in space with high velocity; when it meets obstacle on its way, those are completely knock down by the over-pressure generate by explosion and induced on the structure exceptional actions added up with usual loads acting on the construction. When the blast wave hits the principal wall, it generates a reflection that conduct to higher loads conditions. On the wall acts this reflected over-pressure, higher than dynamic pressures caused by the explosion. On the edges of the building it is possible to note a rift of the incident wave; some is reflected, as we saw, some goes on, involving others facade of the building. At the same time, on the principal wall, the over-pressure gradually reduced.

To obtain a general idea of the blast loading process, a simple object, namely, a cube with one side facing toward the explosion will be selected as an example. Another important consideration is that, during this dissertation, the cube is considered rigidly attached to the ground surface, to create ideal condition for the analysis. On the reality it is not possible to considered the perfect rigidly connection with the ground, because it is needed the analysis of the properties of the terrain.

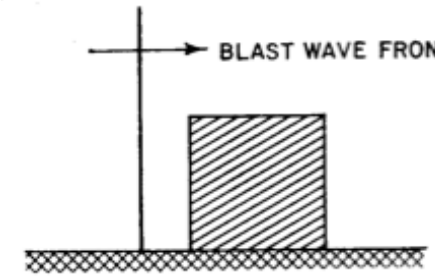

Figure 10 – Blast Wave Front

EXPLOSION FORCES

When the blast wave strikes the front of the cube, reflection occurs producing reflected pressures which may be form two to eight times as great as the incident overpressure. The blast wave then bends (or diffracts) around the cube exerting pressures on the sides and the top of the object, and finally on its back face. The object is thus engulfed in the

high pressure of the blast wave and this decay with time, eventually returning to ambient conditions.

Because the reflected pressure on the front face is greater than the pressure in the blast wave above and to the sides, the reflected pressure cannot be maintained and it soon decays to a "stagnation pressure", which is the sum of the incident overpressure and the dynamic pressure (usually called as drag pressure).

The pressure on the sides and on the top of the cube, build up to the incident overpressure when the blast front arrives at the points in question. This is followed by a short period of low pressure caused by a vortex formed at the front edge during the diffraction process and which travels along or near the surface behind the wave front. After the vortex has passed, the pressure returns essentially to that in the incident blast wave, which decays with time. The air-flow causes some reduction in the loading to the sides and top, and the drag pressure here has a negative value.

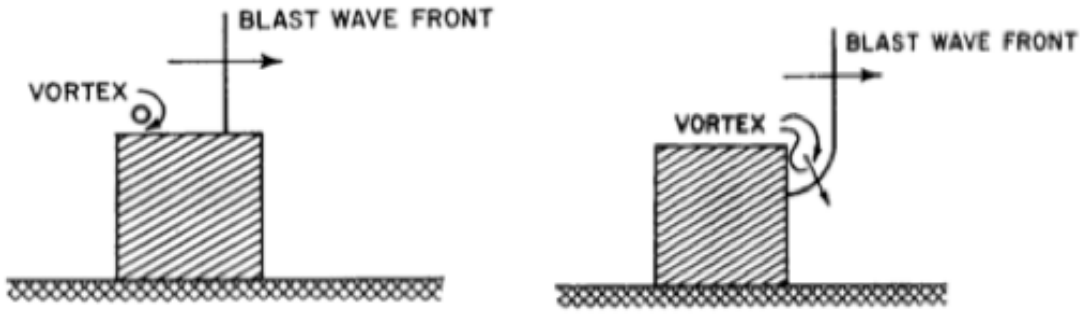

Figure 11 - Blast Wave front

When the blast wave reaches the rear of the cube, it diffracts around the edges, and travels down the back surface. The pressure takes a certain time ("rise time") to reach a more-or-less steady state value equal to the algebraic sum of the overpressure and the drag pressure, the latter having a negative value in this case.

When the overpressure at the rear of the cube attains the value of the overpressure in the blast wave, the diffraction process may be considered to have terminated. Subsequently, essentially steady state conditions may be assumed to exist until the pressures have returned to the ambient value prevailing prior to the arrival of the blast wave. The total loading on any given face of the cube is equal to the algebraic sum of the respective overpressure, p(t) and the drag pressure q(t).

Afterwards, as described above, it is possible to say that the blast load, involving a structure cannot be considered like a static load. Thus, knowing the dynamic process of the blast wave, when it involves a structure, the next step is to analyze its behavior and what kind of consequences occurs on its.

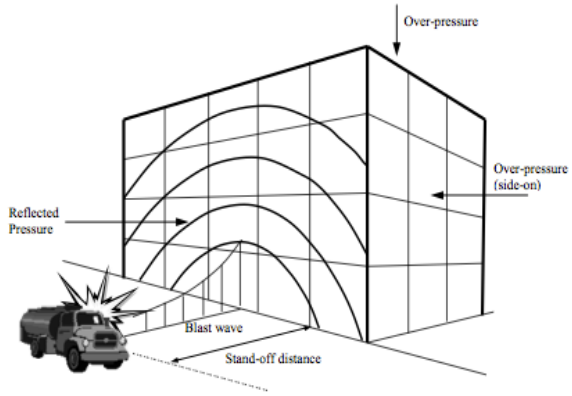

Figure 12 – Blast Wave Phenomena

So considering this event as a dynamic load, on varying of the blast load by the time, it produced structural accelerations and the motion of the construction is associated with inertial forces that generate a higher level of stress. When the structure is involved by blast waves, its behavior can be divided into two different types: elastic behavior and elastic-plastic behavior. The first one occurs when the construction, under loads, has elastic strain; generally, cause the structure is not able to dissipate loads generate by the explosion, this cumulated energy is dissolved during the unloaded phase, converting it in kinetic energy, as a result of free vibrations of the structure. In theory, the behavior of the structure is totally similar with the motion of pendulum, considering that constructions always have damping properties for dissolving blast energy caused by the explosion.

But to know the behavior of the structure, it is needed to know the distribution of the pressures, which represent the load involving the building. Thus, considering the general blast event, occurring after an explosion, it is possible to notice that particles of air with $u_2 >> u_1$, strike against the structures surface. In the case of external explosion, chemical reactions take place where a sudden temperature and pressure rise within the surrounding air; thus, creating an outward moving pressure pulse.

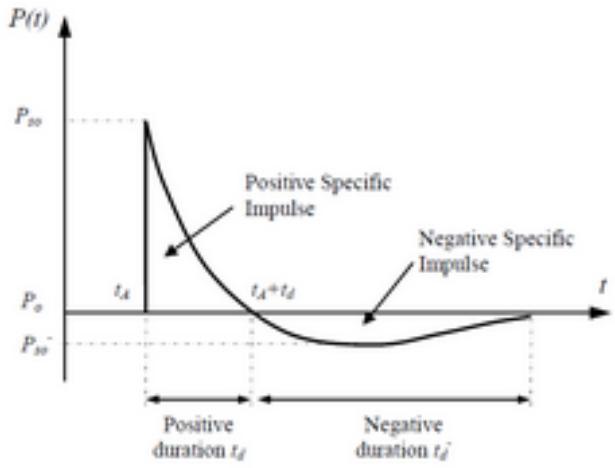

Figure 13 – Blast Wave evolution Charts

Parts of this outspreading pressure field, which are close to the explosion center, move faster due to higher temperature and pressure than parts farther away. As a

consequence of gas expansion due to heat and inertial effects, the pressure discontinuity at the front is later on followed by negative and than, once again, positive pressure phases. An obstacle exposed to such a shock wave, principally shows a p(t) distribution of forces along the elements, and the peak overpressure and duration time under special conditions may be calculated from the equivalent TNT-mass. Examining the pressure distribution on a building in greater detail necessities the distinguish between the stagnation pressure p_{st} at the front of an obstacle in the freely moving high speed airstream and the drag pressure p_d which is the resulting pressure difference between p_{st} at the front and p_{st}-p_d at the rear side of the obstacle. An even higher pressure p_r results from shock wave reflection for a rather short time after the shock-front has reached the front face of the structure. Hence, an initially overpressure p_r from the incoming shock wave occurs at the front face of a structure at time t_1.

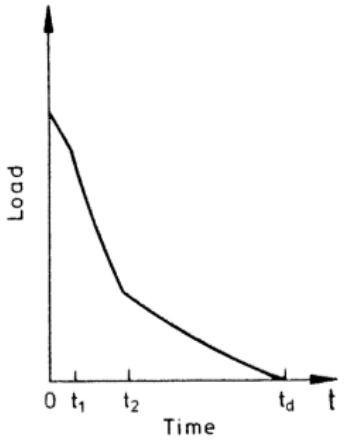

Figure 14 Load-Time Chart

As the pressure gradually surround the building, the pressure drops to the stagnation level at time t_2 and follows this curve until duration time t_d.

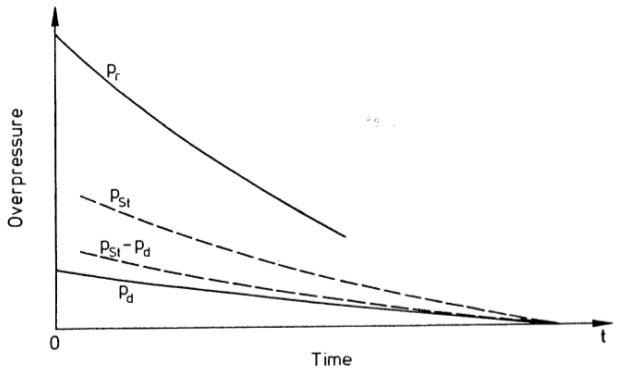

Figure 15 – Pressure wave Charts

PREDICTING DAMAGE LEVELS

Past events show that the specifics of the failure sequence for an individual building, due to air-blast effects and debris impact, significantly affect the overall level of damage. For instance, two adjacent columns of a building may be roughly the same distance from the explosion, but only one fails, because it is struck by fragment in a particular way, that initiates collapse. Afterwards, the details of the physical setting surrounding a particular occupant may

greatly influence the levels of injuries incurred. Direct air-blast effects are damage caused by the high-intensity pressures of the air blast close to the explosion. These may induce localized failure of exterior walls, windows, roof systems, floor systems and columns. To produce a progressive collapse, the weapon must be in close proximity to the critical load-bearing element. The shock wave also acts in directions that the building may not have been designed for, such as upward pressure on the floor system. As the shock wave continues to expand, it enters the structure, pushing both, upward on the ceilings and downward on the floors.

Floor failure is common in large-scale vehicle-delivered explosive attacks, because floor slabs typically have a large surface area for the pressure to act on and a comparably small thickness. Floor failure is particularly common when the weapon is really closed to the target or inside of the building. For hand-carried weapons, that are brought into the building and placed on the floor, away from a primary vertical load-bearing element, the response will be more localized with damage and injuries, extending a bay or two in each direction. Although the weapon is smaller, the air blast effects are amplified due to multiple reflections from interior surface.

More extensive damage, possibly leading to progressive collapse, may occur if the weapon is strategically placed directly against a primary load- bearing element, such as a column.
In comparison to other hazards, such as earthquake or wind, an explosive attack has several distinguishing features:

- Intensity of the localized pressures acting on the building component, can be several orders of magnitude greater than these other hazards (it is not uncommon for the peak pressure to exceed values like 100 [psi]);
- Explosive Pressure decay extremely rapidly with distance from the source (as a result, air blast tend to produce more localized damage than others hazards that have a more global effect);
- Duration of the events is very short, measured in thousands of second (milliseconds). In terms of timing, the building is engulfed by the shock-wave and direct air-blast damage occurs within tens to hundreds of milliseconds from the time of detonation, due to the supersonic velocity of the shock wave and nearly instantaneous response of the structural elements;

4.1 Design Guidance

According with the F.E.M.A. Manual for the design guidelines referred to blast load events, it is possible to draw up a list useful for all buildings designer.

- *Architectural Design*:

The exterior envelope of the building is most vulnerable to an exterior explosive threat, because it is the part of the building closest to the weapon, and it is typically built using brittle materials. It also is a critical line of defense for protecting the occupant of the building. A common, but unfortunate practice is to create a large plaza area in front of the building, but to leave little set back on the sides and rear of the building. Though this practice may increase the monumental character of the building, but it also increases the vulnerability of the other three sides.

The shape of the building can have a contributing effect on the overall damage to the structure. Re-entrant corners and over-hangs are likely to trap the shock wave and amplify the effect of the air-blast. It also is better to use curved surface, when we projected the shape of the building. In case that curved surfaces are used, convex shapes are preferred over concave shapes. Generally simple geometric shape and minimal ornamentation are preferred for the general architectural design of the building, for the just explain reasons. The importance to minimize ornamentation, leads to avoid the injuries caused by the flying debris, on the closest buildings. Considering the example of military constructions, it is possible to notice that, for the architectural design is used berm-wall and buried roofs tops. In fact, soil can be highly effective in reducing the impact of a major explosive attack.

Designing building interior, it is important to separate lobby pavilion or loading dock area outside of the main footprint of the building, provides enhanced protection against damage and potential building collapse in the event of an explosion at the locations. Similarly, placing parking areas outside the main footprint of the building can be highly effective in reducing the vulnerability to catastrophic collapse. Other important rule is to located secondary stairwells, elevator shafts, corridors and storage areas, between public and secured areas. Adequate queuing areas should be provided in front of lobby inspection stations, so that visitors are not forced to stand outside, during bad weather conditions or in a congested line inside a small lobby while waiting to enter the secured areas. Occupied areas or emergency functions should not be placed immediately adjacent to the lobby, but should be separated by buffer area such as storage area or corridor. The interior wall area and exposed structural

columns, in unsecured lobby areas, should be minimized. Emergency functions and elevator shafts are to be placed away from internal parking areas, loading docks and other high-risk areas. False ceilings, light fixtures, venetian blinds, ductwork, air conditioners and others non structural components may become flying debris in the event of an explosion. Wherever possible it is recommended that the design be simplified to limit these kinds of hazards.

- *Structural Design*:

ASCE-7 defines three ways to approach the structural design of buildings to mitigate damage due to progressive collapse.

1. Indirect Method:
   While calculations demonstrating the effects of explosions on buildings, one may use an implicit design approach that incorporates measures to increase the overall robustness of the structure;
2. Alternative Load Path Method:
   Localized response by designing the structure to carry loads by means of an alternative load path in the event of the loss of a primary load-bearing component.
3. Specific Load-Resistance Method:
   Explicitly design critical vertical load-bearing building components to resist the design level explosive forces. Explosive loads for a defined threat may be explicitly considered in design by using nonlinear dynamic analysis methods.

To resist the direct effects of air-blast, it is important to assign to the building structure, mass, shear capacity and capacity for reversing loads, like structural characteristics to resist to the effects of the explosive weapons.

To reduce the risk of progressive collapse in the event of the loss structural elements, the structural traits that should be incorporated are redundancy, ties and ductility. In general, reinforced concrete has a number of attributes that make it the construction material of choice. It has significant mass, which improves response to explosions, because the mass is often mobilized only after the pressure wave is significantly diminished, reducing deformations. Members can be readily proportioned and reinforced for ductile behavior. The construction is unparalleled in its ability to achieve continuity between the members. Finally, concrete columns are less susceptible to global buckling in the event of the loss of a floor system. On the other hand, pre-tensioned or post-tensioned construction provides little capacity for abnormal loading patterns and load reversal.

DIRECT DESIGN METHOD:

This approach ensures that the design meets all the requirements for gravity and natural hazards in addition to air-blast effects. Take note that measures taken to mitigate explosive loads may reduce the structure's performance under other types of loads, and therefore an iterative approach may be needed. As an example, increased mass generally increases the design forces for seismic loads, whereas increased mass generally improves performance under explosive loads.

Non-linear dynamic analysis techniques are similar to those currently used, in advanced seismic analysis. Analytical models range from handbook methods to equivalent single-degree-of-freedom (SDOF) models to finite element (FE) representation. For SDOF and Finite Elements Methods, numerical computation requires adequate resolution in space and time to account for high-intensity, short duration and non-linear response.

Difficulties involve the selection of the models and appropriate failures modes, and finally, the interpretations of the results for structural design details. Charts are available that provide damage estimates for various types of construction, as a function of the peak pressure and peak impulse, based on analysis or empirical data. Military design handbooks typically provide this type of design information. Components such as beam, slabs or wall can often be modeled by SDOF system and the governing equation of motion solved by using numerical methods. There are also charts available in textbooks and military handbook for linearly decaying loads, which provide the peak response and circumvent the need to solve differential equations. These charts require only knowledge of the fundamental period of the element, its ultimate resistance force, the peak pressure applied to the element and the equivalent linear decay time to evaluate the peak displacement response of the system.

The design of the anchorage and supporting structural system can be evaluated by using the ultimate flexural capacity obtained from the dynamic analysis. Furthermore, the mass and the resistance are multiplied by mass and load factors, which estimate the actual portion of the mass or load participating in the deflection of the member along its span. For more complex elements, the engineer must resort to finite element, numerical time integration techniques and/or explosive testing. A dynamic non-linear approach is more likely than a static approach to provide a section that meets the design constraints of the project. Elastic static calculations are likely to give overly conservative design solutions if the peak pressure is considered without the effect of load duration.

By using dynamic calculations, instead of static, we are able to account for the very short duration of the loading. Because peak pressure levels are so high, it is important, to account for the short duration, to properly model, the structural response. In dynamic non-linear analysis, response is evaluated by comparing the ductility (the peak displacement divided by the elastic limit displacement), and/or support rotation (the angle between the support and the point of the peak deflection) to empirically established maximum values that have been established by the military through explosive testing.

Chapter

2

The Blast Phenomena

1. Introduction

As presented before, the aim of this work is to analyze the effects on structural elements generated by a blast load event. So, in this chapter the author will propose theoretical information about blast phenomena, explaining each properties that characterized an explosive event.

Talking about charge, solid explosives must detonate to produce any explosive effect other than a fire. The term detonation refers to a very rapid and stable chemical reaction which proceeds through the explosive material at a speed, called the detonation velocity, which is supersonic in the unreacted explosive. Detonation velocities range are from 6705,6 to 8534,4 [m/sec] for most high explosives. The detonation wave rapidly converts the solid or liquid explosive into a very hot, dense, high pressure gas and the volume of this gas, which had been the explosive material is then the source of strong blast waves in air. Pressure front range, immediately behind the detonation, is from 18,61 to 33,78 [MPa]. Only about one-third of the total chemical energy available in most high explosives is released in the detonation process. The remaining two-third is released more slowly in explosions in air as the detonation products mix with air and burn. This afterburning process has only a slight effect on the blast wave properties because it is so much slower than detonation. The blast effects of an explosion are in the form of a shock wave composed of a high-intensity shock front, which expands outward from the surface of the explosive into the surrounding air. As the wave expands, it decays in strength, lengthens in duration and decreases in velocity. This phenomena is caused by spherical divergence as well as by the fact that the chemical reaction is completed, except for some afterburning associated with the hot explosion products mixing with the surrounding atmosphere.

As the wave expands in air, the front impinges on structure located within its path and then the entire structure is engulfed by the shock pressures. The magnitude and the distribution of the blast loads on the structure arising from these pressure are a function of the following factors:

- Explosive properties, namely type of explosive material, energy output (high or low order detonation), and weight of explosive;
- The location of the detonation relative to the protective structures;
- The magnitude and reinforcement of the pressure by its interaction with the ground barrier, or the structure itself.

2. The Blast Phenomena

In order to analyzed the blast phenomena, it is important to introduce the threats and their influence on the explosion. The threat for a conventional bomb is defined by two equally important elements, the bomb size (or charge weight W) and the standoff distance between the blast source and the target. For example, the blast occurred at the basement of World Trade Center in 1993, has the charge weight of 816,5 [kg] of TNT. The Oklahoma bomb in 1995 has a charge weight of 1814 [kg] at a standoff distance of 4,5 [m]. As a terroristic attack may range from the small letter bomb to the gigantic truck bomb as experienced in Oklahoma City, the mechanics of a conventional explosion and their effects on a target must be addressed.

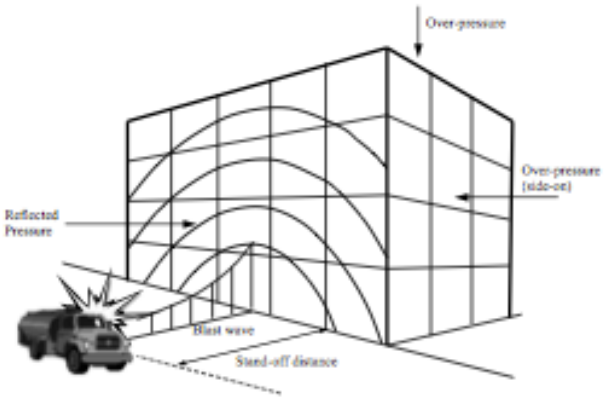

Figure 1 – Blast Evolution Phenomena

The observed characteristics of air blast waves are found to be affected by the physical properties of the explosion source. As shown in the following pressure chart, the air blast phenomena can be explain with a typical blast pressure profile:

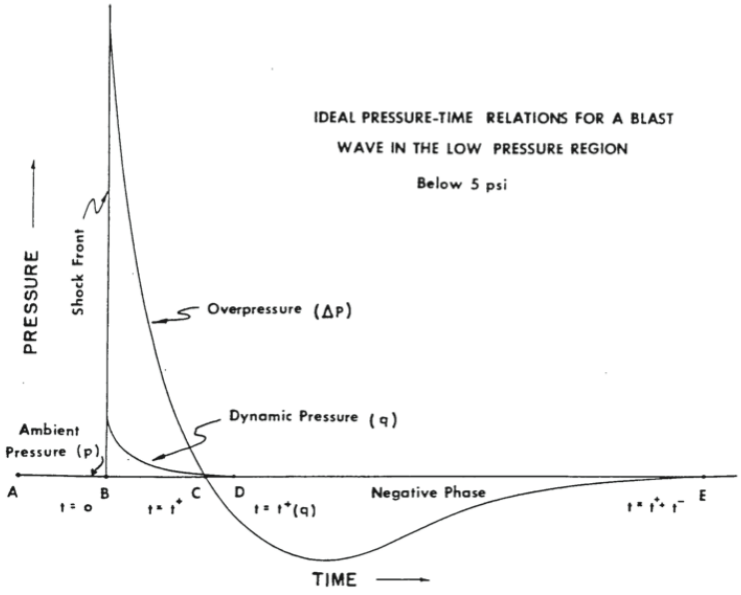

Figure 2 – Blast Load Chart

The head of the blast wave, called the shock front, causes an abrupt of rise in both overpressure and dynamic pressure. First, it is important to explain which are the difference between "Overpressure" and "Dynamic Pressure", and their properties.

- ***Overpressure (Δp)*:** describes the increase in pressure over the ambient. The peak overpressure is highest overpressure reached during the passage of the blast wave.
- ***Dynamic pressure (q)*:** a wind of high velocity blowing in the direction of the shock motion exists immediately behind the shock front. The dynamic pressures are a measure of the drag forces associated with these winds and are a function of the density and particles velocity of the air behind the shock front.

As the blast wave moves out from the fireball region, various changes in its physical characteristics occur as a function of time and distance.

2.1 The Shock Waves

A disturbance in a medium travels at the local speed of sound in that medium, where the speed of sound is a function of the local pressure and temperature. Therefore, if the pressure and the temperature increase, the speed of sound also increases. This has a dramatic influence on the propagation of a pressure pulse of arbitrary shape and finite amplitude through the medium. Considering an idealized triangular pulse, as shown below in picture 1A, since each individual portion of the pulse has a different pressure, the local sound speed for each portion is different. Thus each region of the pulse travels with this local sound speed. The higher-pressure regions thus move faster than the preceding lower pressure regions. They catch up with these slower moving regions and the wave profile becomes steeper, as shown in picture 1B. This process continues until in the limit, a sharp discontinuity is formed, picture 1C, and this is called a shock wave. The velocity of a shock wave is supersonic relative to the undisturbed medium into which it is travelling.

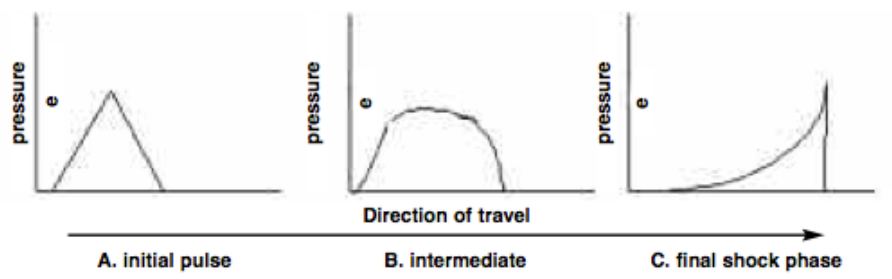

Figure 3 – Type of Blast Load pressure evolution

From the perspective of an observer at rest in the undisturbed medium, the arrival of a shock wave is characterized by an abrupt acceleration, a sudden jump in pressure and density and a local rise in temperature. As a shock wave is supersonic compared to the local sound speed in the surrounding medium it is often convenient to describe it by a quantity called the MACH Number. The MACH Number (M) is the ratio of the shock speed to the local speed of sound, usually under ambient conditions. Shock waves undergo reflection from surface in the same way as a sound or light wave, but unlike sound waves, where their effect, on the properties of the medium is negligible, shock waves charge the medium through which they are travelling. Their reflection from a surface is therefore very complex and non-intuitive. Shock waves exhibit three kinds of reflection phenomena:

- Normal Reflection associated with head-on impact with a non yielding surface;
- Oblique Reflection associated with a small angle of incidence with a surface;
- Mach Stem Formation, a spurt-type effect associated with angles of incidence with a surface near grazing incidence.

In the case of normally reflecting sound wave from a rigid surface, the pressure doubles on reflection. However in the case of shock waves the reflection pressure is a non-linear function of the Mach Number (M) of the incident shock wave. Thus, if we consider a sound wave to be a very weak shock we can say for low Mach Number (M=1) the reflection coefficient (the ratio of the reflected to the incident pressure) is 2. For very strong shock waves in air, the theoretical upper limit of the reflection coefficient is 8.

In the case of oblique reflection, the incident shock wave impinges upon a surface with a small angle of incidence and a shock wave is reflected back into the flow. In this respect they resemble sound wave. However, in general, unlike a sound wave the angle of reflection does non equal the angle of incidence.

A shock front impinging in a surface near grazing incidence does not reflect directly, but is deflected so that it spurts along the surface. As the angle of incidence increases and exceeds 40° the flow travels parallel to the surface with the shock front perpendicular to the surface. This is called a Mach Stem. This surface shock extends from the surface out into the flow until in connects with a line of intersection between the incident shock and the reflected shock. The reflected shock is thus detached from the surface. The Mach Stem regime is very important in the behavior of blast waves. The most important feature is the direction of the blast wind behind it, which is parallel to the surface and travelling with a much higher velocity than in the incident wave.

In free air, in a homogeneous atmosphere where no boundaries or surfaces are present, the changes take place in a definite manner as a result of spherical divergence and irreversible energy losses to the air through which the blast wave propagates.

When an incident air blast wave strikes a more dense medium, such as the earth's surface, it is reflected as shown:

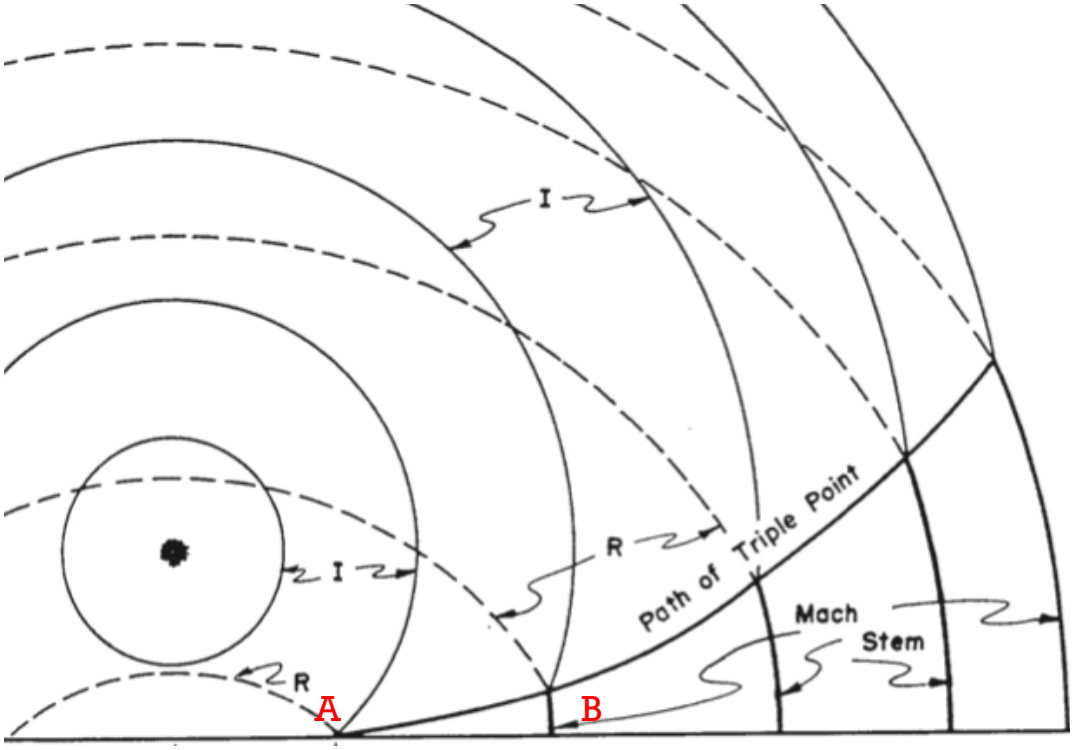

Figure 4 – Triple Point Evolution

Where:

I = incident wave front;

R = reflected wave front.

Furthermore, the portion of surface where firstly occur the reflection, point "A", it is called "Regular Region", while the portion where incident and reflected waves marge, as in point "B", forming a single shock front called Mach Stem, it is indicate as the "Region of the Mach Reflection".

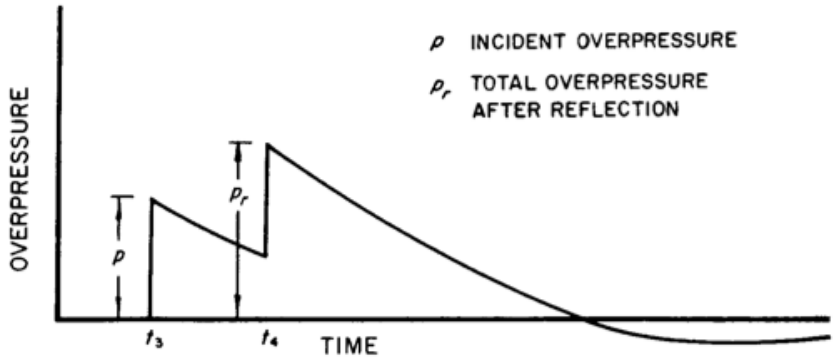

Figure 5 – Over Pressure and Reflected Pressure

The reflected wave near the surface moves faster than the incident wave, because the former travels through a region, as a result of the passage of the incident shock front, is hotter and more dense than the ambient atmosphere. Therefore, under appropriate conditions, that portion of the reflected shock near the surface overtakes and merges with the incident shock to form a single shock front called the "Mach Stem". Due to the reflection process, higher peak overpressure and higher peak dynamic pressures are realized at or near the surface, than would be obtained at the same distance in free air.

The characteristics of the blast wave at or near the surface, as well as the formation of the Mach Stem, are dependent upon yield, height of burst, and the boundary or reflecting surface conditions.

As the Mach Stem travels along the surface, the triple point (the point of intersection of the incident wave, reflected wave and the Mach Stem) rises.

To the fusing of the reflected and incident blast waves to form a Mach Stem as just described, that portion of the reflected wave passing through the fireball of a burst in the transition zone will also fuse with that portion of the incident wave directly above the fireball. This fusion is primarily a result of the increased velocity of the reflected wave as it passes through the fireball, and as a consequence, is relatively narrow in lateral extent.

In general, the evolution of this phenomenon of reflection and the formation of the Mach Stem can be described with the pictures presented below:

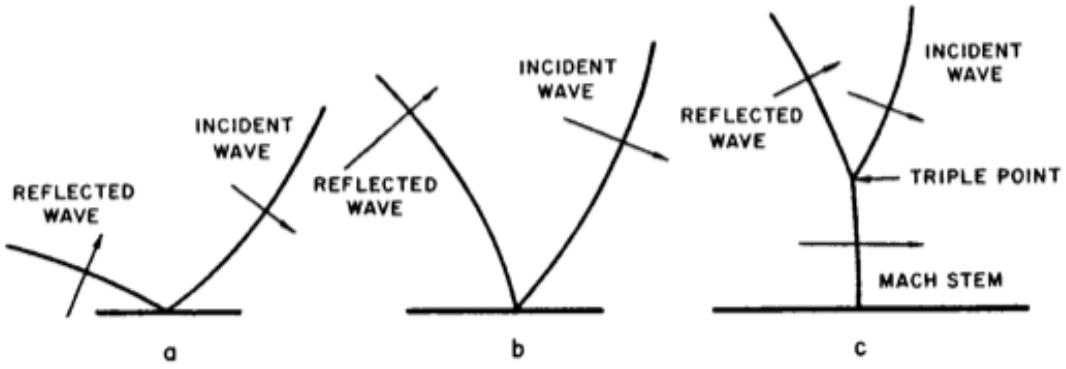

Figure 6 – Mach Stem Phenomena

The picture "c" shows the merging of the incident and reflected waves, forming the "Mach Stem". The situation at a point fairly close to the ground zero, such as in picture "a", represents the first step occurring when reflected and incident waves firstly meet. The point at which these two waves meet, is referred as the "Triple Point".

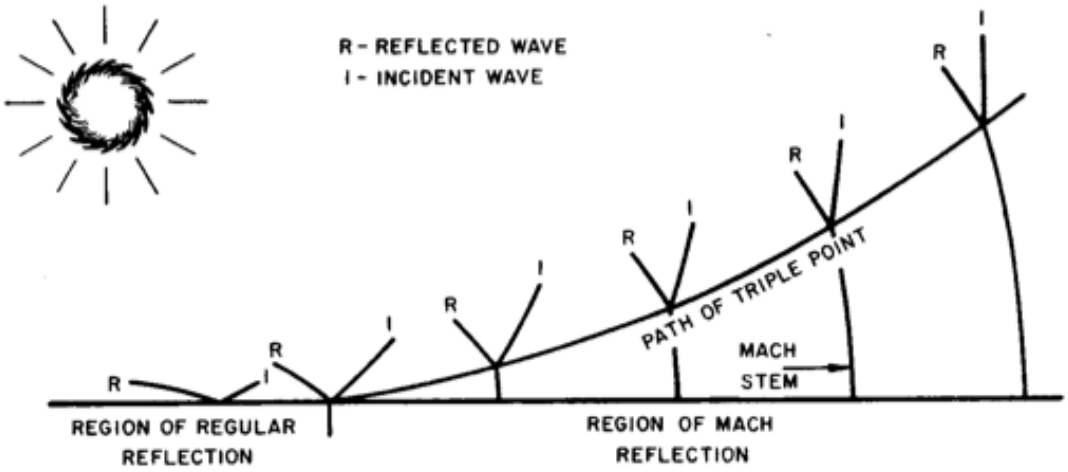

Figure 7 – Mach Stem Phenomena

As shown above, the triple point continues to grow up his height, with Mach stem increase.
As far as the destructive action of the air blast is concerned, there are at least two important aspects of the reflection process to which attention should be drawn. First, only a single pressure increase is experienced in the Mach region below the triple point as compared to the separate incident and reflected waves in the region of regular reflection. Second, since the Mach Stem in nearly vertical, the accompanying blast wave is traveling in a horizontal direction at the surface, and the transient winds are approximately parallel to the ground. Thus, in the Mach region, the blast forces on aboveground structures and other objects are directed nearly horizontally, so that vertical surfaces are loaded more intensely than horizontal surfaces.

The distance from ground zero at which the Mach Stem begins to form, depends primarily upon the yield of the detonation and the height of the burst above the ground. Provided the height of the burst is not too great, the Mach Stem forms at increasing distances from ground zero as the height of burst increases for a given yield, and also as the yield decreases at a specific height of burst.

In general, to explain this phenomenon, it is needed to consider the fluid-dynamic theories and their properties, as presented in [2].
Solving the fluid-dynamic equations in a spherical geometry is a difficult task both analytically and numerically. In order to simplify the problem, a spherical shock system is assumed to be instantaneously modeled as a planar system with a similar configuration.
The angle of incidence of the spherical shock, as measured by the tangent to the shock, is the same as the angle of incidence in the planar shock. The wedge angle O_w of the planar shock system is equivalent to the angle C_9. Once the pressure and triple point trajectory angle are determined for the planar system, they assumed to be the same for the spherical system. Solving these multiple problems will enable the prediction of the path of the triple point.
The medium in which the shock flows is a perfect diatomic gas.

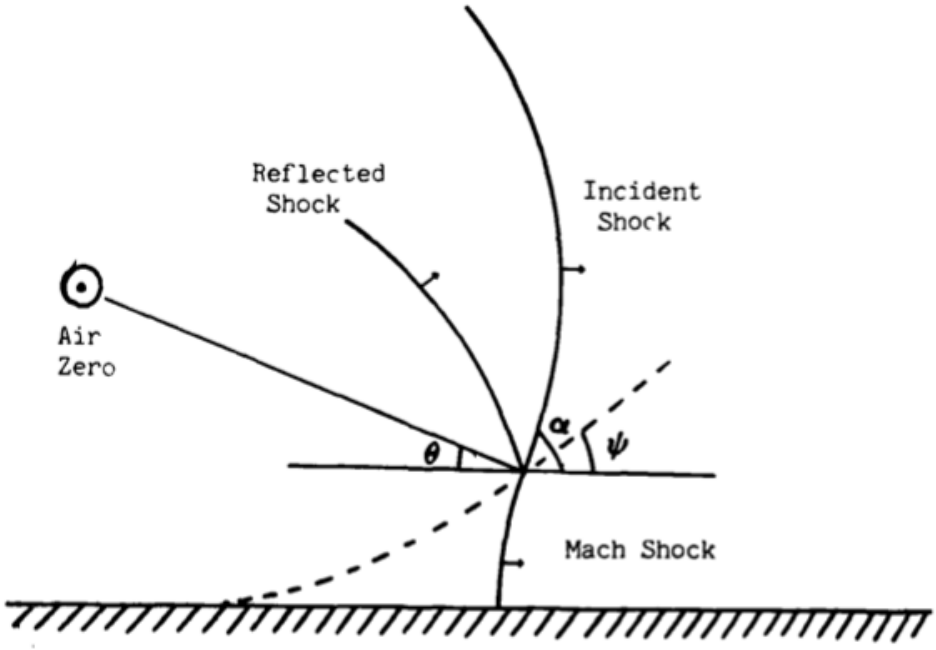

Figure 8 - The spherical shock configuration of the event

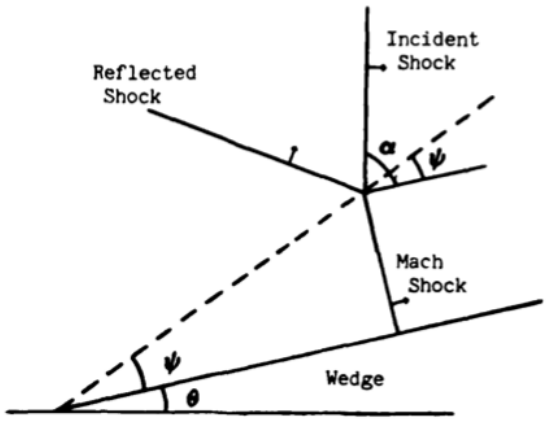

Figure 9 - The planar shock configuration of the event

γ is a variable function of the incident overpressure. The problem can be described at any point in terms of the new variables x/t and y/t. Thus the components of velocity in the x and y directions are constant. It is further assumed that, when two shock solutions are possible, the weaker of the two solutions will be the physically correct one.

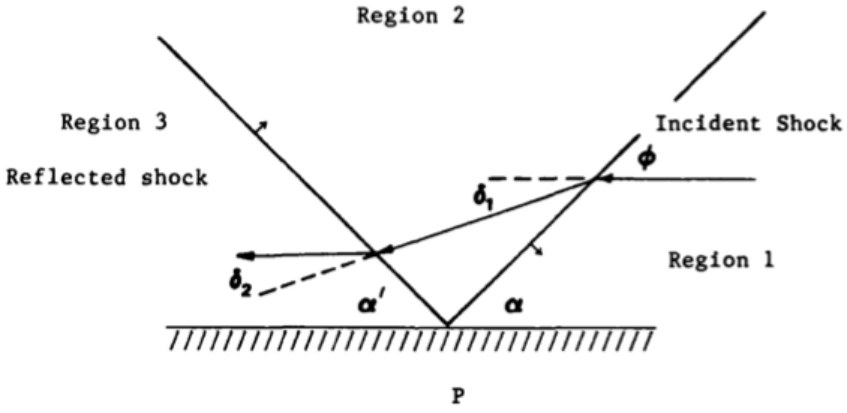

Figure 10 – Reflected and Incident Wave

Two shock wave theory deals with the reflection of an oblique shock wave from an ideal reflector. When an oblique shock wave strikes a surface, a reflected wave is formed.

The strength and angle of reflections may be found from the analysis of the air flow in the vicinity of the point of reflection (designated P in the upper figure). With respect to an observer travelling in the point of reflection, P, the ambient air (region 1) is flowing toward him with a velocity equal to $U_s/\text{sen}\alpha$.

The flow of air is depicted in the figure by arrows. The conditions across the shock from region 1 to region 2 are expressed by the following four equations, which are statements of conservations of mass, momentum and energy:

$$\rho_1 tan\alpha = \rho_2 \tan(\alpha - \delta_1)$$

$$\rho_1 U_1 sen\alpha = \rho_2 U_2 \operatorname{sen}(\alpha - \delta_1)$$

$$P_1 + \rho_1 {U_1}^2 sen^2\alpha = P_2 + \rho_2 {U_2}^2 \operatorname{sen}^2(\alpha - \delta_1)$$

$$H_1 + \frac{1}{2}{U_1}^2 sen^2\alpha = H_2 + \frac{1}{2}{U_2}^2 \operatorname{sen}^2(\alpha - \delta_1)$$

Where:

- ρ_1 and ρ_2 are the air densities in regions 1 and 2;
- U_1 and U_2 are the velocities of air in regions 1 and 2;
- U_s is the velocity of the incident shock;
- P_1 and P_2 are the pressures in regions 1 and 2;
- α is the angle of incidence;
- δ is the angle of deflection of the incoming flow;
- H_1 and H_2 are the enthalpies of the air in regions 1 and 2.

Similar four equations could be written about the conditions for the reflection occurring between region 2 and 3. Because the flow near the wall must move parallel to the ground, the strength and angle of the reflection shock must be such that it causes a deflection of the flow through an angle equal to the first deflection, but opposite in direction. As the angle of incidence increases, the magnitude of the reflected shock increases until at the some angle the strength of the reflected shock is greater than that of the incident shock.
The angle at which the reflected shock becomes greater than the incident shock is found from the relation:

$$\alpha = \frac{1}{2}\arccos\frac{(\gamma - 1)}{2}$$

As the angle of incidence increases past this angle, the reflection shock increases in magnitude.

3. Blast-wave phenomena at the surface

So now, explained in general the blast wave phenomenon, their effects and the contribution of the reflected waves on pressure loads, it is important to better analyze the case of study.
In this case, the goal is to understand the contribution of reflected waves for surface burst, and the evolution of the phenomenon, when the shock meets a vertical surface (such as a façade of a building).

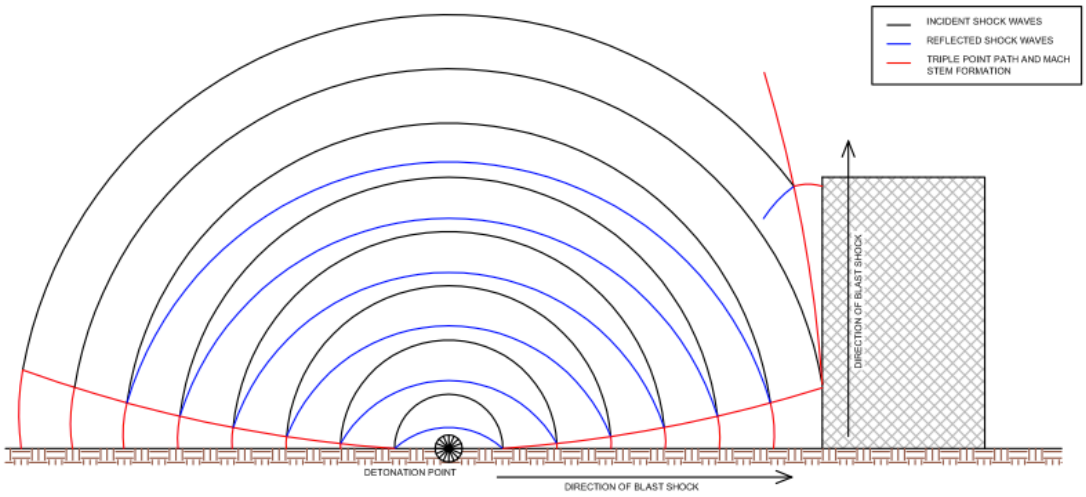

Figure 11 – Surface Blast Wave Phenomena

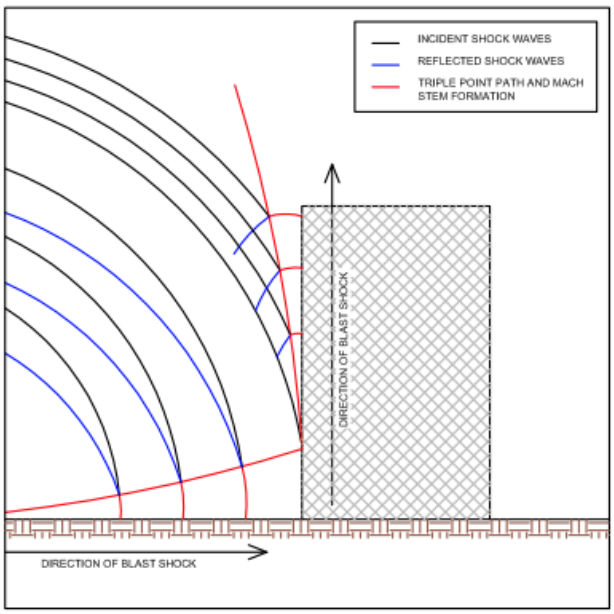

Figure 12 – Intersection of a Blast Wave with an Obstacle

The general air blast phenomena resulting from a contact surface burst are somewhat different from those for an air burst as described above. In a surface explosion the incident and reflected waves merge instantly, and there is no region of regular reflection. All objects and structures on the surface, even close to ground zero, are thus subjected to air blast similar to that in the Mach region below the triple point for an air burst.

For an ideal surfaces (absolutely rigid), reflecting surface the shock wave characteristics, overpressure and dynamic pressure, at the shock front would correspond to that for a "free air" burst, in the absence of a surface, with twice the energy yield.

Behind the front, the various pressures would decay in the same manner as for an air burst. Because of the immediate merging of the incident and reflected air blast waves, there is a single shock front, which is hemispherical in form, as shown in the picture below.

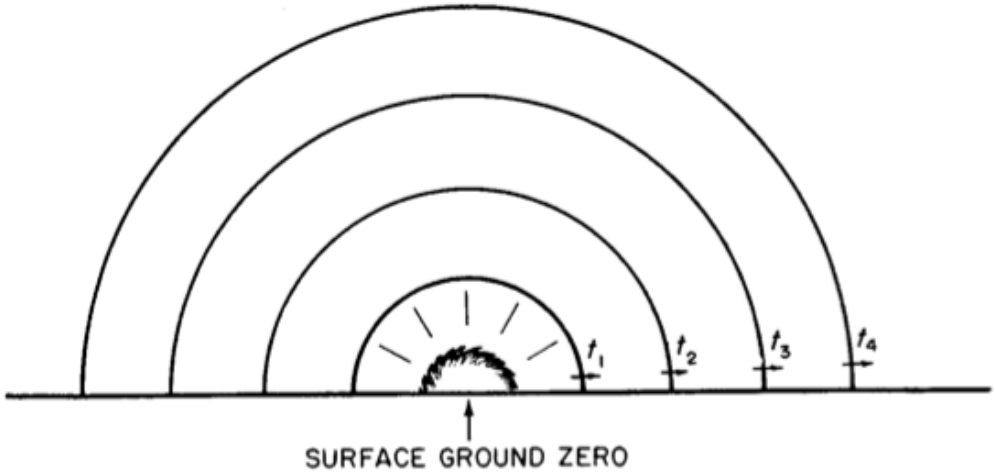

Figure 13 – Surface Explosion

Near the surface, the wave front is essentially vertical and the transient winds behind the front will blow in a horizontal direction.

The general evolution of pressures, in function of time and distance from the detonation point, is well shown in the following picture:

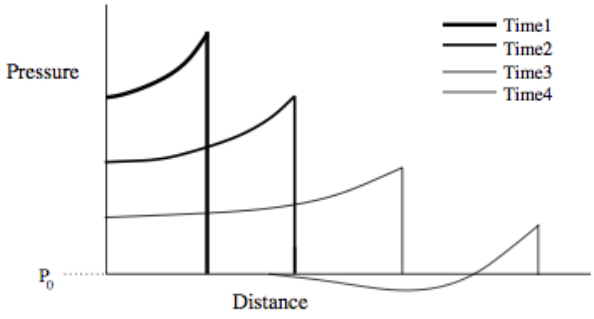

Figure 14 – Pressure Wave Evolution

Another important aspect of the blast wave problem is the possible effect of an air burst on underground structures as a result of the transfer of some of the blast wave energy into the ground. A minor oscillation of the surface is experienced and a ground shock at any point is determined by the overpressure in the blast wave immediately above it. For large overpressure with long positive phase duration, the shock will penetrate some distance into the ground, but blast waves, which are weaker and of shorter duration are attenuated more rapidly. The major principal stress in the soil will be nearly vertical and about equal in magnitude to the air blast overpressure.

So, as shown upper, the general conditions of a surface burst and the evolution of the blast phenomenon in the space is quite similar to an explosion in a free air, and considering the differences presented in previous annex, it is possible now to do a theoretical analysis of what append when a blast shock occurs.
When an air blast wave strikes a denser medium such as the earth surface, it is reflected. If the surface is hard and flat, and if the incident blast wave has a very low peak overpressure, reflection follows simple laws, much like the reflection of light. If the overpressures are moderate and high, or if the surface acts as a non-ideal reflector, interaction between the blast waves at the surface can be complex. Study of the blast wave at the surface is largely concerned with these complex aspects of surface interactions.

3.1 Reflection at normal incidence

The peak reflected overpressure, Δp, produced by a normally incident blast wave depends on the peak overpressure and the peak dynamic pressure, q, of the incident blast wave. An approximate equation for peak reflected overpressure is:

$$\Delta p_r = 2\Delta p + (\gamma + 1)q$$

where Δp_r is the peak reflected overpressure, γ is the ratio of specific heats of the medium, and the others quantities are known.
If γ for the air is considered equal to 1,4, at moderate temperature and pressure, the upper equation becomes:

$$\Delta p_r = 2\Delta p + 2{,}4\ q$$

Using the defined value of the dynamic pressure q as follows:

$$q = \frac{1}{2}\rho_s u^2$$

with the Rankine-Hugoniot equations (view the Appendix) leads to the relation:

$$q = \frac{\Delta p^2}{2\gamma P + (\gamma + 1)\Delta p}$$

and considering q=1,4 the value of the dynamic pressure is calculate as followed:

$$q = \frac{5}{2} * \frac{\Delta p^2}{7P + \Delta p}$$

Inserting this value of q into the equation for the reflected overpressure gives:

$$\Delta p_r = 2\Delta p \left(\frac{1 + 4\Delta p/P}{1 + \Delta p/P}\right)$$

This equation shows, in the limiting case of low overpressures (at overpressures sufficiently low that dynamic pressure is negligible), the peak overpressure of the reflected wave. This

relation is a general one that is valid for any angle of incidence. It is valid because at low overpressure the reflected shock wave has the same strength as the incident shock wave, and the peak reflected overpressure is the sum of the overpressures of the incident and reflected waves.

3.2 Regular and Mach reflection

The reflected wave near the surface travels through a region that is heated and made denser than the ambient atmosphere by the incident shock front as it passes. Since, a portion of the reflected shock can, under appropriate conditions, overtake and merge with the incident shock. This forms a single shock front, called "Mach Stem", which produces higher peak overpressures and peak dynamic pressures at or near the surface than would be produced at the same distance in free air. The characteristics of the blast wave at or near the surface depend on yield, height or burst, and properties of the reflecting surface. The region where the incident and reflected shocks have not merged to form a Mach Stem is referred to as the region of regular reflection; the region where they have merged is referred to as the region of Mach reflection. As the Mach Stem travels along the surface, the triple point rises.

3.3 Surface Conditions

Explain the general properties of reflection phenomena, it is now important, to better understand, considered which kinds of surface are involved and their properties.
The preceding description of the reflection process considers the earth's surface as if it were an ideal reflector. An ideal surface is defined as a perfectly flat surface that reflects all (and absorbs none) of the energy, both thermal and blast, that strikes it. In general the nature of the reflecting surface can affect the peak overpressure and the formation and growth of the Mach Stem.
For bursts over real target areas, however, the condition and the nature of the surface must be considered, since it has been determined that under certain circumstances, severe modifications of the blast wave may occur. These modifications are due to the physical characteristics of the surface, which result thermal and mechanical effects on the blast wave. The surface, which more closely approach the ideal one are ice, snow and water. These surfaces are considered "good", since the influence of such surfaces in altering the blast wave is expected to be a minimum.

In general, in many target areas, it is expected that a significant thermal layer will form near the surface prior to the shock arrival. The interaction of the incident blast wave with this thermal layer may affect the reflection process to a considerable degree, depending on the intensity of the thermal layer.

Thus individual blast wave parameters such as shock velocity, peak overpressure, particles velocity, peak dynamic pressure and duration, as well as arrival times, wave's forms and impulsive values, will be affected.

The nature of these perturbations depends on the height of burst and ground range involved, and to a lesser extent on the yield.

In general these thermal effects are not expected in regions where pressures are below 6 [psi] for burst over any surface.

Many others surfaces, especially when the explosion can raise a cloud of dust, are defined as non-ideal because they absorb substantial amounts of heat energy. In these circumstances, the properties of the blast wave may be modified by the formation of an auxiliary wave, called "precursor", that precedes the main incident wave.

3.4 The Rankine-Hugoniot Equations

To better understand the relations presented before, it is important to explain the theory of Rankine-Hugoniot and the origin of their equations.

-ASSUMPTIONS:

- One-dimensional steady flow;
- Constant area tube;
- Ideal-gas; constant and equal specific heats;
- Adiabatic conditions;
- Body forces are negligible.

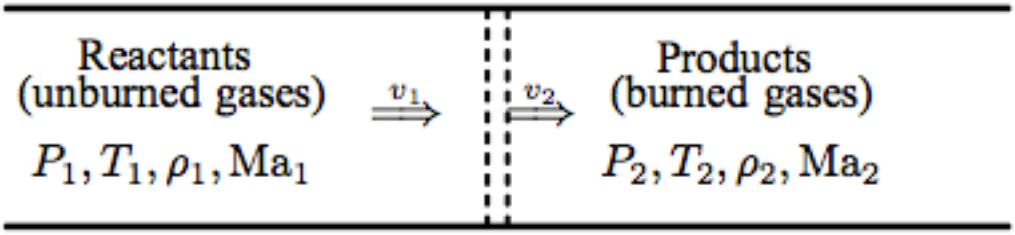

Figure 15 – Rankine–Hugoniot Physical Explanation

- Mass conservation:

$$\dot{m}'' = p_1 v_1 = p_2 v_2 \qquad (1)$$

- Momentum conservation: only force acting on the control volume is pressure:

$$P_1 + p_1 v_1^2 = P_2 + p_2 v_2^2 \qquad (2)$$

- Energy conservation:

$$h_1 + \frac{v_1^2}{2} = h_2 + \frac{v_2^2}{2} \qquad (3)$$

If we split the total enthalpy to sensible and heat of formation contribution, it is possible to write:

$$h(T) = \sum Y_i \, h_{fi}^o + \sum Y_i \int_{T_0}^{T} c_{pi} dT \qquad (4)$$

with constant specific heat assumption:

$$h(T) = \sum Y_i \, h_{fi}^o + c_p(T - T_0) \qquad (5)$$

Substituting eq. (5) into eq. (3):

$$c_p T_1 + \frac{v_1^2}{2} + \sum_{state\ 1} Y_i h_{fi}^0 - \sum_{state\ 2} Y_i h_{fi}^0 = c_p T_2 + \frac{v_2^2}{2} \qquad (6)$$

where:

$$\sum_{state\ 1} Y_i h_{fi}^0 - \sum_{state\ 2} Y_i h_{fi}^0 = q\ (heat\ addition)$$

Then energy equation is:

$$c_p T_1 + \frac{v_1^2}{2} + q = c_p T_2 + \frac{v_2^2}{2} \qquad (7)$$

and the ideal-gas assumption yields:

$$P_1 = \rho_1 R_1 T_1$$
$$P_2 = \rho_2 R_2 T_2$$

Now, combining eq. (1) and (2):

$$\frac{P_2 - P_1}{\frac{1}{\rho_2} - \frac{1}{\rho_1}} = -\dot{m}''^2$$

that represents the Rayleigh Line. For fixed values of P_1 and ρ_1:

$$P = a\left(\frac{1}{p_2}\right) + b$$

$$a = -\dot{m}''^2 \qquad and \qquad b = P_1 + -\dot{m}''^2\left(\frac{1}{\rho_1}\right)$$

where "a" is the slope and "b" the intercept.

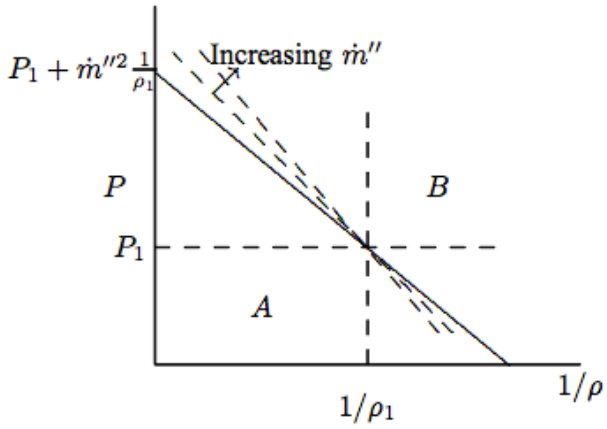

Figure 16 – Rayleight Line Graphs

Looking the graphs, it is possible to say that:

- Rayleigh line for state 1 fixed by P1 and 1/ρ1;
- Increasing mass flux m" causes the line steepen;
- In the limit of infinite mass flux, Rayleigh line would be vertical; while at the opposing limit of zero flux, it is horizontal;
- Two quadrants labeled A and B are physically inaccessible.

Rankine-Hugoniot curve is obtained when we required that the energy equation (7) be satisfied in addition to the continuity and momentum. Combining eq. (1), (2) and (7) and using ideal gas relations:

$$\frac{\gamma}{\gamma-1}\left(\frac{P_2}{\rho_2}-\frac{P_1}{\rho_1}\right)-\frac{1}{2}(P_2-P_1)\left(\frac{1}{\rho_1}+\frac{1}{\rho_2}\right)-q=0 \qquad (8)$$

The upper relation becomes a transcendental relation between P and 1/ρ:

$$f\left(P,\frac{1}{\rho}\right)=0$$

In general the point (P_1,$1/\rho_1$) is known as the origin of the Rankine-Hugoniot curve. Note that this curve does not pass through the so-called origin.

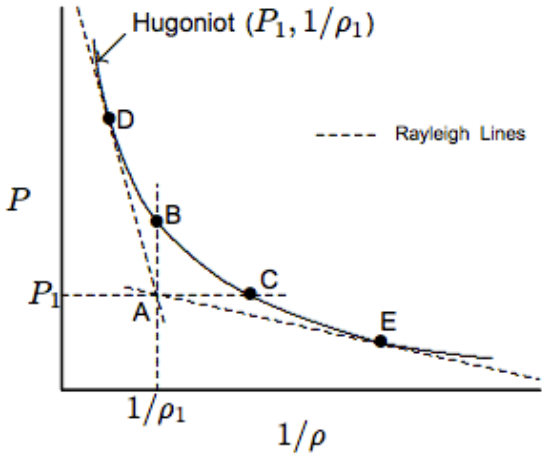

Figure 17 – Hugoniot Line Graphs

Now the question is: What points on the Hugoniot curve correspond to realizable physical states? So, the four limiting Rayleigh lines divide the Hugoniot curve into five segments:

- ***Above D:*** *strong detonations;*
- ***D-B:*** *weak detonations;*
- ***C-E:*** *weak deflagrations;*
- ***Below E:*** *strong deflagrations.*

Chapter

3

Conceptual Approach And Calculation of Blast Load on Structures

1. Introduction

In this chapter the author analyzes the energy generated by the explosion and the relative load involving the structures. As shown before, the phenomena of explosion is divided into two different categories:

- ***Deflagration***
- ***Detonation***

Both phenomena present similar properties, describing the evolution of explosion, but the time's variable distinguish which one we have to consider for the analysis. The aim of this work, as describes on the introduction, is to analyze the behavior of structures subjected to terroristic attack, and so the arise of detonations.

In general, the majority of explosives, despite their different chemical and physical properties, products detonation, that well approximate the general ideal explosion. A simple way to predict the effects of explosion consists in considering the energy released by weapon and compared that, with the properties of a reference explosive, called TNT. It means, that it is possible to convert energy, products by every kind of explosive, into an equivalent quantity of TNT. For example, considering high explosives, the conversion into "TNT equivalent mass" it is possible increasing the weight of the source with specific coefficient, as shown below.

SOURCE	COEFFICIENT	SOURCE	COEFFICIENT
TNT	1	RDX	1,25
Torpex	1,23	HMX	1,27
Gelatins-Dynamite	0,8	Pentrite	1,3
C 4	1,2	Nitroglycerin-dynamite	0,9
Amatol 50/50	0,97	Fulminate Mercury	0,39
Compound B	1,15	Pentolite	1,3

Table 1 – TNT Equivalence

The TNT method could be used also in case of VCE explosion, rounding up the effects of deflagration with an ideal detonation approach using solid source. Indeed, though these two phenomena have different properties and way to evolve, just knowing that 1 [kg] of TNT release 4520 [KJ/kg], it is possible to convert the blast effects of a certain explosive source with the TNT equivalence method. To better understand the phenomena and the meaning of the TNT equivalence, below it is analyze this method, and its applications just for detonation.

2. The Blast Wave Parameters

Now the goal is to calculate the "TNT equivalence" in order to obtain the blast load that involves the structural elements considered in this work. To better understand the high explosives event, it is important to specify the surrounding conditions characterized by the ambient.

In case of detonation, it is important to distinguish an air explosion and a ground surface explosion. Generally, considering the first type, the reaction generate by the explosion create a gasses cloud, characterized by the very high temperature and pressure. This cloud will compress the surrounding air, generating, with the motion of the adjacent air layers, the blast wave. That wave includes the 50% of the original power of the weapon. As shown below, the evolution of a blast wave could be sketch in a graph, function of time and pressure:

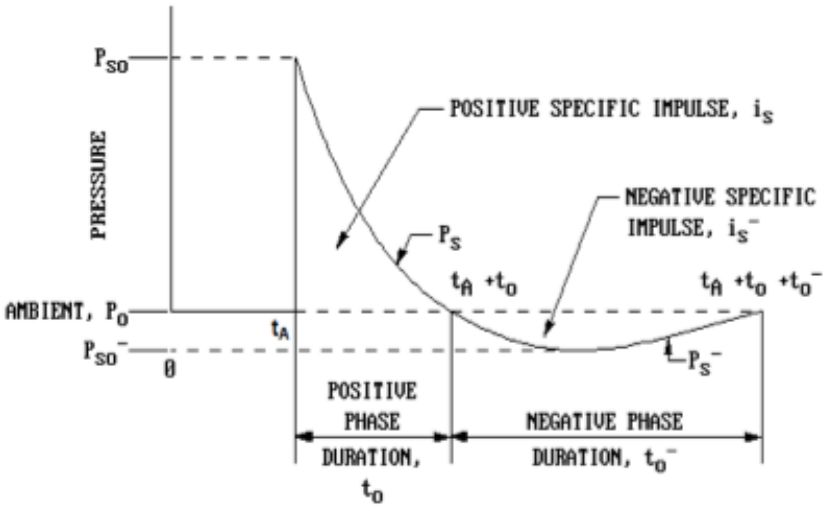

Figure 1 – Blast Wave Function

So the blast wave is a compression wave, with a peak pressure (P_{S0}) representing the maximum value of pressure involving the structures, follow by a rapid drop of the intensity of the impulse. After this first phase, the blast wave loses her power, getting off a second phase characterized by the free vibration of the structure, called negative phase. In general the evolution of blast phenomena could be sketch as follow:

- ***T_A*** *represents the arrival time of the blast wave on the structure;*
- ***P_{S0}*** *is the peak of overpressure involving the structure, followed by the rapid drop of the pressure since to the atmospheric pressure P_0;*

- t_0 *is the duration of the positive phase, when the high pressures of the blast wave involve the structure;*
- P^-_{S0} *is the maximum value of pressure occurs during the free vibration period;*
- t^-_0 *is the duration of the free vibration period (negative phase)*

Below, the author will explain how to calculate all of blast wave properties, dividing into ten different cases of study, function of TNT mass and the distance from the target:

- W_{TNT} *=250 [kg] at the stand-off distance d =20[m];*
- W_{TNT} *=500 [kg] at the stand-off distance d =20[m];*
- W_{TNT} *=750 [kg] at the stand-off distance d =20[m];*
- W_{TNT} *=250 [kg] at the stand-off distance d =50[m];*
- W_{TNT} *=500 [kg] at the stand-off distance d =50[m];*
- W_{TNT} *=750 [kg] at the stand-off distance d =50[m];*
- W_{TNT} *=130 [kg] at the stand-off distance d =20[m];*
- W_{TNT} *=130 [kg] at the stand-off distance d =50[m];*
- W_{TNT} *=130 [kg] at the stand-off distance d =10[m];*
- W_{TNT} *=15 [kg] at the stand-off distance d =5[m].*

So now the goal, it is to find all parameters to obtain the blast wave properties, for each case of studies.

2.1 Scale Distance "Z"

As explained before, now it is important to distinguish between air explosion and ground surface explosion. The general method used for the analysis is quite similar for both, but considering in this work only ground surface explosion, it is important to evaluate the amplification effects generated by the ground surface. In that case, we have to increase the TNT masses with the coefficient 1,8, finding its "TNT equivalent" values:

Weapon Source defined for W_{TNT}	**AMPLIFICATION $1{,}8*W_{TNT}$**
250 [kg]	450 [kg]
500 [kg]	900 [kg]
750 [kg]	1350 [kg]
130 [kg]	234 [kg]
15 [kg]	27 [kg]

Table 2 – Scale Distance "Z"

An other important parameter, generally used to describe this problem is stand-off distance "d", defined as the distance between the position of the charge and the target. In that work we defined four different values of d:

- ***d = 20 [m]****;*
- ***d = 50 [m]****;*
- ***d =10 [m]***;
- ***d = 5 [m]***.

These variables (stand-off distance and the mass of TNT) are expressed by means of a new quantity called "Scale Distance", by the equation:

$$Z = \frac{d}{W_{TNT}^{0,333}}$$

Obtaining ten different "Z" for each case considered:

CASE	W_{TNT} [kg]	Stand-off distance "d" [m]	Scale Distance "Z" [m/kg^{0,333}]
1	450	20	2,6099
2	900	20	2,0714
3	1350	20	1,8096
4	450	50	6,5247
5	900	50	5,1787
6	1350	50	4,5240
7	234	20	3,2455
8	234	50	8,1139
9	234	10	1,6227
10	27	5	1,6666

Table 3 – Stand-Off Distance

2.2 Peak Overpressure

A blast wave peak overpressure could be obtained using various specific formulas. Just for the case of a ground surface detonation, the peak overpressure will results amplifies, cause the presence of a reflecting surface (hemispheric detonation).

Two kind of method can be used for the calculation of the blast peak overpressure, each one dependent from the scale distance "Z". The first method was proposed by Henrych (1979), generalized few years later by Gelfand and Silnikov (2004).

- ***Henrych Method:***

$$P_{S0} = 1{,}4072 * Z^{-1} + 0{,}554 * Z^{-2} - 0{,}0357 * Z^{-3} + 0{,}000626 * Z^{-4} \quad when\ 0{,}05 < Z < 0{,}3\ [\frac{m}{kg^{0{,}333}}]$$

$$P_{S0} = 0{,}6194 * Z^{-1} + 0{,}0326 * Z^{-2} + 0{,}2132 * Z^{-3} \quad when\ \ 0{,}3 < Z < 1{,}0\ \ [\frac{m}{kg^{0{,}333}}]$$

$$P_{S0} = 0{,}0662 * Z^{-1} + 0{,}405 * Z^{-2} + 0{,}3288 * Z^{-3} \quad when\ \ 1{,}0 < Z < 10\ \ [\frac{m}{kg^{0{,}333}}]$$

- ***Gelfand and Silnikov Method:***

$$P_{S0} = 1{,}7 * 10^3 * e^{(-7{,}5 * Z^{0{,}28})} + 0{,}0156 \quad air\ exp. \quad 0{,}1 < Z < 8{,}0\ \ [\frac{m}{kg^{0{,}333}}]$$

$$P_{S0} = 1{,}7 * 10^3 * e^{(-7{,}14 * Z^{0{,}28})} + 0{,}0156 \quad ground\ exp. \quad 0{,}1 < Z < 8{,}0\ \ [\frac{m}{kg^{0{,}333}}]$$

$$P_{S0} = 8{,}0 * 10^3 * e^{(-10{,}7 * Z^{0{,}1})} + 0{,}0156 \quad air\ exp. \quad Z > 8{,}0\ \ [\frac{m}{kg^{0{,}333}}]$$

$$P_{S0} = 8{,}0 * 10^3 * e^{(-10{,}46 * Z^{0{,}1})} + 0{,}0156 \quad ground\ exp. \quad Z > 8{,}0\ \ [\frac{m}{kg^{0{,}333}}]$$

So, considering the second one method, as ground surface explosion, for each case we obtain:

CASE	Scale Distance "Z" [m/kg^{0,333}]	P_{S0} [MPa]
1	2,6099	0,16490596
2	2,0714	0,28363443
3	1,8096	0,38661577
4	6,5247	0,02532024
5	5,1787	0,03630068
6	4,5240	0,04712197
7	3,2455	0,09854551
8	8,1139	0,02014703
9	1,6227	0,49357781
10	1,6666	0,46515186

Table 4 – Overpressure Values

2.3 Pressure Bend

The equation of Friedlander (Baker 1967) describes the wave front of a blast wave, with a curve as a function of pressure and time:

$$P(t) = P_0 + P_m * (1 - \frac{t}{t_0}) e^{-\alpha t/t_0}$$

where P_0 represents the pressure at time t [msec], P_m is the maximum peak of overpressure (in case of air explosion it is equal to P_{S0}) and α is an experimental parameter relate to pressure wave. It is possible to calculate the α value using the Wei and Dharani formula:

$$\alpha = -0{,}0697 * Z - \frac{9{,}63}{Z} + \frac{15{,}9}{Z^2} - \frac{5{,}65}{Z^3} + 2{,}735$$

Looking the Friedlander equation, it is possible to notice that is a function of pressure and time. The time t_0 represents the positive phase of the blast event, when the peak overpressure occurs and involves for the first time the structure. Its values could be calculate by the Henrych or Sadovsky formulas:

- ***Henrych:***

$$t_0 = 10^{-3}(0{,}107 + 0{,}444 * Z + 0{,}264 * Z^2 - 0{,}129 * Z^3 + 0{,}0335 * Z^4 \quad as \quad 0{,}05 < Z < 0{,}3 \ [\frac{sec}{kg^{0{,}333}}]$$

- ***Sadovsky:***

$$t_0 = 1{,}2 * 10^{-3} * W^{0{,}333} * Z^{0{,}5}$$

When the blast pressure stops, the negative phase begins (rarefaction phase), and generates a free vibration motion of structure. This step is characterized by the pressure P^-_{S0} along the t_0 calculate with Krauthammer method:

- ***Krauthammer (P^-_{S0}):***

$$P^-_{S0} = 10^4 \ [Pa] \qquad at \qquad Z < 3{,}5 \ [\frac{m}{kg^{0{,}333}}]$$

$$P^-_{S0} = \frac{0{,}35}{Z} 10^5 \ [Pa] \qquad at \qquad Z \geq 3{,}5 \ [\frac{m}{kg^{0{,}333}}]$$

- ***Krauthammer (t_0^-):***

$$t_0^- = 0{,}0104 * W^{0{,}333}\ [sec] \qquad at \qquad Z < 0{,}3 \quad [\frac{m}{kg^{0{,}333}}]$$

$$t_0^- = \{0{,}003125 * log_{10}(Z) + 0{,}01201\} * W^{0{,}333}\ [sec] \qquad at \qquad 0{,}3 \leq Z \leq 0{,}3 \quad [\frac{m}{kg^{0{,}333}}]$$

$$t_0^- = 0{,}0139 * W^{0{,}333}\ [sec] \qquad at \qquad 1{,}9 < Z \qquad [\frac{m}{kg^{0{,}333}}]$$

The bend of the pressure blast wave could be drawn considering the method proposed by the U.S. Army Corps of Engineers Protective Design Center:

$$\frac{P(t)^-}{P_{S0}^-} = \frac{27}{4} * \left(\frac{t^-}{t_0^-}\right) * \left(1 - \frac{t^-}{t_0^-}\right)^2$$

So, considering the case of study, below we propose a table that resume all results obtained for each analysis:

CASE	Parameter	Positive Phase	P_{S0}^-	Negative Phase	P_0
	α	t_0 [msec]	[MPa]	t_0^- [msec]	[MPa]
1	0,8797	0,1778	0,01	0,1063	0,101325
2	1,0115	0,0156	0,01	0,1338	0,101325
3	1,1892	0,0151	0,01	0,1412	0,101325
4	1,1574	0,0234	0,0053	0,1063	0,101325
5	1,0666	0,0263	0,0067	0,1338	0,101325
6	1,0068	0,0281	0,0077	0,1532	0,101325
7	0,8858	0,0132	0,01	0,0854	0,101325
8	1,2135	0,0210	0,0043	0,0854	0,101325
9	1,4032	0,0074	0,01	0,0779	0,101325
10	1,3444	0,0038	0,01	0,0381	0,101325

Table 5 – Blast Wave Parameters

2.4 Blast Front Wave Dynamic Parameters

To create a detonation front wave, Rankine and Hugoniot in 1870 found others important parameter, called dynamic parameters, useful to describe the phenomena. For example the air high velocity, generated by the explosion of a weapon, require the analysis of three important variables:

- ***The Front Wave velocity U;***
- ***Static Density ρ_s;***
- ***The Maximum Dynamic Pressure q_s, which has the same envelope of the blast wave overpressure P_{S0}.***

When a detonation occurs, the acceleration of air particles generates a wind and its motion could be describe by the dynamic parameters. Its calculation could be made using specific formulas, efficient when the front wave is perpendicular to the direction of the motion.

- ***The Front Wave velocity "U" formula:***

$$U = \sqrt{\frac{6P_s + 7P_0}{7P_0}} * C_0 \quad [\frac{m}{sec}]$$

- ***Static Density "ρ_s" formula:***

$$\rho_s = \frac{6P_s + 7P_0}{P_s + 7P_0} * \rho_0$$

- ***The Maximum Dynamic Pressure "q_s" formula:***

$$q_s = \frac{5P_s^2}{2(P_s + 7P_0)}$$

Where P_0 represents the atmospheric pressure, C_0 is the sound velocity in air (C_0=340 [m/sec]) and ρ_0 is the density. Each pressure value must be expressed in [bar].

Another fundamental parameter useful to describe the front wave of a blast event is wavelength "L_W", that represents the distance considered between the start point and the target:

$$L_W \approx U * t_0 \quad [m]$$

The last parameter useful to describe the dynamic front wave it is called "Arrival Time t_A", that is the time which the blast wave covers the distance between the start point and the target. There are two possible ways to calculate its value:

- ***1° Method considers the average of the possible front waves velocities "U_{med}", calculated between R_0=0,053* $\sqrt[3]{W}$ (TNT weapon dimension) and the R (distance from the target):***

$$t_a = \frac{R - R_0}{U_{med}} \quad [sec]$$

- ***Empirical Method (UET Taxila-2009):***

$$t_a = \frac{0{,}4 * R^{0,5} * W^{-0,2}}{C_0} \quad [sec]$$

So, considering the cases of study, below we propose a table that resume all results obtained for each analysis:

CASE	U [m/sec]	Density ρ_s [kg/m^3]	q_S [bar]	Wavelength L_W [m]	t_A [sec]
1	533,14	1,934	0,8818	9,479	0,0126
2	635,17	2,428	1,4232	9,971	0,0109
3	711,92	2,763	1,8465	10,751	0,0101
4	379,61	1,172	0,1477	8,898	0,0379
5	393,87	1,243	0,2102	10,361	0,0329
6	407,42	1,311	0,2709	11,465	0,0304
7	466,49	1,609	0,5482	6,203	0,0143
8	372,70	1,138	0,1179	7,836	0,0432
9	783,72	1,051	2,2501	5,803	0,0062
10	765,30	1,980	2,1461	2,847	0,0041

Table 6 – Blast Wave Dynamic Parameters

2.5 Specific Impulse Calculation

The specific impulse is one of the most important parameter of a blast wave, represented by the product between pressure and time. The reaction of a structure and its elements could be evaluate analyzing the specific impulse value, calculated by the Friedlander formula:

$$i_s = \int_{t_A}^{t_0} P(t)dt$$

Sometimes, the specific impulse could be evaluated considering a triangle, function of t_d (acting pressure duration) and blast wave overpressure. Its value is represented by the area of a triangle, equivalent to the area generated under the blast wave bend during the positive phase.Acting this simplification, we must considered $t_d < t_0$, because the hypothetical triangle area increase much than 35% the real area generate by the blast wave bend. So the equivalent value of t_d could be evaluate with $t_d = 2i/P$.

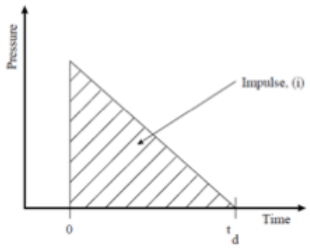

Figure 2 – Pressure-Time Chart

The author present below a table that resume all specific impulses, obtain for each case:

CASE	i_S	t_d [sec]
1	0,0010	0,0124
2	0,0015	0,0109
3	0,0020	0,0105
4	0,0002	0,0164
5	0,0003	0,0184
6	0,0004	0,0196
7	0,0004	0,0093
8	0,0001	0,0147
9	0,0012	0,0051
10	0,0006	0,0026

Table 7 – Impulse and Time Values

2.6 Reflected Pressure

The reflected pressure occurs when the blast wave crash with a structure or a surface. When this phenomena occurs, the blast wave changes its direction of motion, generating a more powerful reflected wave front.

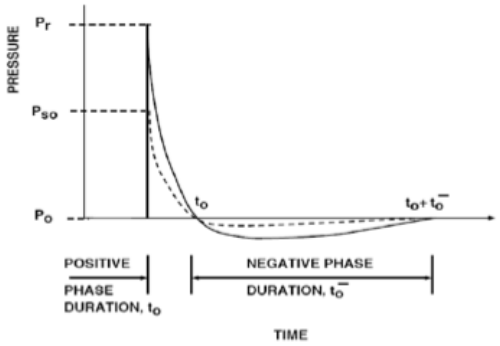

Figure 3 – Reflected Pressure Chart

As shown in the picture, there are represented two bends, one starting from P_r (reflected pressure) and one from P_{S0} (peak overpressure). It is easy to see that the reflected pressure bend is higher than the peak overpressure value, and this difference is caused by the "Mach Stem Phenomena", describes into the previous chapter.

The value of the reflected pressure could be calculated increasing the P_{S0} with a coefficient C_r, counted in the Smith method (1994). This method analyzes the blast wave collision with the surface, considering the crash angle α, and equal to α = 0 for the case of study. Indeed, using this simple method, the reflected pressure is:

$$P_r = C_r * P_{S0} \quad [MPa]$$

with:

$$C_r = 3 * \sqrt[4]{P_{S0}} \qquad and \qquad P_{S0}\ in\ [bar]$$

CASE	C_r	P_r [MPa]
1	3,3996	0,5606
2	3,8932	1,1042
3	4,2066	1,6263
4	2,1280	0,0538
5	2,3287	0,0845
6	2,4855	0,1171
7	2,9890	0,2945
8	2,0098	0,0404
9	4,4715	2,2070
10	4,4057	2,0493

Table 8 – Reflected Pressure Values

2.7 Graphic Analysis Review

To verify that all results, obtained with the analysis of the blast wave parameters, are correct, we can use a graphic method proposed by the U.S. Army Corps of Engineers Protective Design Center, in collaboration with the Protection Engineering Consultants, LLC (PEC) and Baker Engineering and Risk Consultants Inc. Considering a ground surface explosion, the author propose below the two graphs used for the verification of the results, drawn with a logarithmic scale.

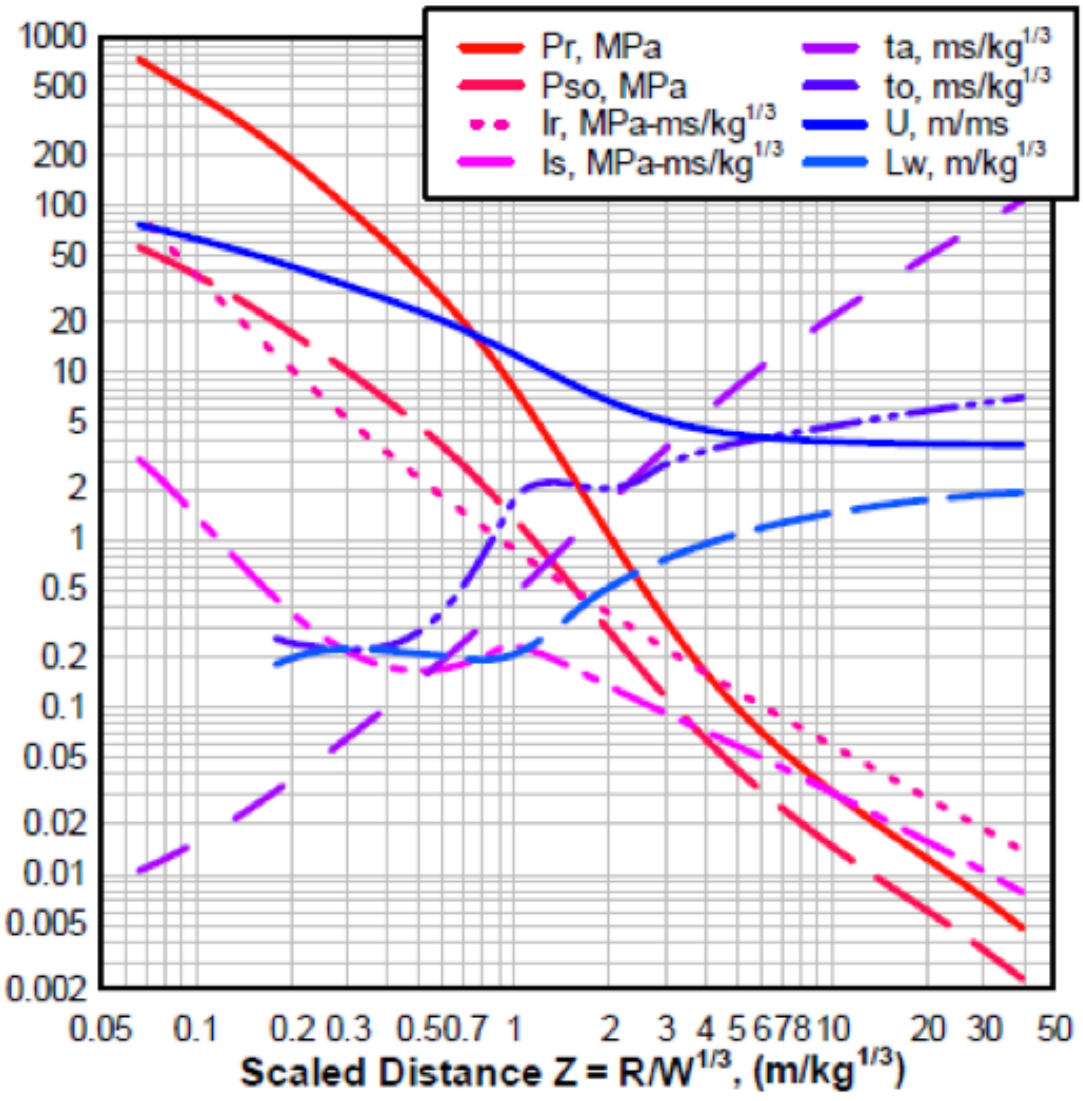

Figure 4 – Graphic Analysis review – Positive Phase

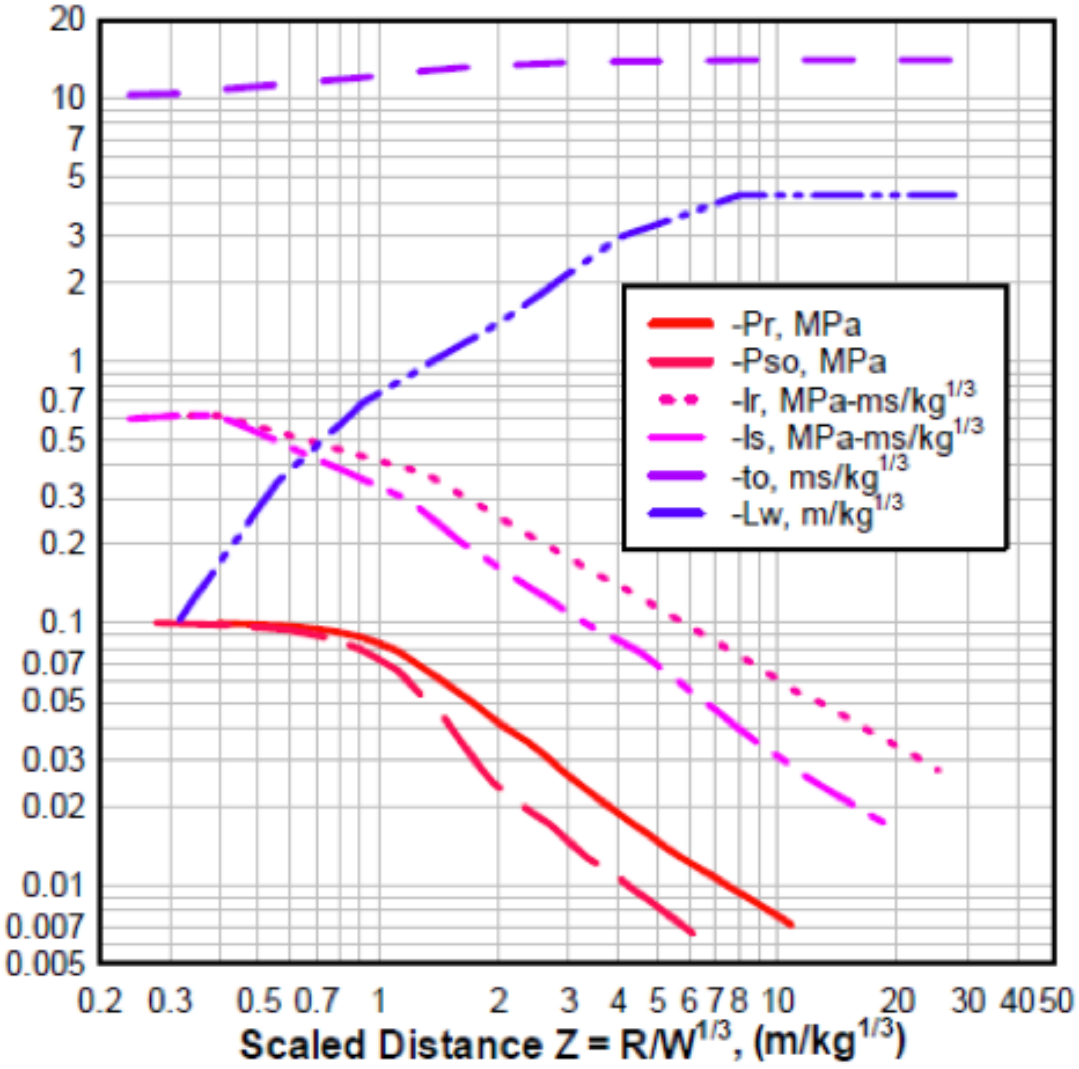

Figure 5 – Graphic Analysis Review – Negative Phase

3. The Blast Load Calculation

The values of pressure, density and temperature, when a blast wave crash against a structure, are much more increased if the surface involved by the explosion, is reflective. So, the blast load will be considered maximum when the pressure is completely reflected by the surface. Below, it is proposed a picture that well describes the evolution of a blast wave involving a structure surface.

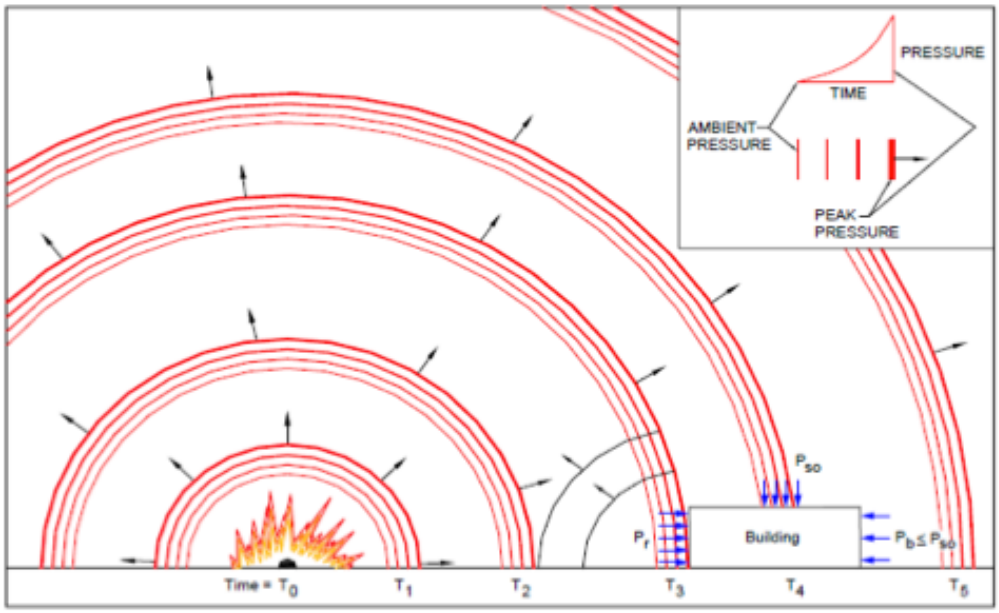

Figure 6 – Surface Blast Wave

As shown, the blast wave rolls up the entire structure, and each surface is involved by the wave, depending on its orientation, as a function of the direction of the phenomena.

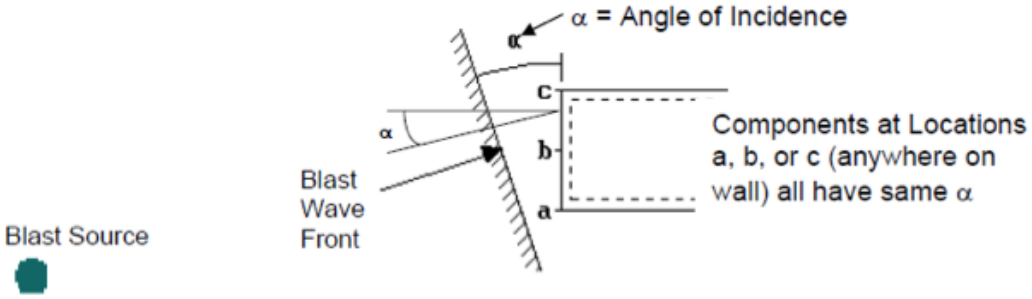

Figure 7 – Incident Wave on a Surface

The ASCE (1997), analyzing the entire phenomena, divided the surface involved by the explosion, as:

- ***Blast Load on the principal surface***

  The principal surface is firstly involved by a reflected pressure P_r. After the time t_c, called clearing time, the value of the pressure decrease to P_S, function of the initial peak overpressure P_{S0} and the dynamic wind pressure q_s. It is also important specify that, the blast load is affected by the time t_c when its value is smaller than $t_{rf} = 2i_r/P_r$. In that case, P_{S0} is the pressure acting on the surface.

$$P_S = P_{S0} + C_D * q_S \quad [MPa]$$

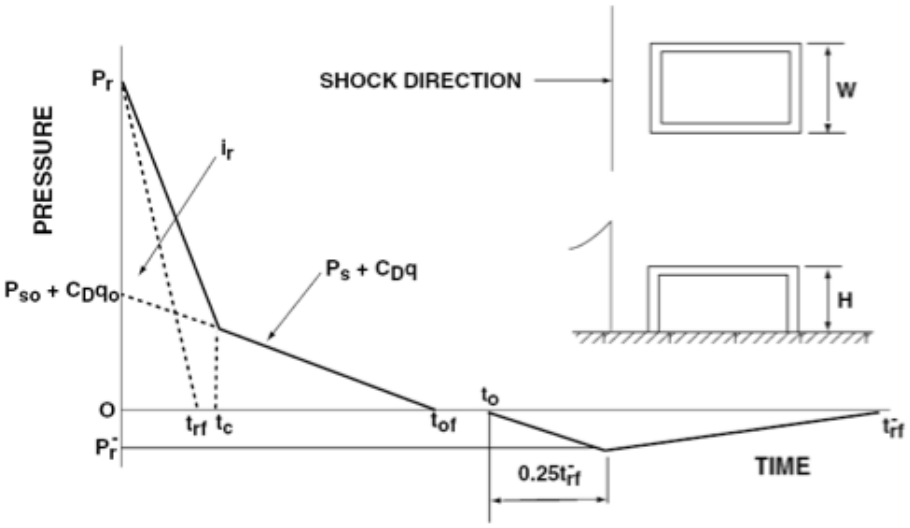

Figure 8 – Blast Load Function

The specific impulse can be evaluated using the triangular method, proposed above, with the formula:

$$i_S = 0{,}5 * (P_r - P_s)t_C + 0{,}5P_s t_0$$

and time t_d:

$$t_d = \frac{2 * i_s}{P_r} = \frac{(t_0 - t_c) * P_s}{P_r + t_C}$$

- ***Blast Load on the lateral surface and the roof***

  Considering lateral surfaces and roof, the dynamic pressure is smaller than the one that involves the principal surface. Furthermore it has not a uniform distribution along the surface and also, it is a function of time and distance, cause the front wave changes quickly its positions. Particularly, if the dimension L it is considered equal to L_W, the overpressure involving the structure overtake the surface and decrease to the ambient pressure. Considering that, for its calculation we must use a reducing coefficient C_e, depending to the length of the surface. Cause the front wave motion is perpendicular to the surface we obtain a not uniform pressure distribution. For that reason, it is possible to considered a length surface equal to L=1, changing the equation of the pressure P_a involving a lateral surface as:

$$P_a = C_e * P_{S0} + C_D * q_s \quad [MPa]$$

The C_e value could be evaluate using the graphs presented below, depending on the ratio L_W/L and C_D (coefficient representing the opposition to the motion and function of q_s):

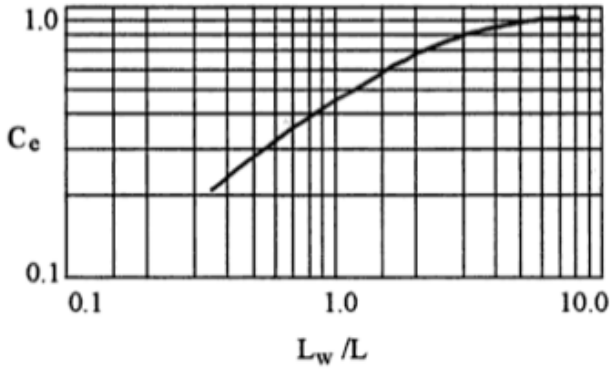

Figure 9 – Reducing Coefficient Charts

The time progress for the load involving the lateral surface, it is represented in the charge below, where t_1 =L/U and t_2 =(L/U)+t_1

Considering the roof, any reflection occurs when the blast wave involves the surface. Consequently, the pressure value could be evaluates with the same equation used for the lateral surface, considering the coefficient C_e and C_D.

Analyzed the methods used for the calculation of the blast load involving the structural elements, now it is possible to resume the values obtain after that analysis process for the cases of study:

CASE	Pressure P_a [MPa]	Coefficient C_D	t_{rf} [sec]	t_c [sec]	Impulse I_W	t_d [sec]
1	0,2530	1,00	0,0062	0,0122	0,0041	0,0147
2	0,4259	1,00	0,0078	0,0102	0,0068	0,0123
3	0,5712	1,00	0,0067	0,0091	0,0091	0,0112
4	0,0401	1,00	0,0283	0,0171	0,0005	0,0218
5	0,0573	1,00	0,0319	0,0165	0,0009	0,0231
6	0,0742	1,00	0,0244	0,0159	0,0013	0,0236
7	0,1533	1,00	0,0083	0,0139	0,0020	0,0136
8	0,0319	1,00	0,0243	0,0174	0,0004	0,0202
9	0,7185	1,00	0,0033	0,0082	0,0088	0,0080
10	0,6797	1,00	0,0014	0,0084	0,0070	0,0069

Table 9 – Resuming Values for Blast Load Function Calculation

3.1 Graphic Analysis Review

At last, considering all the analysis proposed, the author presents below graphs and tables representing the "Blast Load Functions", useful for the next steps analysis with Midas Gen Software. Each case is divided into three subcase, one for each height of columns considered:

CASE 1

- ***Column h = 5 [m] (TNTeq = 250 [kg] and r = 20 [m])***

Time [sec]	Load [kN]
0,00	1401,54
0,012	632,73
0,018	0,00
0,019	-80,00
0,124	0,00

Table 10 – Case 1 Time- Load Values

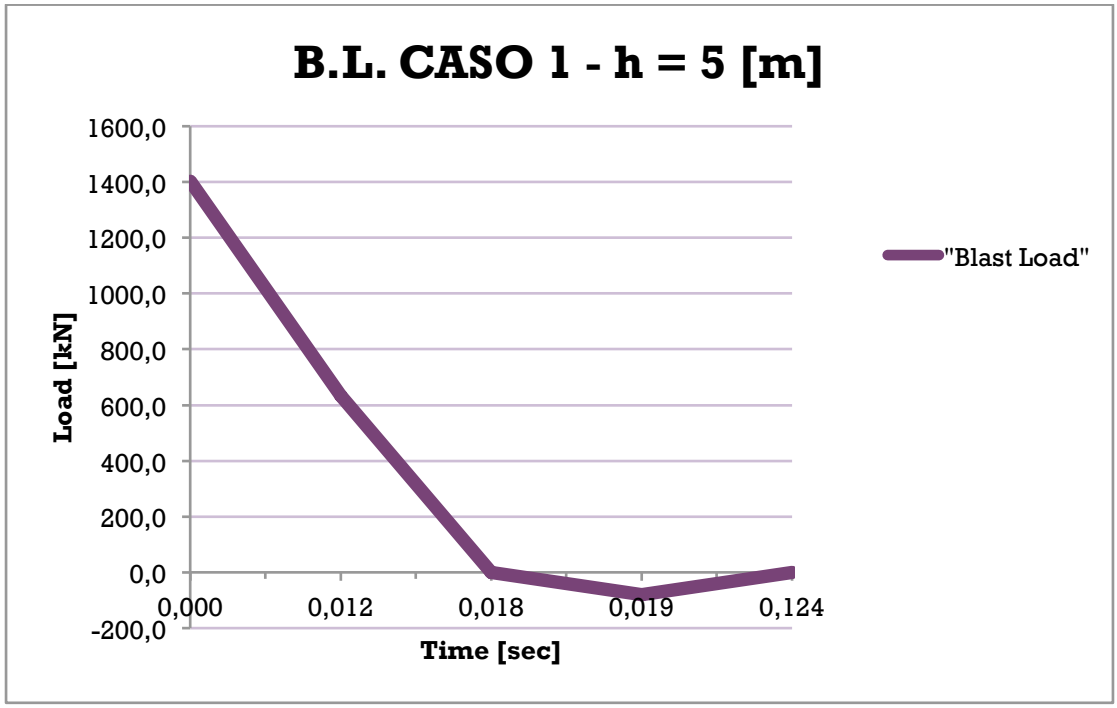

Figure 10 – Case 1 Load Function

- ***Column h = 4 [m] (TNTeq = 250 [kg] and r = 20 [m])***

Time [sec]	Load [kN]
0,00	1121,23
0,012	506,18
0,018	0,00
0,019	-64,00
0,124	0,00

Table 11 – Case 1 Time- Load Values

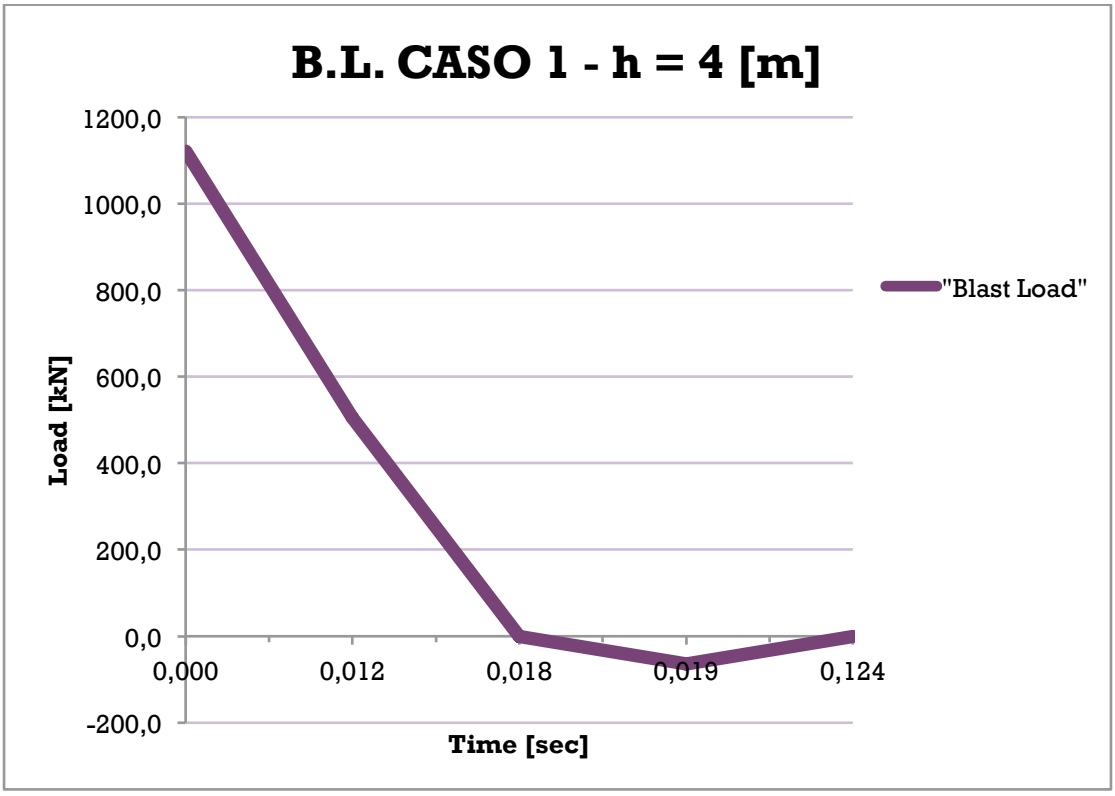

Figure 11 – Case 1 Load Function

- ***Column h = 3 [m] (TNTeq = 250 [kg] and r = 20 [m])***

Time [sec]	Load [kN]
0,00	840,92
0,012	379,63
0,018	0,00
0,019	-48,00
0,124	0,00

Table 12 – Case 1 Time- Load Values

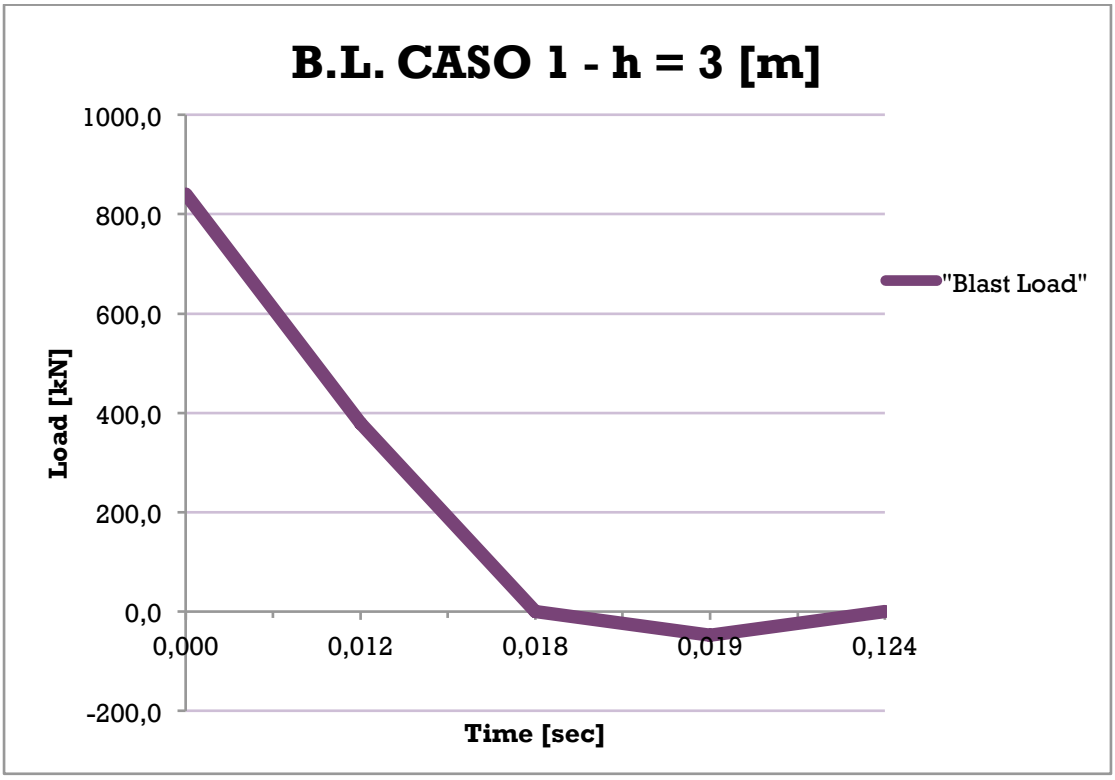

Figure 12 – Case 1 Load Function

CASE 2

- ***Column h = 5 [m] (TNTeq = 500 [kg] and r = 20 [m])***

Time [sec]	Load [kN]
0,00	2760,64
0,010	1064,89
0,016	0,00
0,018	-100
0,150	0,00

Table 13 – Case 2 Time- Load Values

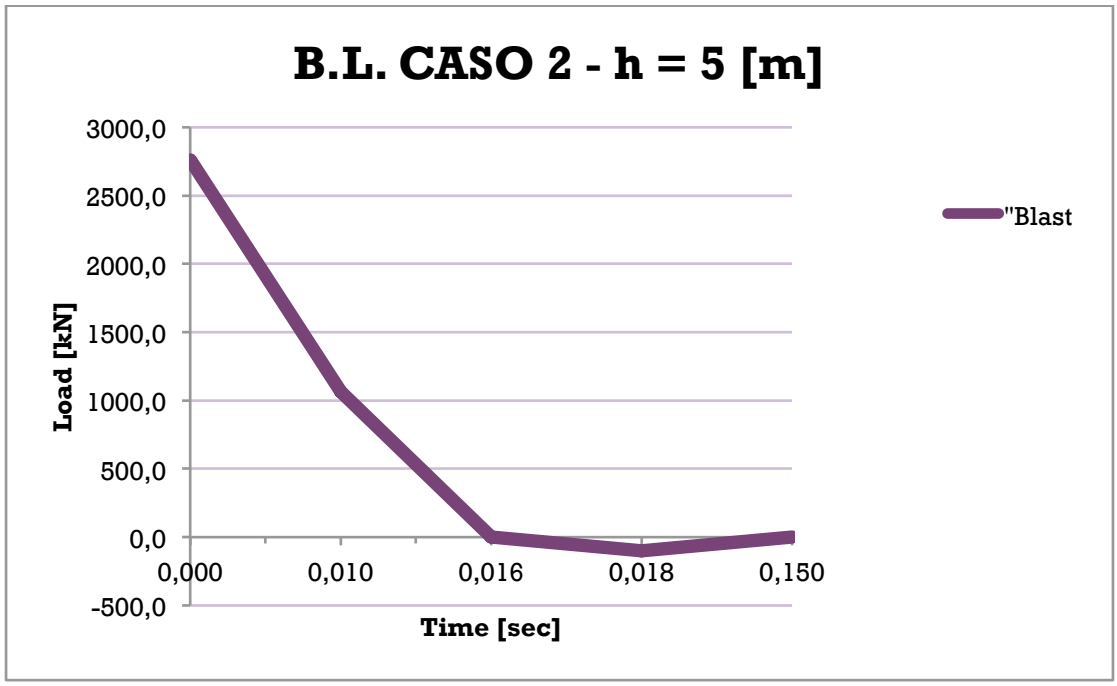

Figure 13 – Case 2 Load Function

- ***Column h = 4 [m] (TNTeq = 500 [kg] and r = 20 [m])***

Time [sec]	Load [kN]
0,00	2208,51
0,010	851,91
0,016	0,00
0,018	-80,00
0,150	0,00

Table 14 – Case 2 Time- Load Values

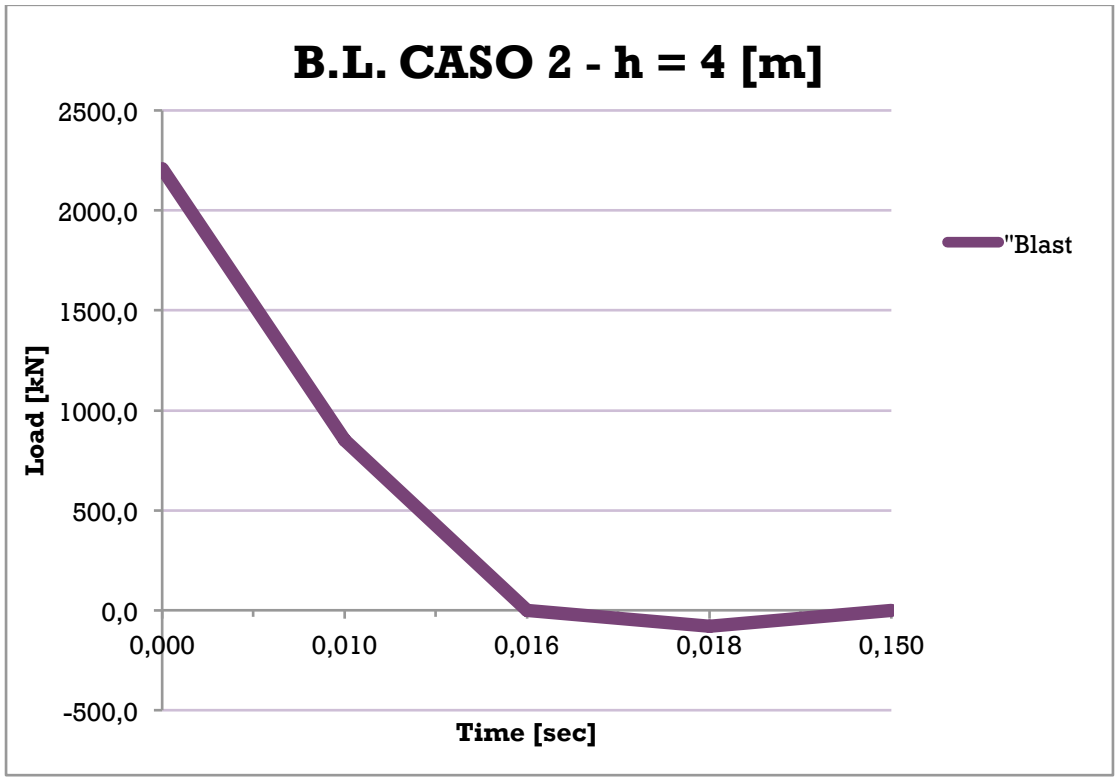

Figure 14 – Case 2 Load Function

- ***Column h = 3 [m] (TNTeq = 500 [kg] and r = 20 [m])***

Time [sec]	Load [kN]
0,00	1656,38
0,010	638,84
0,016	0,00
0,018	-60,00
0,150	0,00

Table 15 – Case 2 Time- Load Values

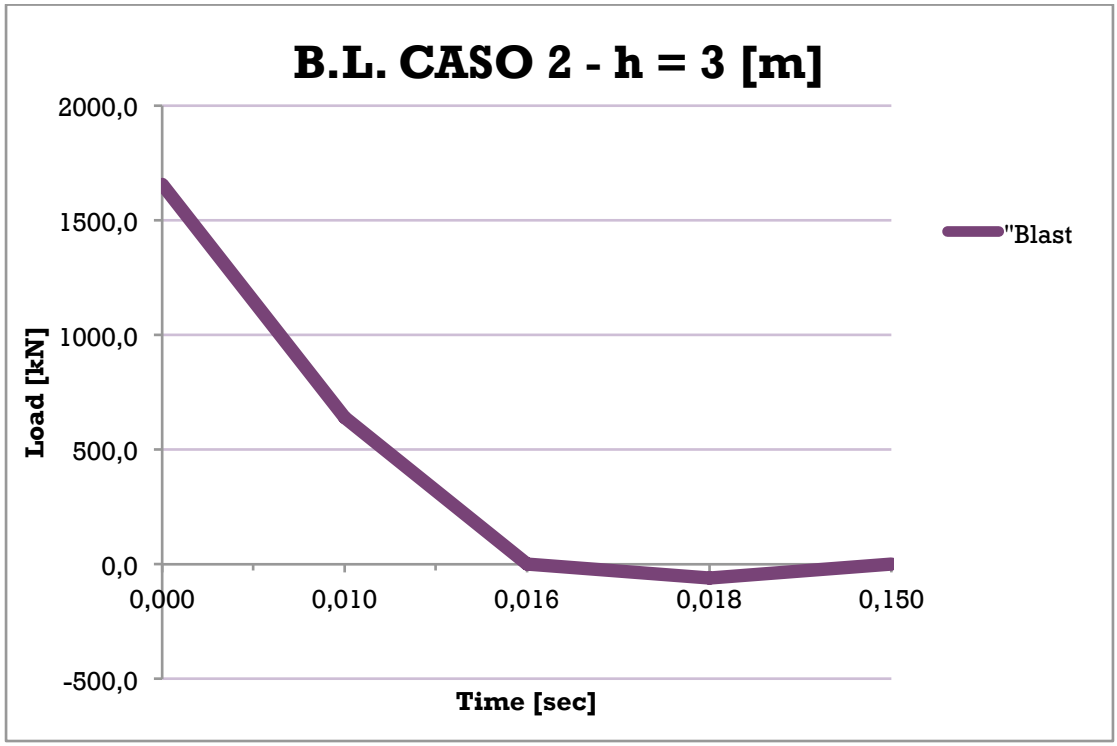

Figure 15 – Case 2 Load Function

CASE 3

- ***Column h = 5 [m] (TNTeq = 750 [kg] and r = 20 [m])***

Time [sec]	Load [kN]
0,00	4065,94
0,009	1428,18
0,015	0,00
0,017	-125,00
0,156	0,00

Table 16 – Case 3 Time- Load Values

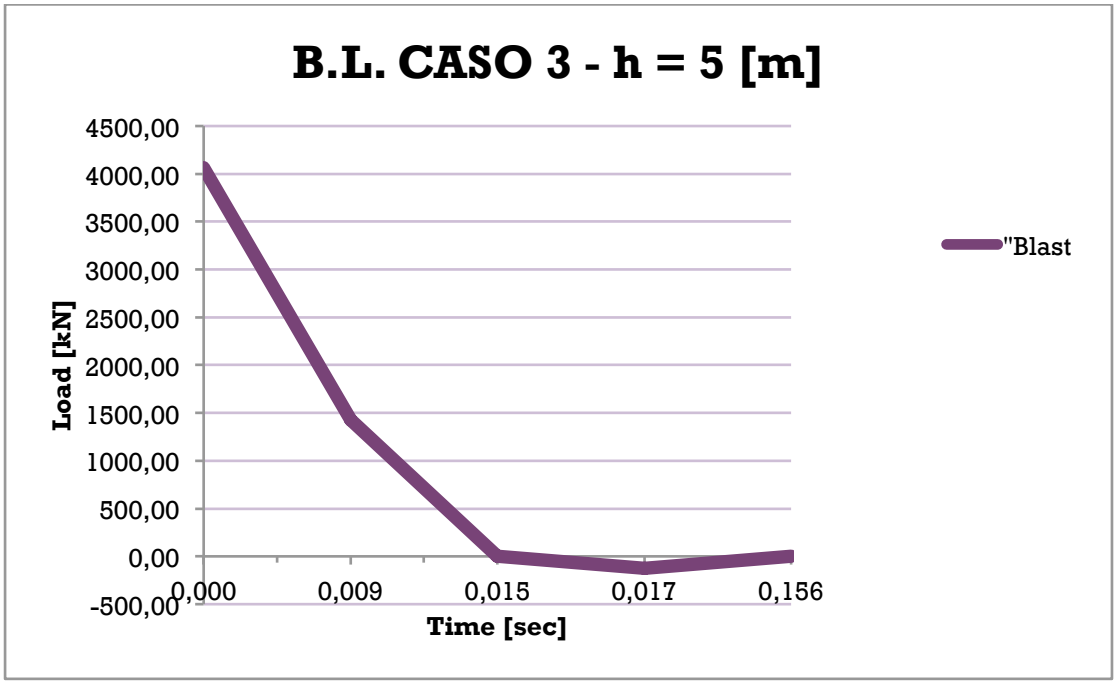

Figure 16 – Case 3 Load Function

- ***Column h = 4 [m] (TNTeq = 750 [kg] and r = 20 [m])***

Time [sec]	Load [kN]
0,00	3252,00
0,009	1142,55
0,015	0,00
0,017	-100,00
0,156	0,00

Table 17 – Case 3 Time- Load Values

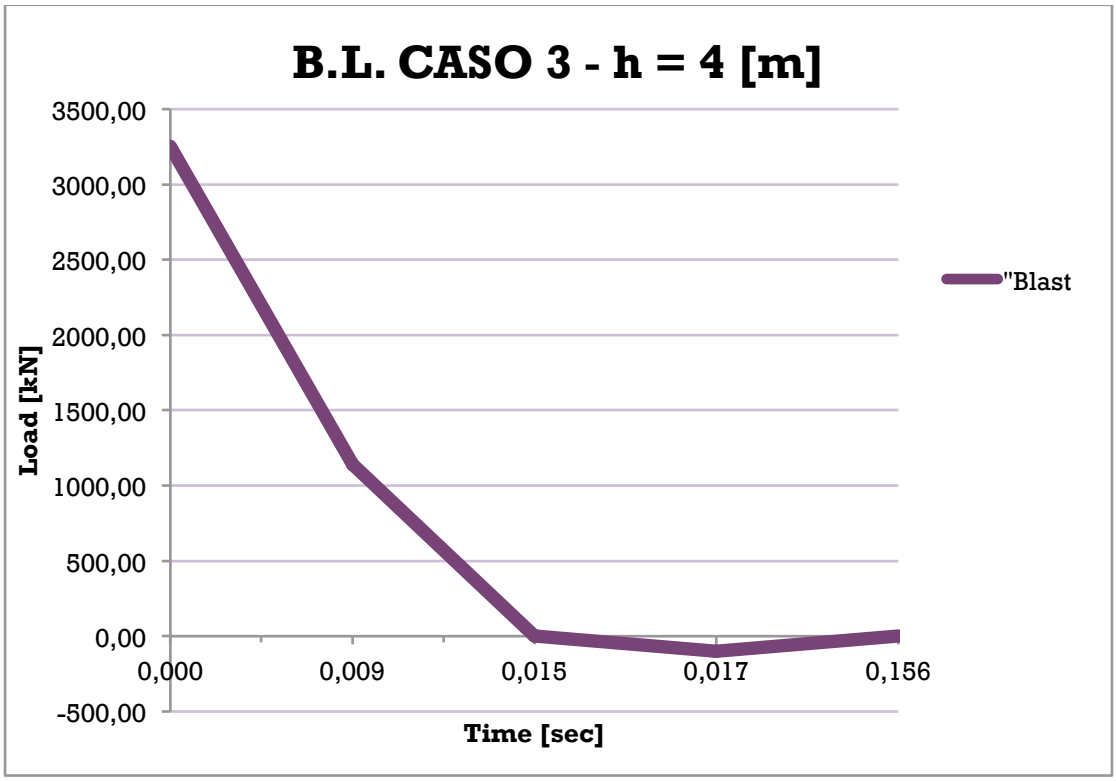

Figure 17 – Case 3 Load Function

- ***Column h = 3 [m] (TNTeq = 750 [kg] and r = 20 [m])***

Time [sec]	Load [kN]
0,00	2439,56
0,009	856,91
0,015	0,00
0,017	-75,00
0,156	0,00

Table 18 – Case 3 Time- Load Values

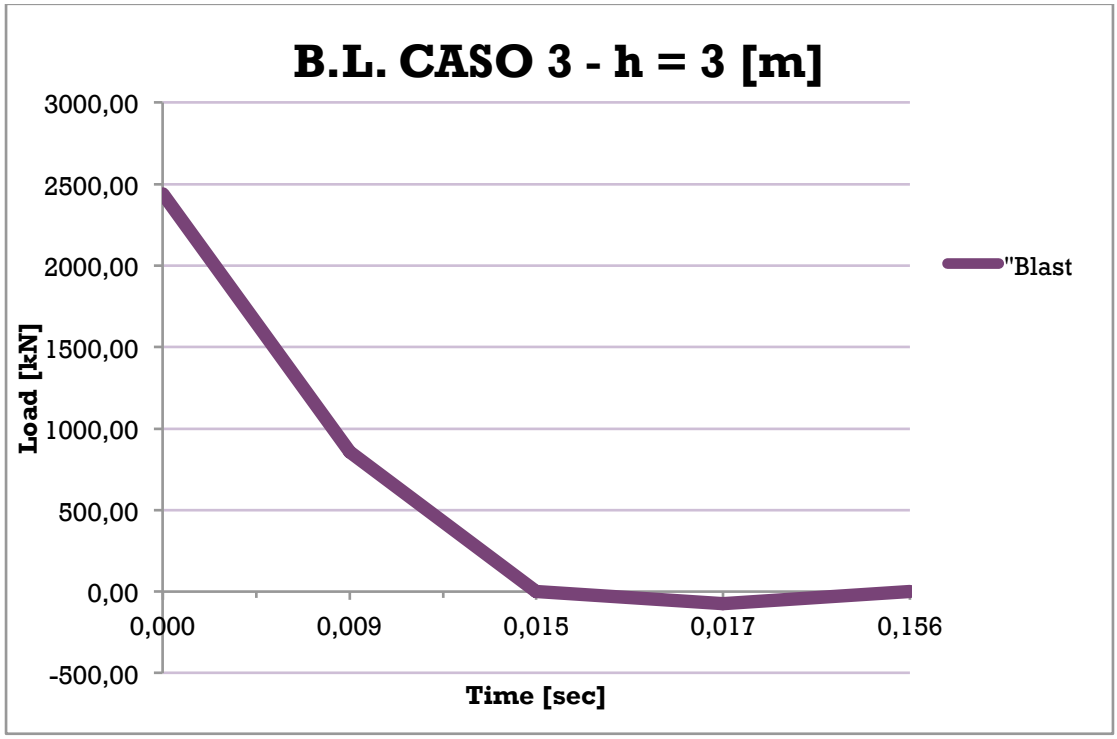

Figure 18 – Case 3 Load Function

CASE 4

- ***Column h = 5 [m] (TNTeq = 250 [kg] and r = 50 [m])***

Time [sec]	Load [kN]
0,00	134,71
0,017	100,23
0,023	0,00
0,031	-32,50
0,130	0,00

Table 19 – Case 4 Time- Load Values

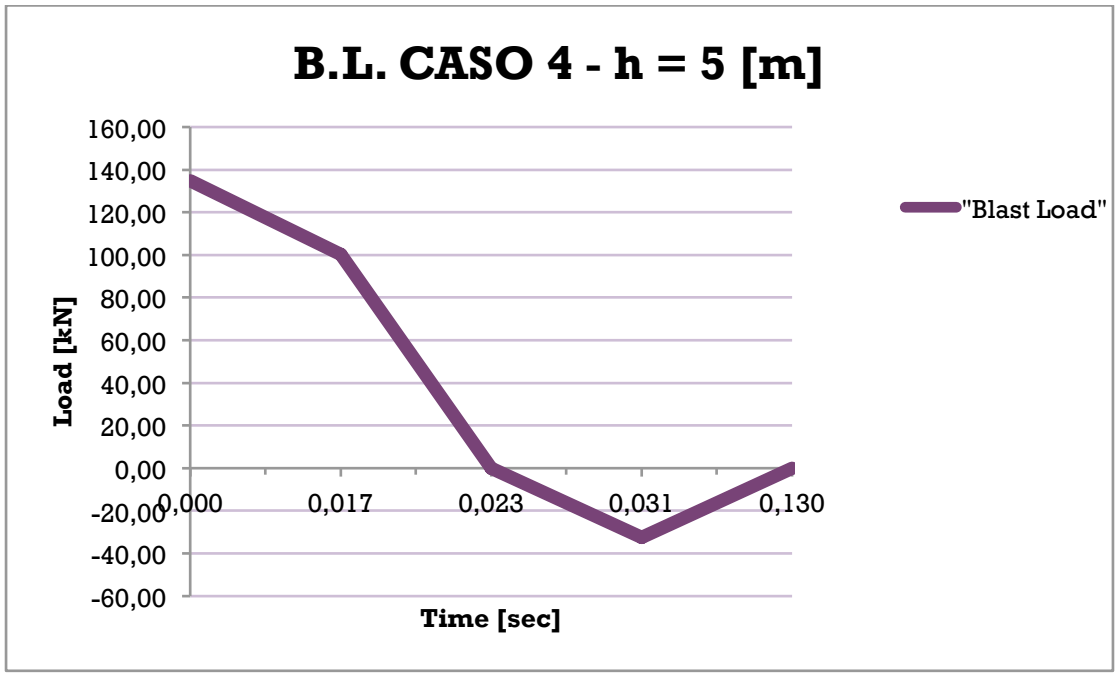

Figure 19 – Case 4 Load Function

- ***Column h = 4 [m] (TNTeq = 250 [kg] and r = 50 [m])***

Time [sec]	Load [kN]
0,00	107,77
0,017	80,18
0,023	0,00
0,031	-26,00
0,130	0,00

Table 20 – Case 4 Time- Load Values

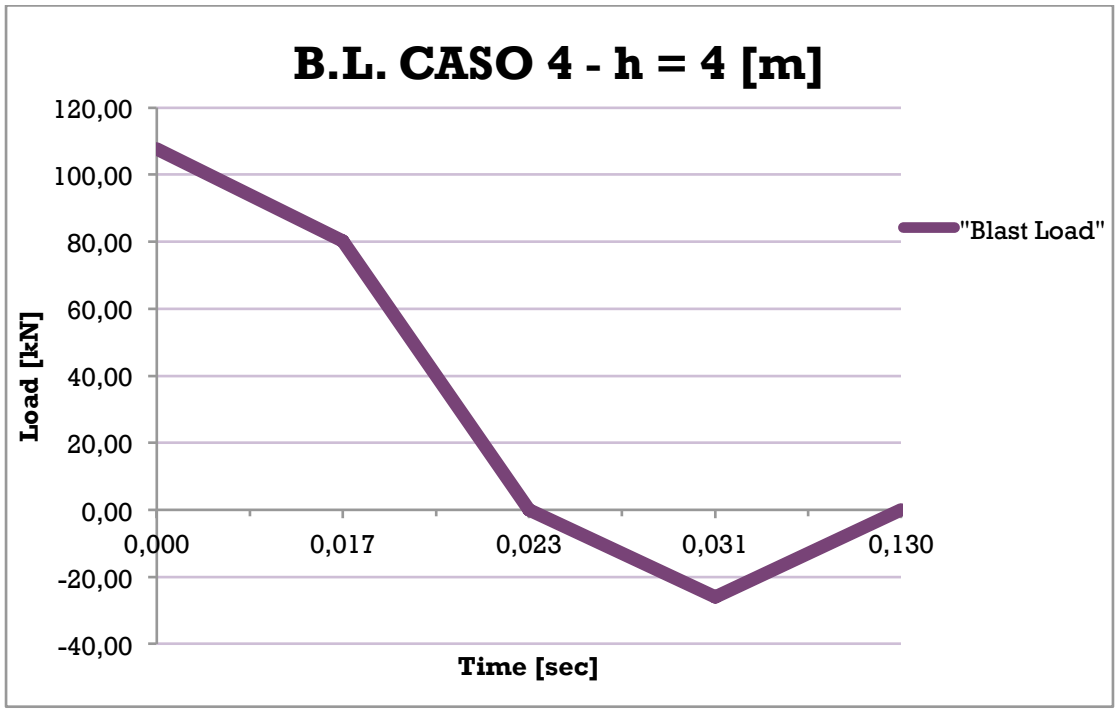

Figure 20 – Case 4 Load Function

- ***Column h = 3 [m] (TNTeq = 250 [kg] and r = 50 [m])***

Time [sec]	Load [kN]
0,00	80,83
0,017	60,14
0,023	0,00
0,031	-19,50
0,130	0,00

Table 21 – Case 4 Time- Load Values

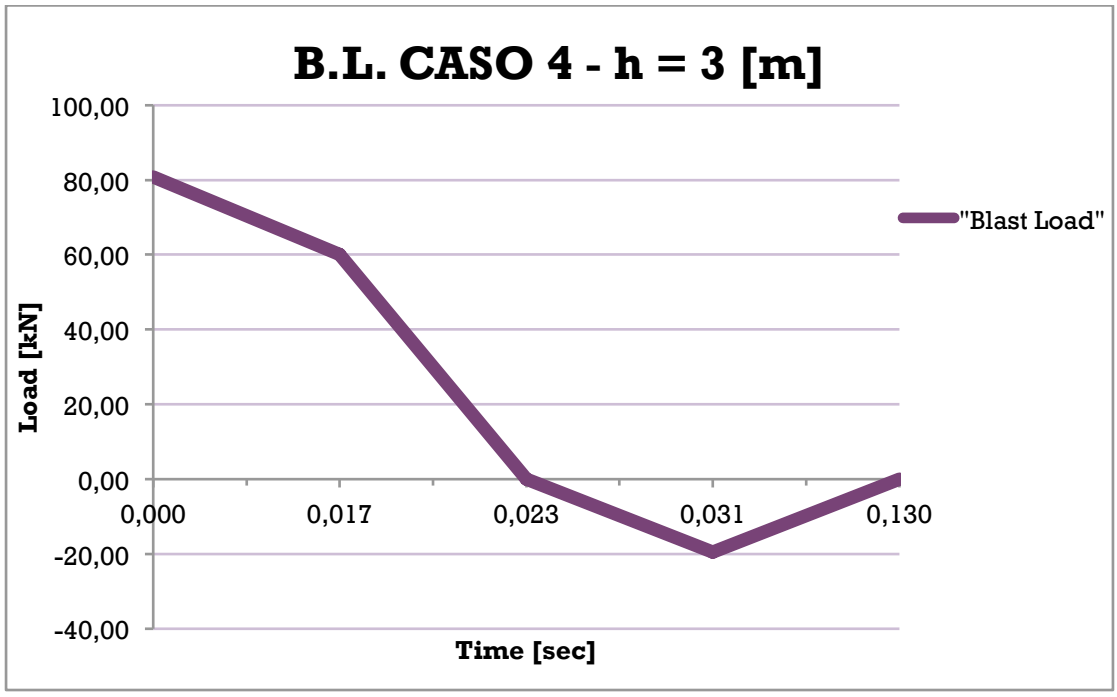

Figure 21 – Case 4 Load Function

CASE 5

- ***Column h = 5 [m] (TNTeq = 500 [kg] and r = 50 [m])***

Time [sec]	Load [kN]
0,00	211,37
0,017	143,33
0,026	0,00
0,034	-40,00
0,160	0,00

Table 22 – Case 5 Time- Load Values

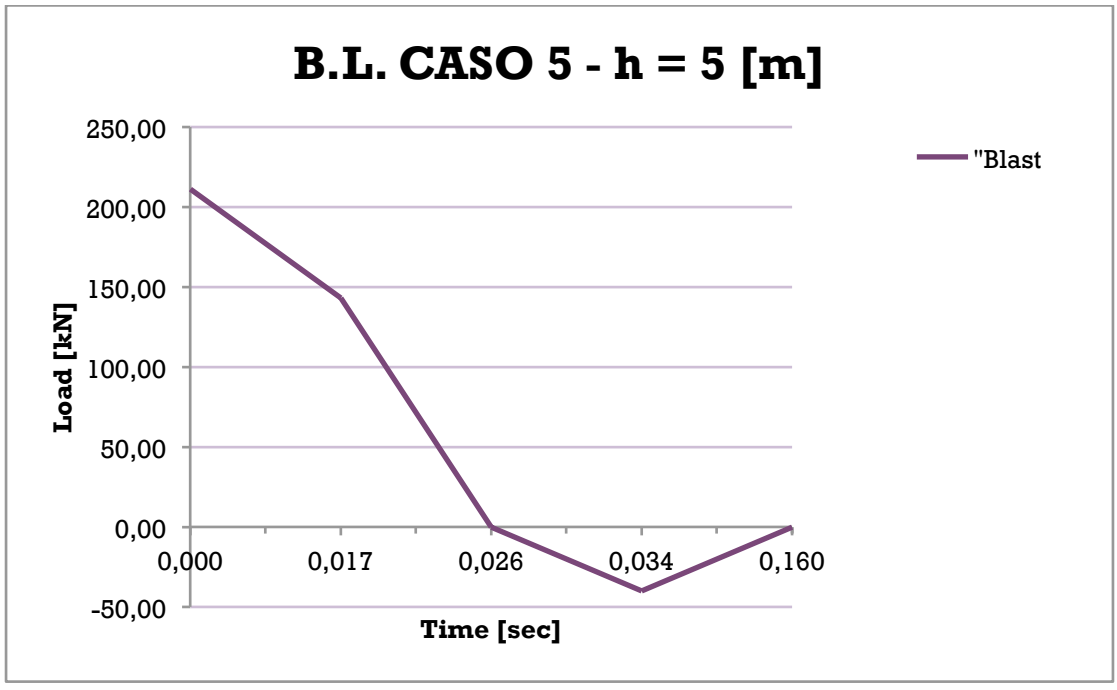

Figure 22 – Case 5 Load Function

- ***Column h = 4 [m] (TNTeq = 500 [kg] and r = 50 [m])***

Time [sec]	Load [kN]
0,00	169,10
0,017	114,66
0,026	0,00
0,034	-32,00
0,160	0,00

Table 23 – Case 5 Time- Load Values

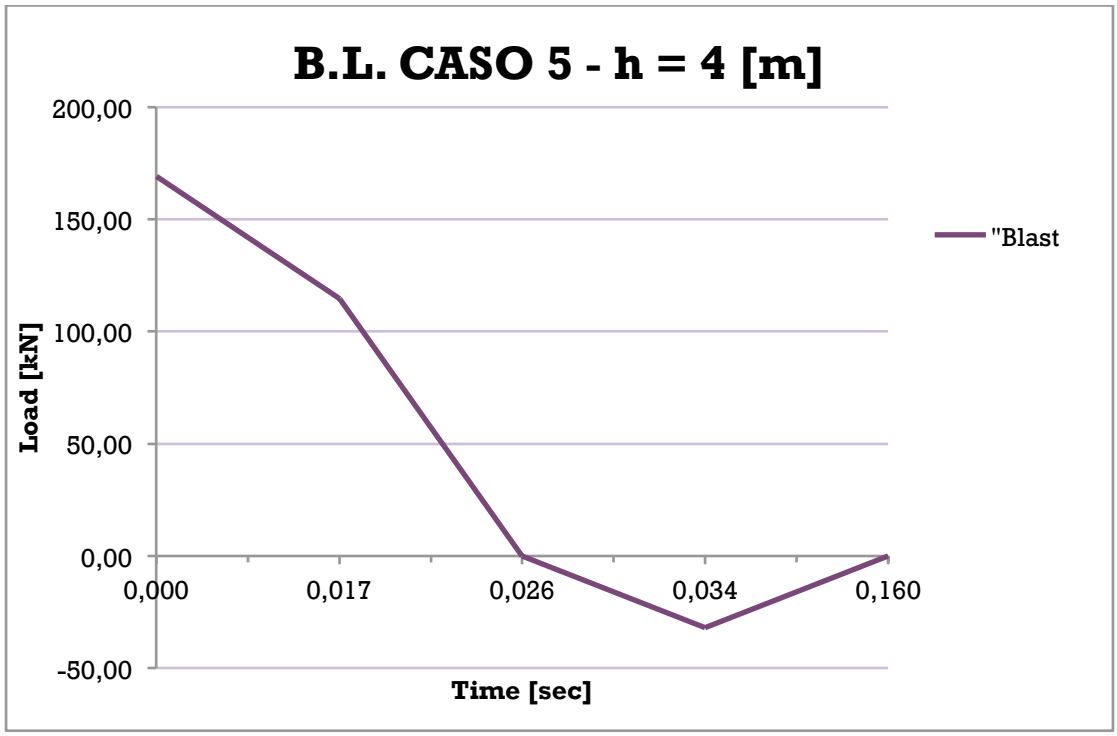

Figure 23 – Case 5 Load Function

- ***Column h = 3 [m] (TNTeq = 500 [kg] and r = 50 [m])***

Time [sec]	Load [kN]
0,00	126,82
0,017	86,00
0,026	0,00
0,034	-24,00
0,160	0,00

Table 24 – Case 5 Time- Load Values

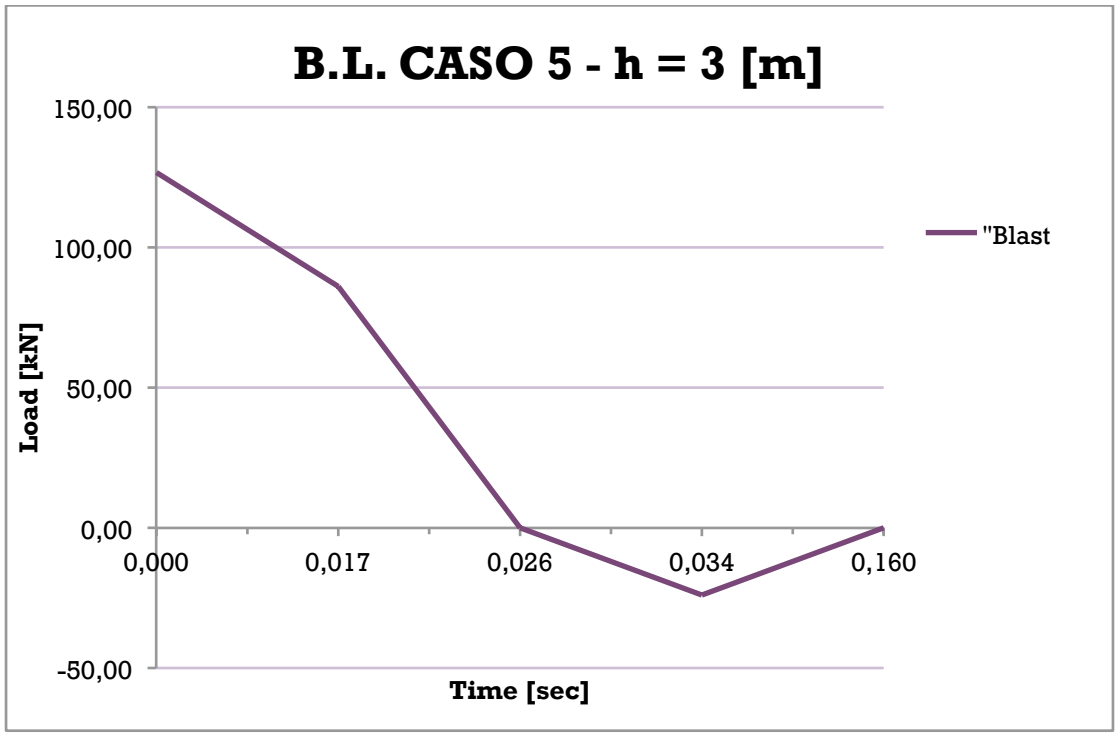

Figure 24 – Case 5 Load Function

CASE 6

- ***Column h = 5 [m] (TNTeq = 750 [kg] and r = 50 [m])***

Time [sec]	Load [kN]
0,00	292,81
0,016	185,53
0,028	0,00
0,034	-45,00
0,181	0,00

Table 25 – Case 6 Time- Load Values

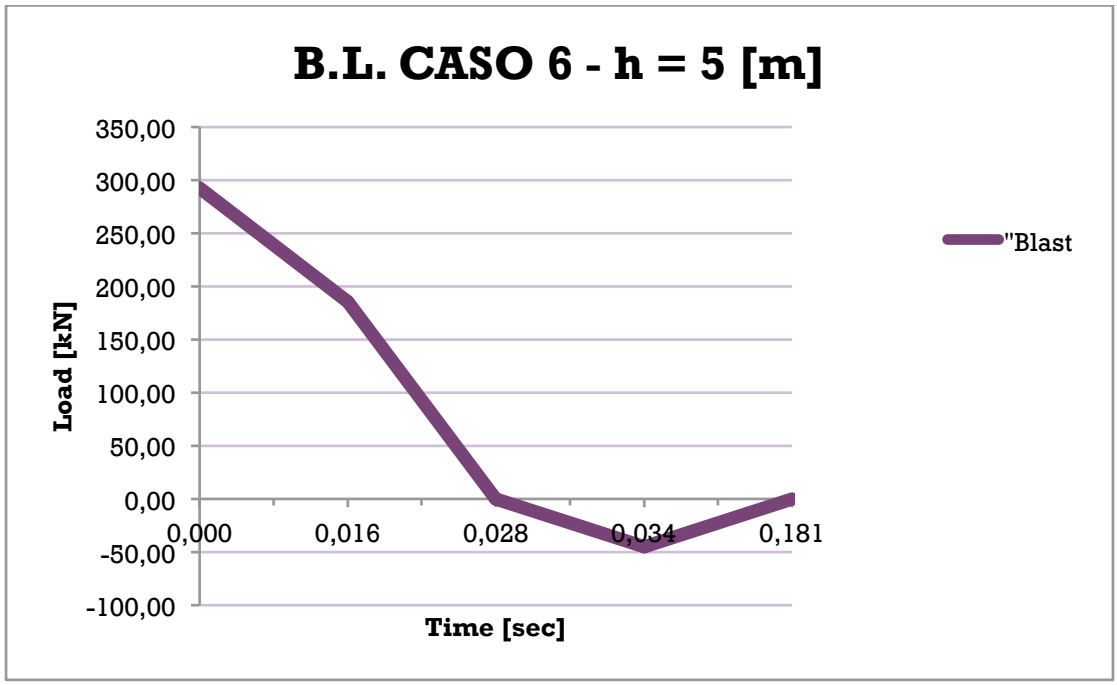

Figure 25 – Case 6 Load Function

- ***Column h = 4 [m] (TNTeq = 750 [kg] and r = 50 [m])***

Time [sec]	Load [kN]
0,00	234,25
0,016	148,43
0,028	0,00
0,034	-36,00
0,181	0,00

Table 26 – Case 6 Time- Load Values

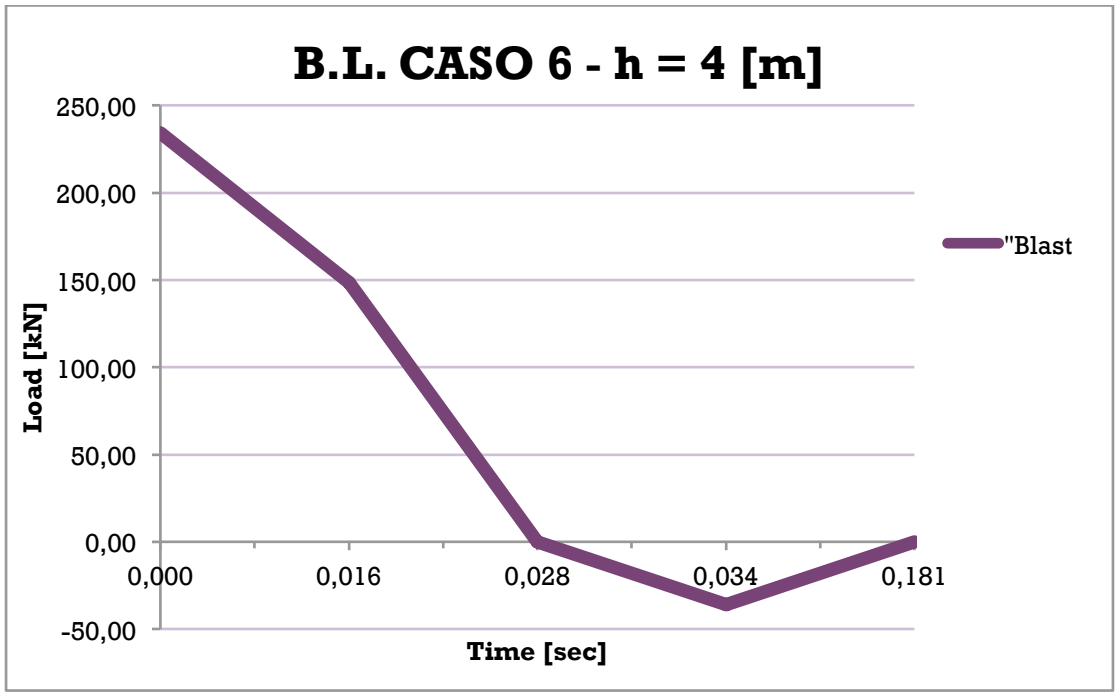

Figure 26 – Case 6 Load Function

- ***Column h = 3 [m] (TNTeq = 750 [kg] and r = 50 [m])***

Time [sec]	Load [kN]
0,00	175,69
0,016	111,32
0,028	0,00
0,034	-27,00
0,181	0,00

Table 27 – Case 6 Time- Load Values

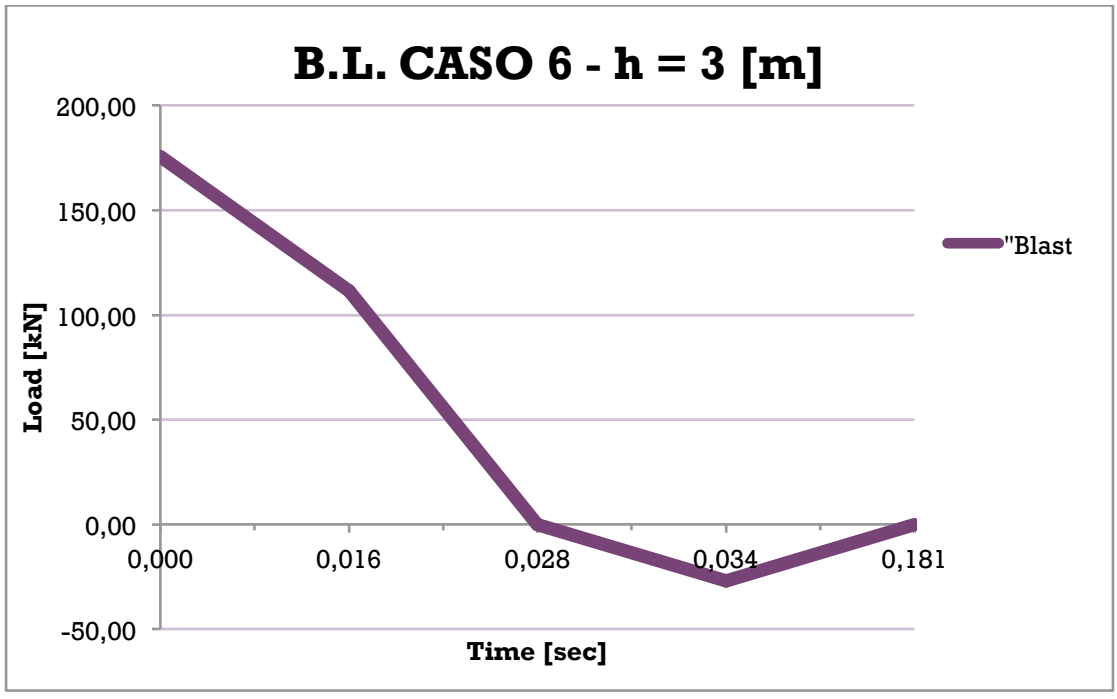

Figure 27 – Case 6 Load Function

CASE 7

- ***Column h = 5 [m] (TNTeq = 130 [kg] and r = 20 [m])***

Time [sec]	Load [kN]
0,00	736,39
0,014	383,42
0,027	0,00
0,029	-62,50
0,099	0,00

Table 28 – Case 7 Time- Load Values

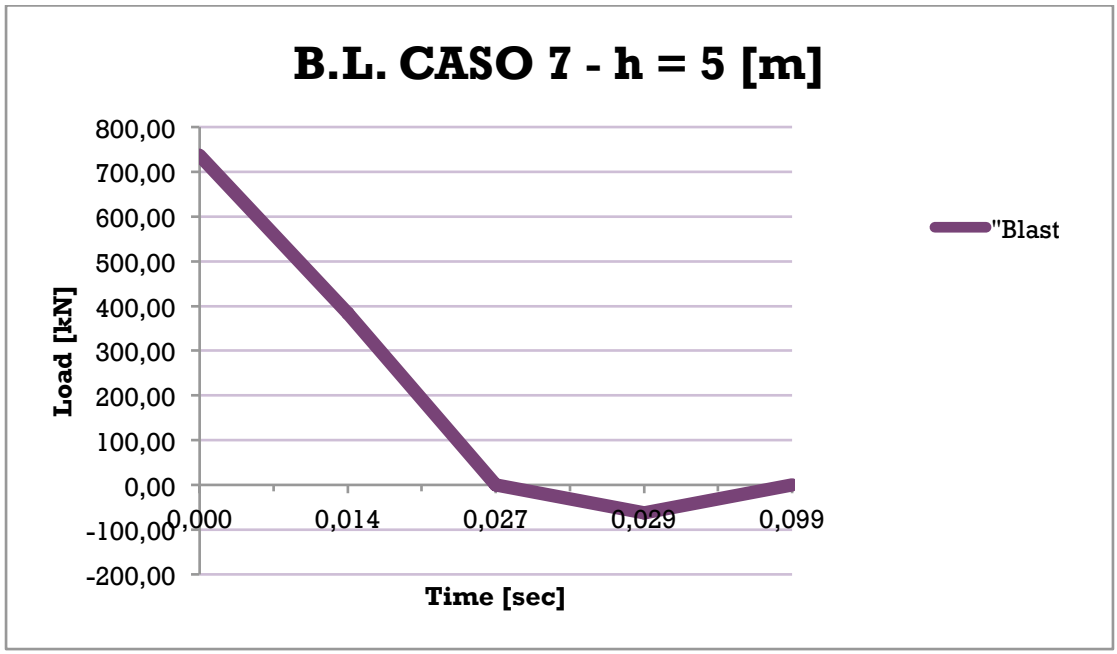

Figure 28 – Case 7 Load Function

- ***Column h = 4 [m] (TNTeq = 130 [kg] and r = 20 [m])***

Time [sec]	Load [kN]
0,00	589,11
0,014	306,73
0,027	0,00
0,029	-50,00
0,099	0,00

Table 29 – Case 7 Time- Load Values

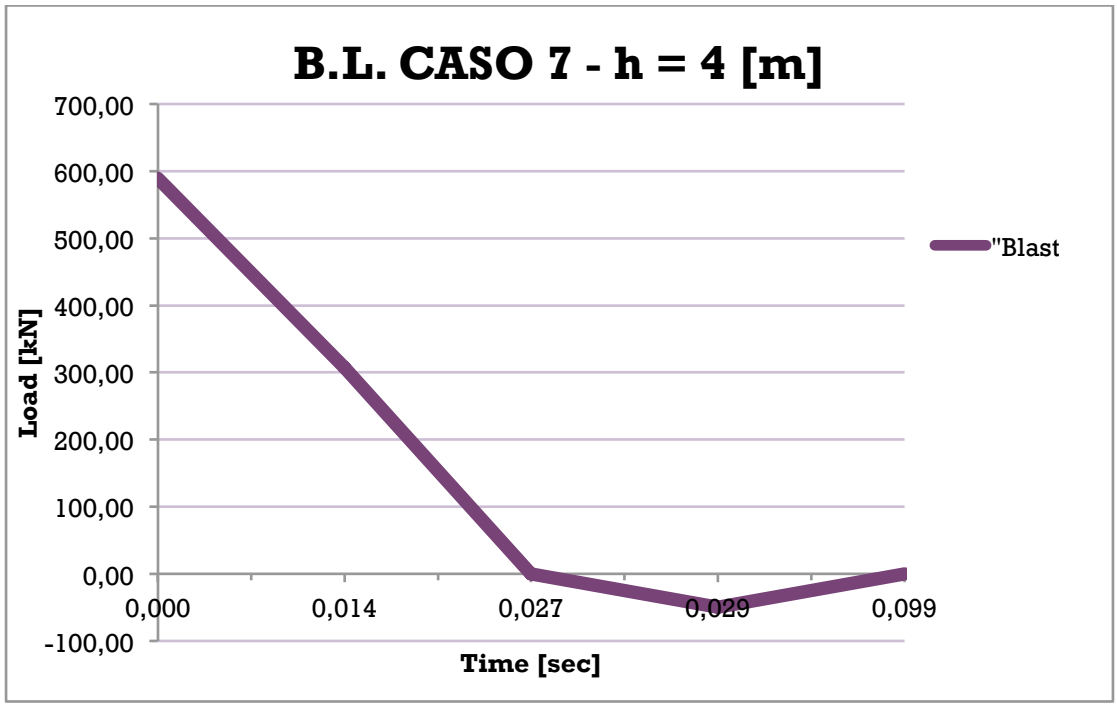

Figure 29 – Case 7 Load Function

- ***Column h = 3 [m] (TNTeq = 130 [kg] and r = 20 [m])***

Time [sec]	Load [kN]
0,00	441,83
0,014	230,05
0,027	0,00
0,029	-37,50
0,099	0,00

Table 30 – Case 7 Time- Load Values

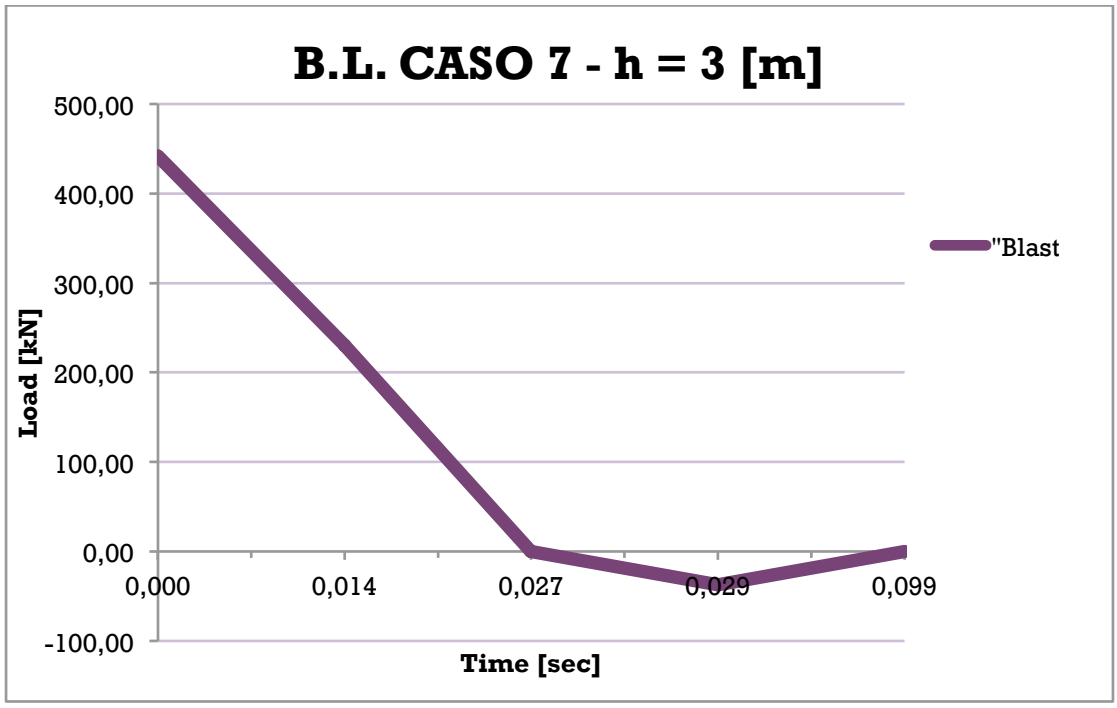

Figure 30 – Case 7 Load Function

CASE 8

- ***Column h = 5 [m] (TNTeq = 130 [kg] and r = 50 [m])***

Time [sec]	Load [kN]
0,00	101,23
0,017	79,85
0,021	0,00
0,027	-22,5
0,107	0,00

Table 31 – Case 8 Time- Load Values

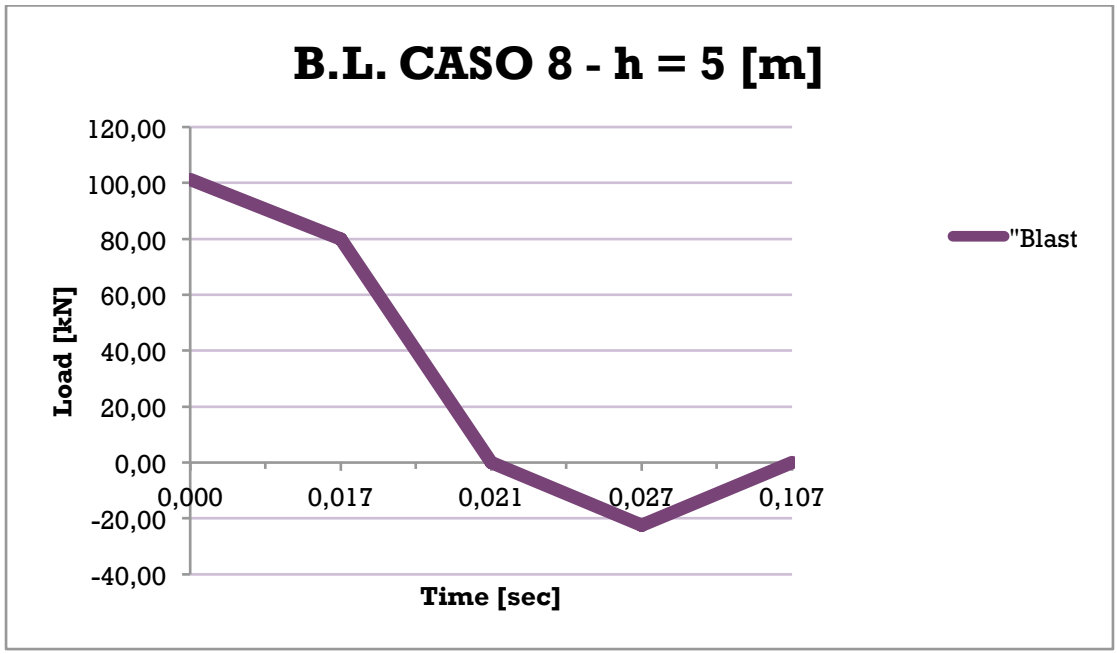

Figure 31 – Case 8 Load Function

- ***Column h = 4 [m] (TNTeq = 130 [kg] and r = 50 [m])***

Time [sec]	Load [kN]
0,00	80,99
0,017	63,88
0,021	0,00
0,027	-18,00
0,107	0,00

Table 32 – Case 8 Time- Load Values

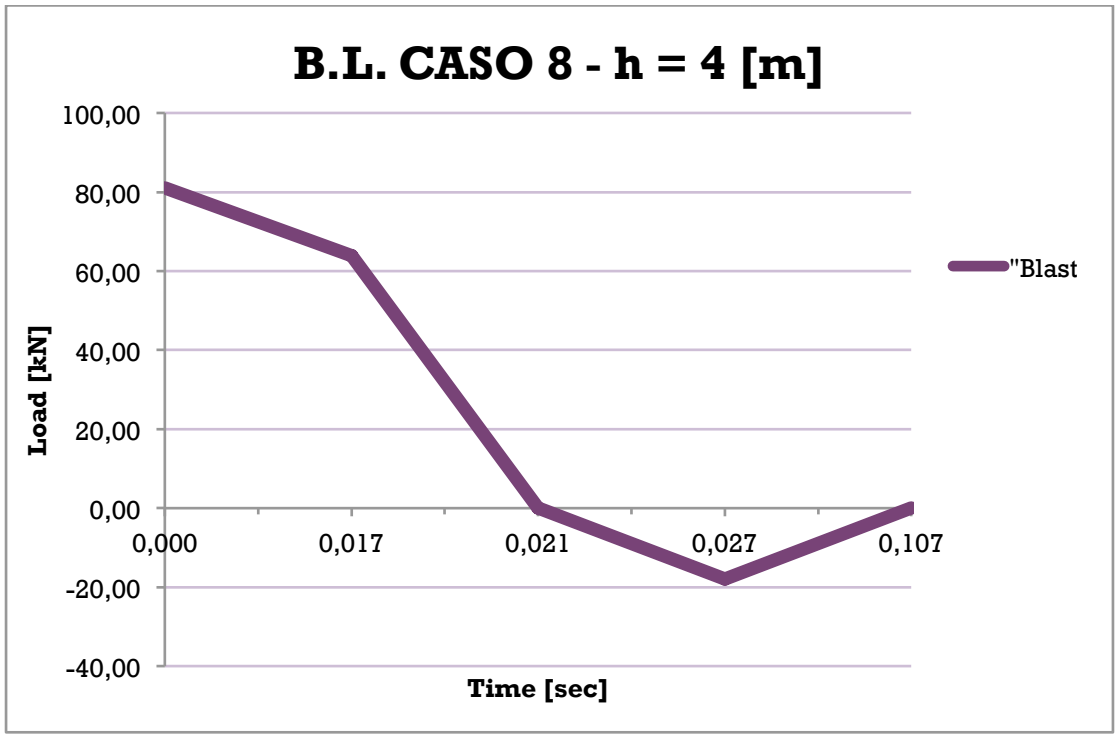

Figure 32 – Case 8 Load Function

- ***Column h = 3 [m] (TNTeq = 130 [kg] and r = 50 [m])***

Time [sec]	Load [kN]
0,00	60,74
0,017	47,91
0,021	0,00
0,027	-13,50
0,107	0,00

Table 33 – Case 8 Time- Load Values

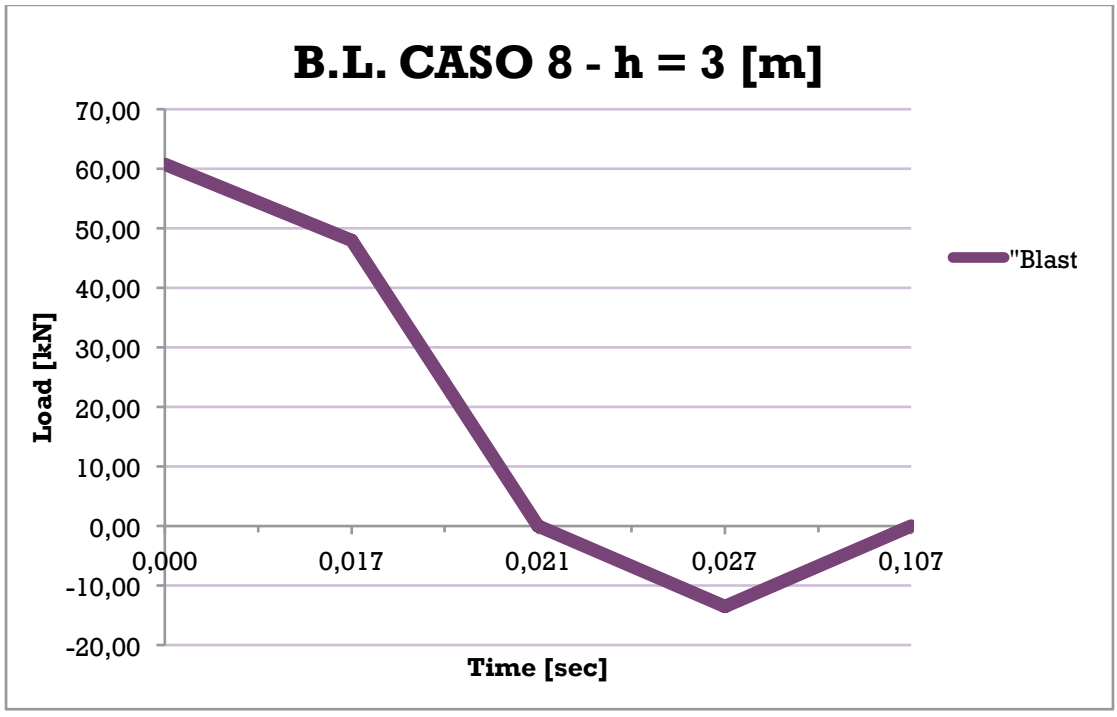

Figure 33 – Case 8 Load Function

CASE 9

- ***Column h = 5 [m] (TNTeq = 130 [kg] and r = 10 [m])***

Time [sec]	Load [kN]
0,00	5517,67
0,008	1796,49
0,016	0,00
0,017	-150,00
0,085	0,00

Table 34 – Case 9 Time- Load Values

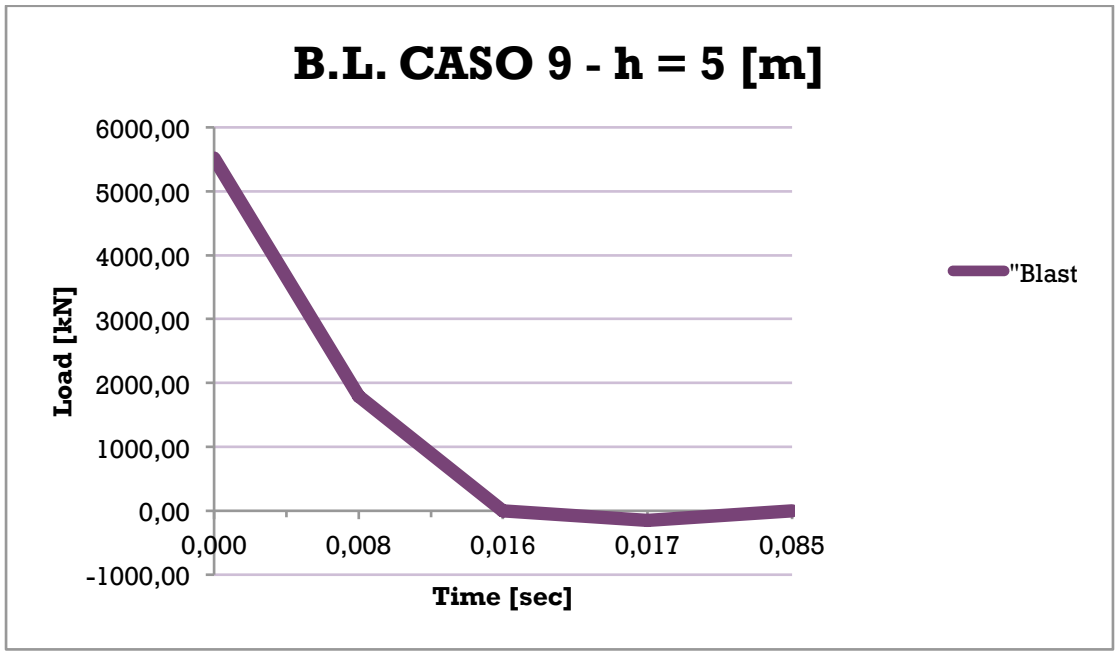

Figure 34 – Case 9 Load Function

- ***Column h = 4 [m] (TNTeq = 130 [kg] and r = 10 [m])***

Time [sec]	Load [kN]
0,00	4414,14
0,008	1437,19
0,016	0,00
0,017	-120,00
0,085	0,00

Table 35 – Case 9 Time- Load Values

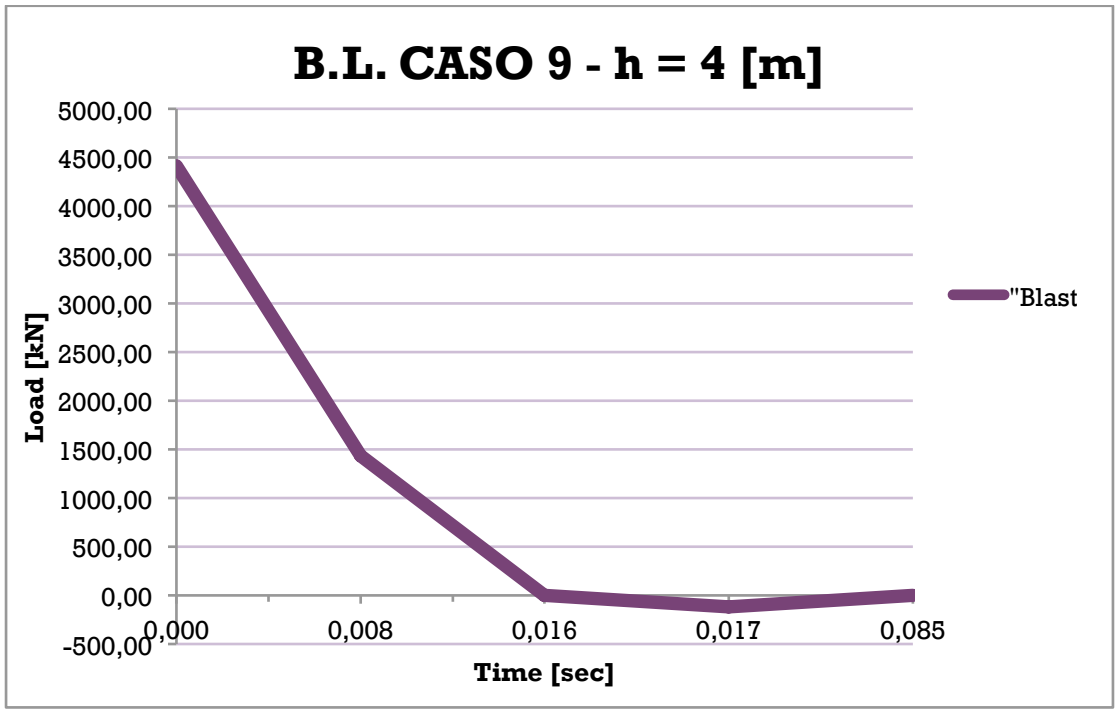

Figure 35 – Case 9 Load Function

- ***Column h = 3 [m] (TNTeq = 130 [kg] and r = 10 [m])***

Time [sec]	Load [kN]
0,00	3310,60
0,008	1077,90
0,016	0,00
0,017	-90,00
0,085	0,00

Table 36 – Case 9 Time- Load Values

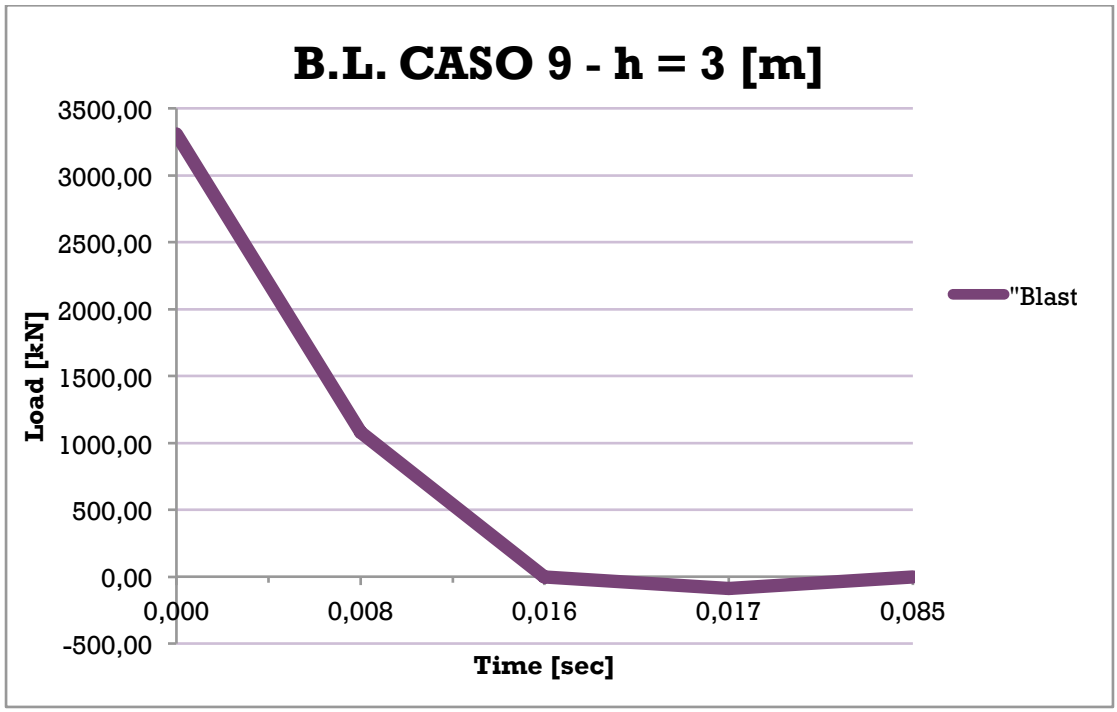

Figure 36 – Case 9 Load Function

CASE 10

- ***Column h = 5 [m] (TNTeq = 15 [kg] and r = 5 [m])***

Time [sec]	Load [kN]
0,00	5123,36
0,008	1699,41
0,012	0,00
0,013	-150,00
0,042	0,00

Table 37 – Case 10 Time- Load Values

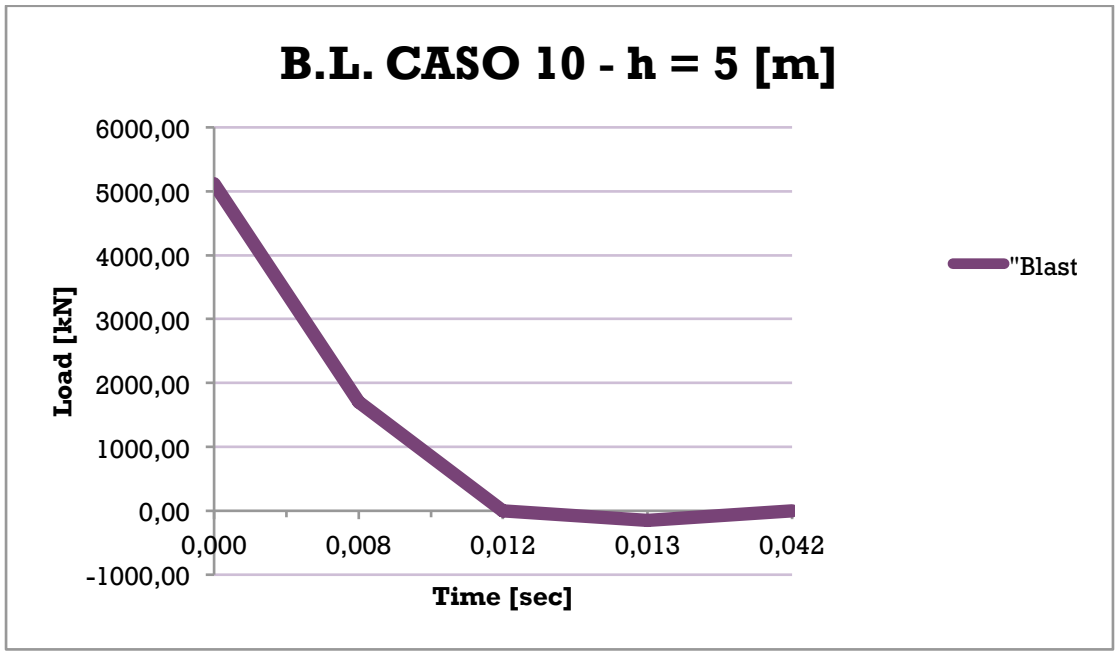

Figure 37 – Case 10 Load Function

- ***Column h = 4 [m] (TNTeq = 15 [kg] and r = 5 [m])***

Time [sec]	Load [kN]
0,00	4098,69
0,008	1359,63
0,012	0,00
0,013	-120,00
0,042	0,00

Table 38 – Case 10 Time- Load Values

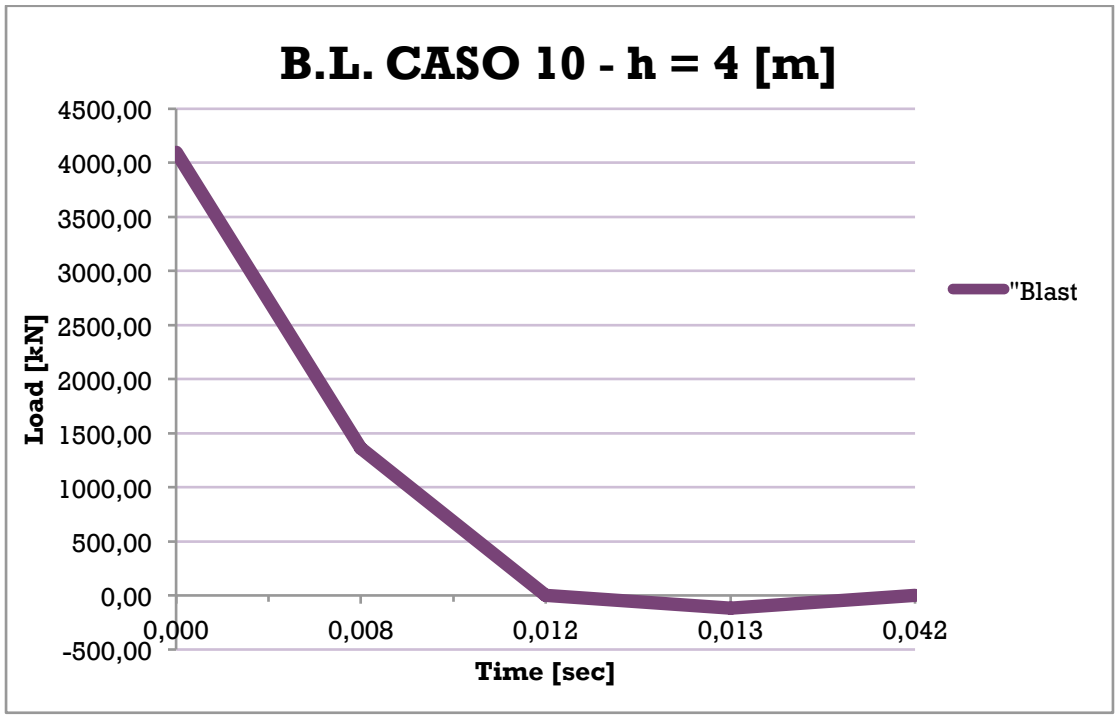

Figure 38 – Case 10 Load Function

- ***Column h = 3 [m] (TNTeq = 15 [kg] and r = 5 [m])***

Time [sec]	Load [kN]
0,00	3074,01
0,008	1019,64
0,012	0,00
0,013	-90,00
0,042	0,00

Table 39 – Case 10 Time- Load Values

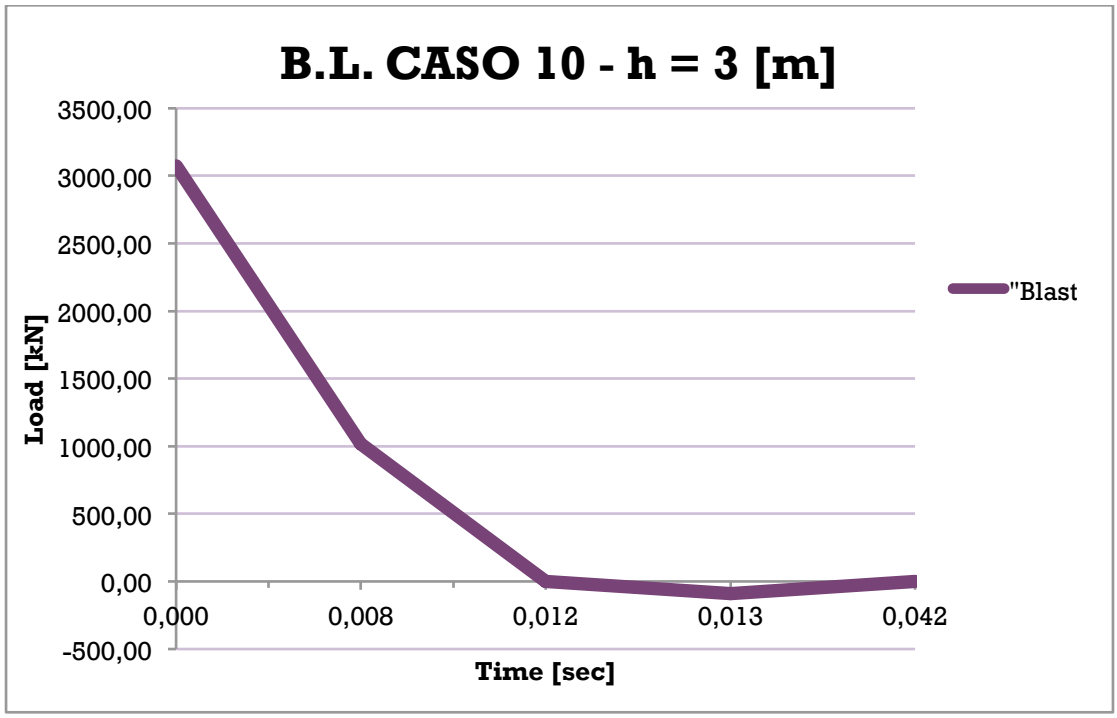

Figure 39 – Case 10 Load Function

Chapter

4

Materials

1. Introduction

Reinforced Concrete (RC) is one of the most commonly used building materials nowadays.It is a composite material made of plain concrete, which has relatively high compressive strength but low tensile strength, and steel bars embedded in the concrete, which can provide the needed strength in tension. The economy, efficiency, strength and stiffness of RC make it an attractive material for a wide range of structural engineering applications, such as nuclear power-plants, bridges, cooling towers and offshore platforms. For RC to be used as a structural material, it should satisfy special criteria including:

- Strength and Stiffness;
- Safety and Appearance;
- Economy.

By applying the principles of structural analysis, the laws of equilibrium and the consideration of the mechanical properties of the components studied; RC design procedure should yield a sufficient margin of safety against collapse under ultimate loads. Serviceability analysis is conducted to control the deflections under service loads and to limit the crack width to an acceptable level for the structural component to perform and appear safe and inhabitable for the human eye. Economical considerations are satisfied by optimizing the usage of steel/concrete quantities to account for the difference in unit costs of steel and concrete.

The ultimate objective of design is the safety and economy of the RC structural member. The design process is usually based on a linear elastic analysis to calculate the internal forces in the member which are then used to design the reinforcement and the details of the member using some code provision. Codes are usually based on empirical approaches that utilize experimental data and provide design rules to satisfy safety and serviceability requirements. Although the design of RC structures based on linear-elastic stress analysis is adequate and reliable in many cases, the extent and impact of a disaster in terms of human and economical losses in the event of structural failure of large scale modern structures necessitate more careful and detailed structural safety analysis. Thus, Nonlinear Finite Element Analysis (NFEA) is often required to obtain detailed information regarding the ultimate loading capacity and the post-failure behavior of RC structures.

The complex behavior of concrete, which arises from the composite nature of the material, is characterized by a reduction of the load carrying capacity with increasing deformations after reaching a certain limit load. This global behavior is usually caused by a material behavior which is described as strain softening and occurs in tension and in compression. This necessitates the development of appropriate constitutive models to describe such behavior.

In RC, the response of the structure is even more complicated. In general a number of cracks will develop in the structure due to the bond action between concrete and reinforcement. This results in a redistribution of the tensile loads from concrete to the reinforcement. This phenomenon is called tension-stiffening, because the response is stiffer than the response with a brittle fracture approach.

The behavior of RC is highly nonlinear which is caused by mechanisms such as cracking, crushing, creep and shrinkage of concrete, but also caused by the interaction between reinforcement and concrete, where the load transferring mechanism of the interface between concrete and reinforcement plays an important role. Because all these mechanisms are interacting, it is not realistic to try to formulate a constitutive model which incorporates all these mechanisms, but a model has to be formulated to adequately describe the behavior of a structure within the range of application which has been restricted in advance. Although the constitutive models which are developed within this phenomenological approach are usually simplified representations of the real behavior of the material, it is believed that more insight can be gained by tracing the entire response of a structure in this manner, than modeling a structure with highly sophisticated material models which do not result in a converged solution after failure load and are computationally expensive and complicated.

A large variety of models have been proposed to characterize the stress-strain relation and failure behavior of RC materials. All these models have certain inherent advantages and disadvantages which depend to a large degree on their particular application and complexity. Macroscopic constitutive studies have been conducted with different levels of complexity and applicability in order to address the different aspects of the concrete material behavior. On the other hand, microscopic modeling and multi-scale modeling offer useful ways to model the material behavior, but their applicability to full-scale structural problems is still problematic, due to their requirement for huge amounts of computer resources. Therefore, further development in the macroscopic constitutive modeling of concrete is justified and needed, with the motivation of incorporating contemporary experimentally observed features of the material behavior in the modeling.

Concrete and reinforcing steel are represented herein by separate material models which are combined together using a model that describes the interaction between reinforcing steel and concrete to simulate the overall behavior of the composite RC material. Generally an elasto-plastic damage constitutive model is used to describe the behavior of concrete, while steel reinforcement is modeled as an elasto-plastic material with strain hardening using the classical von Mises plasticity. Bond considerations are accounted for within the steel reinforcement model. Coupling between damage and plasticity in the constitutive model is employed to capture the observed phenomenological behavior of concrete. In this combined approach, damage theory is used to model the material deterioration, while the permanent deformation and some other behavioral features of concrete can be captured using plasticity theory. All features of the two theories can be incorporated in this combined approach, making it very promising for use in constitutive modeling or RC structures.

In general in this section the author will analyze those different method of approach for the study of a reinforced concrete element, explaining for each case the theoretical approach assumed.

2. Materials

As explained before, when we study the response of loaded structures, the behavior of the material is often complex but in general can be simplified with the help of linear elastic, ideal plastic and elasto-plastic response. These simplifications usually give close approximations to the actual material response. Often these approximations are seen as potential sources of error but since comparisons between different methods are made, all using these approximation, it is disregarded in this master thesis. So that, in this chapter an introduction to the different responses is presented.

In general describing RC structures, it is possible to say that they are made up of two materials with different characteristics, namely, concrete and steel. Steel can be considered as a homogeneous material with generally well defined material properties. Concrete, on the other hand, is a heterogeneous material made up of cement, mortar and aggregates. Its mechanical properties are widely scattered and cannot be defined easily. For the convenience of analysis and design, however, concrete is often considered a homogeneous material at the macroscopic scale. Similar relations are obtained for other types of RC structural elements. This nonlinear response can be roughly divided into three ranges of behavior: the uncracked elastic stage, the crack propagation and the plastic (yielding or crushing) stage (Chen, 1982).

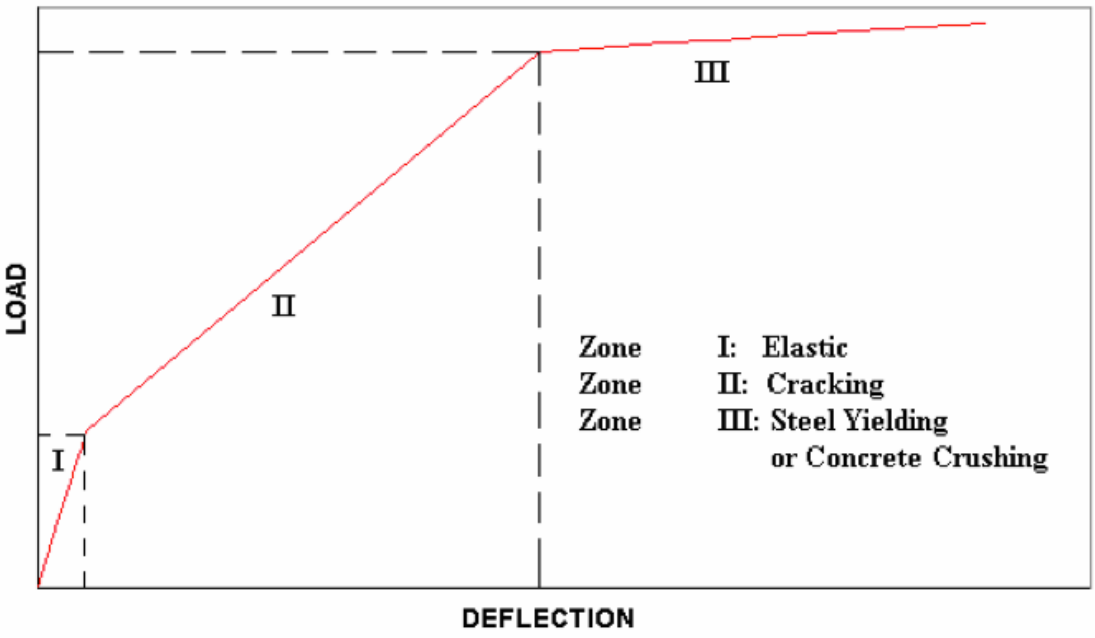

Figure 1 – Load-Deflection Graphs

The nonlinear response is caused by three major effects, namely, cracking of concrete in tension, yielding of the reinforcement or crushing of concrete in compression, and the interaction of the constituents of RC. Interaction includes bond-slip between reinforcing steel and surrounding concrete, aggregate interlock at a crack and dowel action of the reinforcing steel crossing a crack. The time-dependent effects of creep, shrinkage and temperature variation also contribute to the nonlinear behavior. Furthermore, the stress-strain relation of concrete is not only nonlinear, but is different in tension than in compression and the mechanical properties are dependent on concrete age at loading and on environmental conditions, such as ambient temperature and humidity. The material properties of concrete and steel are also strain-rate dependent to some extent.

The earliest publication on the application of the finite element method to the analysis of RC structures was presented by Ngo and Scordelis (1967). In their study, simple beams were analyzed with a model in which concrete and reinforcing steel were represented by constant strain triangular elements, and a special bond link element was used to connect the steel to the concrete and describe the bond-slip effect. A linear elastic analysis was performed on beams to determine principal stresses in concrete, stresses in steel reinforcement and bond stresses. Ngo and Scordelis (1967) reported that one of the main difficulties in constructing an analytical model for RC member is due to the composite action of steel and concrete. Prefect bonding between steel and concrete can only exist at an early stage under low load intensity. As the load is increased, cracking as well as breaking of bond inevitably occurs, and a certain amount of bond slip will take place in the beam, all of which will in turn affect the stress distributions in concrete and steel.

An adequate numerical analysis of the nonlinear behavior of RC structures is based on the coupled modeling of different inelastic processes in concrete and in reinforcement. Macroscopic representation of crystal dislocation in steel reinforcement within the framework of elastoplasticity yields a reliable prediction of deformation history of reinforcement. The realistic constitutive behavior of concrete is, however, more complex. It has resulted in the appearance of many different concepts to its theoretical description. Concrete failure is usually characterized by many macroscopic cracks. If the discrete cracks are considered, the necessary adaptation of the FE mesh to the trajectory of each crack under new load step makes the FE analysis cumbersome. Even in the two- dimensional case, it limits the applicability of conventional fracture mechanics to simple specimens with one or two cracks. Therefore, the use of models based on continuum damage mechanics and elastoplasticity have found large application in the numerical modeling of concrete fracture.

The development of analytical models for the response of RC structures is complicated due to the following factors (Kwak and Fillipou, 1997):

- RC is a composite material made up of concrete and steel, two materials with very different physical and mechanical behavior;
- Concrete exhibits nonlinearities even under low level of loading due to nonlinear material behavior, environmental effects, cracking, biaxial stiffening and strain softening;
- Reinforcing steel and concrete interact in a complex way through bond-slip and aggregate interlock.

Because of these factors and the differences in short and long term behaviors of the constituent materials, it is common practice among researches to model the short and long term response of RC members and structures based on separate material models for reinforcing steel and concrete, which are then combined along with models of interaction between the two constituents to describe the behavior of the composite RC material.

2.1 Linear Elastic Response

For linear elastic behavior there is a linear relationship between stress and strain, as can be seen in the figure…. The strain increases with increased stress and after unloading the strains will go back to zero. This means that the strain is proportional to the stress for material with linear behavior and the stress σ, can be expressed with Hooke's Law:

$$\sigma = E*\varepsilon$$

where E represents the Young's Modulus and ε is the strain.

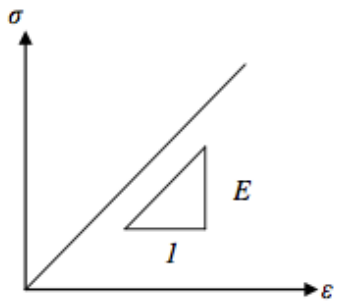

Figure 2 – Young Modulus and Strain relationship

When a structure of linear elastic material is deformed, it will gain an internal resisting force, "R", proportional to the displacement "u", as shown in the figure….. This relation is described by:

$$R = k*u$$

Where k is the structural stiffness.

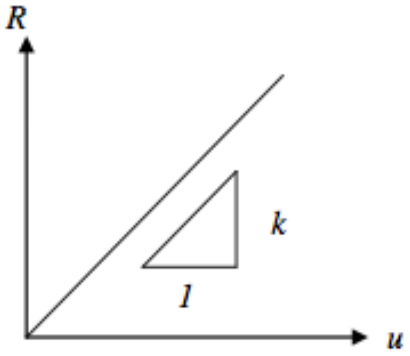

Figure 3 – Structural Stiffness

A simply supported beam with linear elastic material response will deform, when subjected to a uniformly distributed load, with the shape shown in figure below.

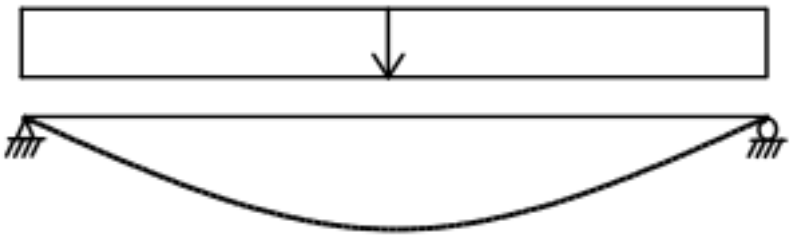

Figure 4 – Linear Elastic Deformation

2.2 Ideal Plastic Response

For material with ideal plastic behavior the deformation are zero until the strees reaches the material yield stress. When this happens the deformations will occur. As seen in figure…. In theory these deformations are infinite but in reality there are limits such as the plastic rotation capacity for beams subjected to a bending moment and the ultimate strain limit for tensioned reinforcement bars. With the external static load, F, on the structure, the internal force, R, can be expressed as:

$$R = \begin{cases} F \; for \; F < R_m \; and \; u = 0 \\ R_m \; for \; F \geq R_m \; for \; all \; u > 0 \end{cases}$$

where R_m is the maximum internal force.

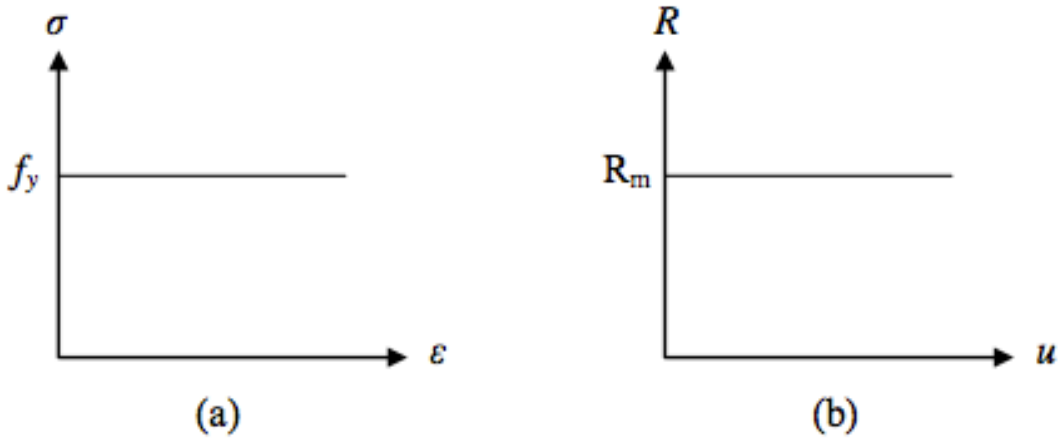

Figure 5 – Stress-Strain and Force-Deformation Graphs

A beam with ideal plastic material response will deform with the shape shown in figure below, when subjected to a uniform distributed load.

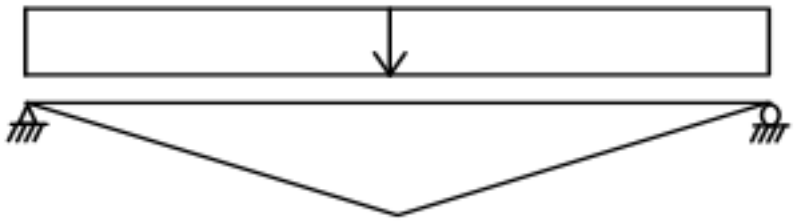

Figure 6 – Ideal Plastic Deformation

2.3 Elasto-Plastic Response

The elasto-plastic material behavior is the combination between linear elastic behavior and ideal plastic behavior, see figure…. The material is fully reversible while in its elastic phase but when the load reaches the yield limit it will initiate permanent deformations. When unloaded, the deformations will decrease, following a curve parallel to the linear elastic curve. If the body is loaded again, the deformations will follow the elastic behavior until the yield limit is reached and the plastic deformations will continue where it last ended. Whit the external load, F, on the structure, the internal force, R, can be expressed as:

$$R = \begin{cases} ku_{el} \; for \; F < R_m \\ R_m \; for \; F \geq R_m \end{cases}$$

where u_{el} is the elastic displacement.

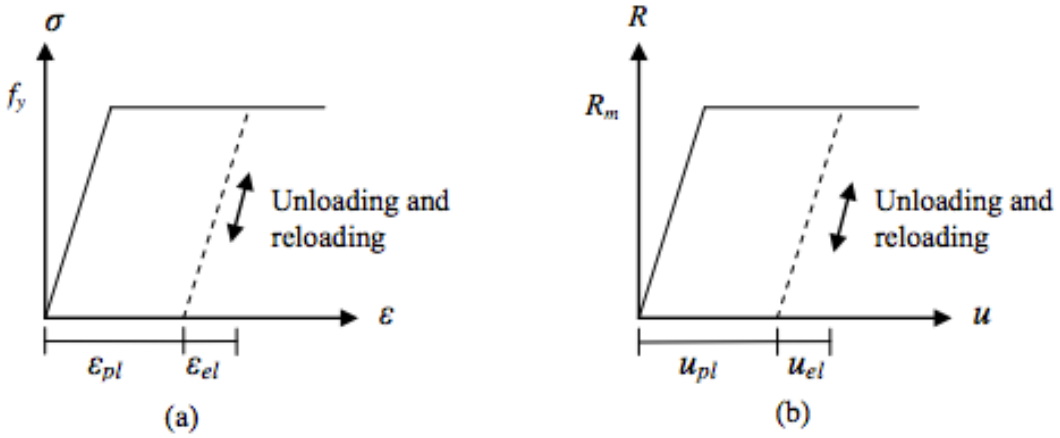

Figure 7 – Elasto-Plastic Response

2.4 Theory of Plasticity and Plastic Hinges

When looking at a beam with rectangular cross-section subjected to pure bending, it is assumed for both theory of elastic and theory of plasticity that the stress and the strain is symmetric and linearly distributed over the height of the cross-section, see figure… While the stresses in the beam are below the yield stress, the cross-section will have an elastic response according to Hooke's Law, and the elastic moment can be described as:

$$M_{el} = \frac{\sigma * I}{h/2}$$

where σ is the stress in the other fiber and I is the moment of inertia for the cross-section. For a rectangular cross-section this is calculated as:

$$I = \frac{w * h^3}{12}$$

where w is the width and h is the height of the cross-section. Combining those equations, the elastic moment can be written as:

$$M_{el} = \sigma * W_{el}$$

with

$$W_{el} = \frac{w * h^2}{6}$$

When the stress reaches the yield stress f_y, the cross-section will start to yield. If the load is further increased the beam enters an elasto-plastic behavior until the whole cross-section has yielded, see figure…. When the elasto-plastic state is reached only the inner elastic part will follow Hooke's Law. For the plastic part the strain response stays linear but the stresses are modified to not exceed the yield limit.

Just before the whole cross-section yields the maximum moment capacity, M_{pl}, is reached and so for rectangular cross-section it can be described as:

$$M_{pl} = f_y * W_{pl}$$

where

$$W_{pl} = \frac{w * h^2}{4}$$

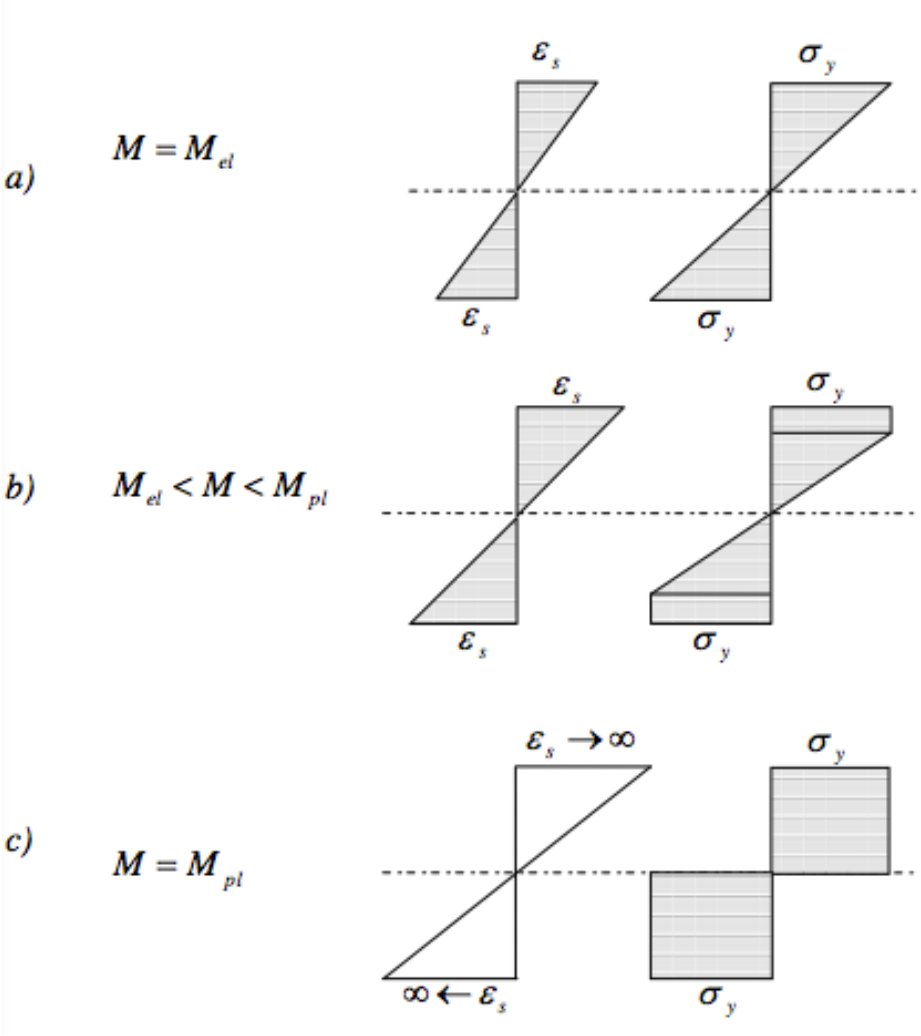

Figure 8 – Stress Evolution of the Section

When the beam reaches its full plastic capacity the majority of deformation will occur in the most strained area of the beam. The moment and the curvature of this small area will be large in comparison to the rest of the beam and this will cause a local plastic rotation to the area. The small deformable area where this large curvature is developed is called a plastic hinge, and the moment in the plastic hinge will develop, and a mechanism is formed. For statically undetermined systems of order n there will be n+1 plastic hinges before the mechanism is formed. This is illustrated in figure 9. If the beam is subjected to a dynamic load more plastic hinges can be formed.

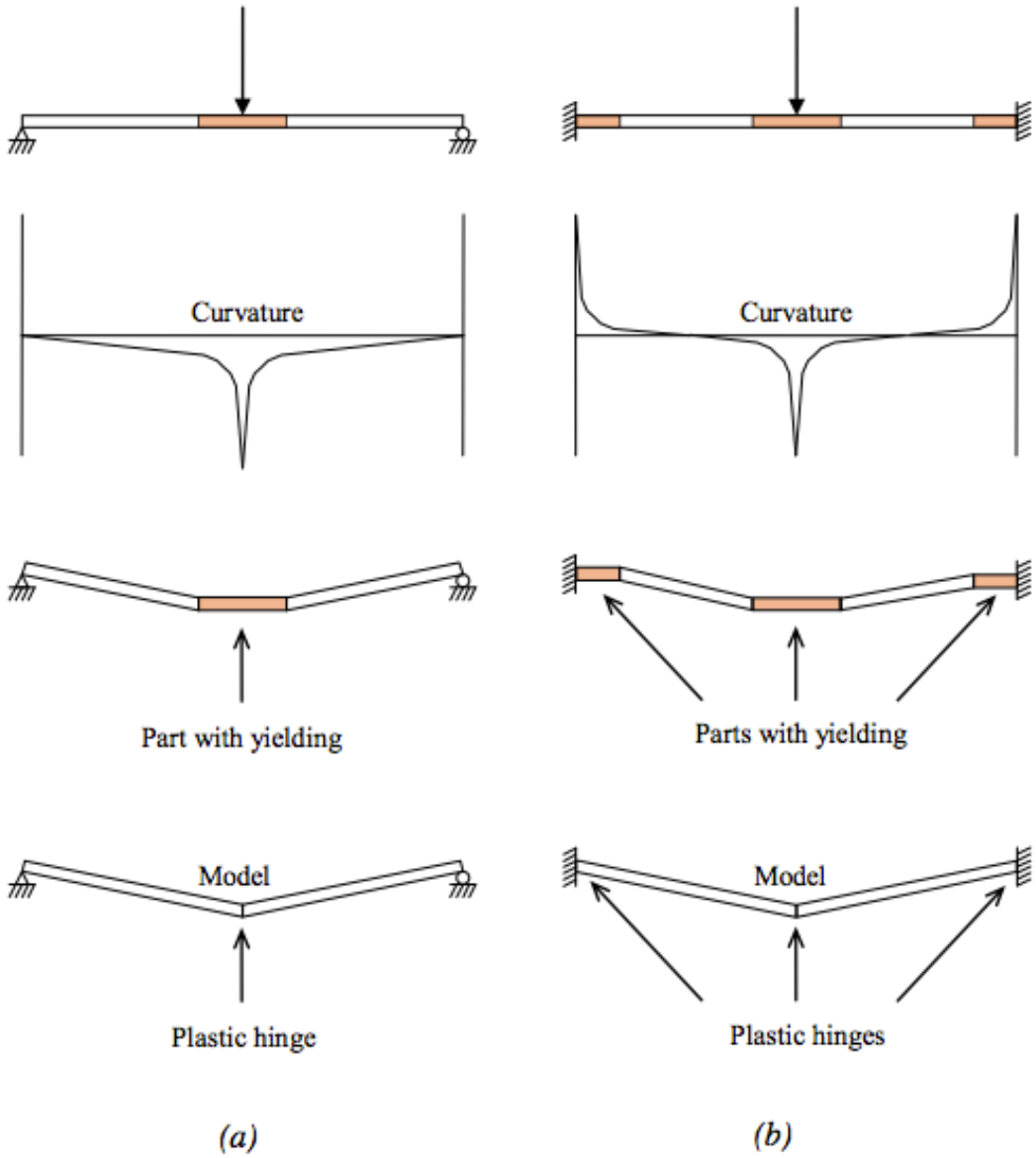

Figure 9 – Plastic Hinges Formation

After the plastic hinge has been developed the beam can still be deformed. How much, though, in determined by the plastic rotation capacity.

2.5 Plastic Rotation Capacity

The actual load-bearing capacity of reinforced concrete structures can be utilized in the design by using the theory of plasticity or by admitting redistribution of moments. In this case it is presupposed that the plastic hinges forming in the highly stressed areas have a large enough rotation capacity. However, this capacity is not arbitrarily large, but narrowly limited. Knowledge of the rotation capacity of reinforced concrete hinges is therefore a prerequisite for the reliable application of the theory of plasticity in reinforced concrete design.

The current methods for determining the rotation capacity of plastic hinges are based either on the statistical evaluation of tests or on theoretical approaches. For example in the CEB-FIP Model Code the plastic rotation capacity is given as a function of the related height of the compression zone. The curve was obtained by a statistical evaluation of 350 tests. The scatter of the experimental results is very large as shown below, indicating that basic influencing factors are neglected by the approach. In this case a statistical evaluation is relatively meaningless.

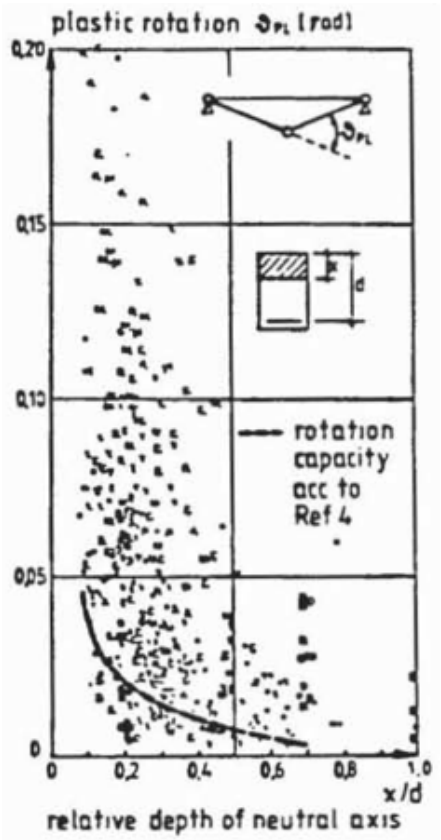

Figure 10 – Plastic Rotation Capacity

The basic work on analytical models of plastic hinges was performed by Dilger and Bachmann. While Dilger disregards the important influence of the contribution of concrete between cracks (tension stiffening) on the rotation capacity, Bachmann assumes constant bond stresses between cracks thus neglecting the influence of displacements on the bond behavior. Both authors assume simplified relationships to describe the behavior of the bars in the inelastic range. Because the rotation capacity significantly depends in the shape of the stress-strain curve of the steel and on the bond behavior, these results cannot be transferred to reinforcement commonly used today. Because of this unsatisfactory situation, an analytical model for plastic hinges was developed.

Based on the given dimensions of the cross section (concrete and reinforcement) and the assumed stress-strain relationships of steel and concrete, the moment-curvature relationship or the tensile force-curvature relationship, respectively, assuming plaine sections remain plaine. The distribution of moments along the beam is calculated taking into account the width of the loading plate. The load is increased until the ultimate moment previously calculated is reached. In statically indeterminate structures an statically determinate beam with a length equal to the distance between two adjacent points of zero moment is cut out of the real system. If shear cracks must be expected, the shifting of the tensile force compared to the M/z-line (M =Moment, z =lever arm) (truss analogy) is taken into account assuming an angle of the inclined compression struts. From the tensile force distribution and the tensile force-curvature relationship the curvature in the cracks is reached. The crack distance is calculated.

The contribution of concrete between cracks is calculated for every beam section between two cracks by means of an iterative solution of the differential equation of bond, using a modified version of the program described. On the basis of the calculated steel strain distribution, the distribution of curvature between the cracks is derived by using the distance of the tensile reinforcement to the neutral axis. Integration of these curvatures over the beam length yields the rotation capacity of the beam. The plastic rotation is defined as the difference between the rotation at ultimate load and at a load causing yielding of the reinforcement at the point of maximum moment. The mathematical model can only yield reliable results if the actual material is described very accurately. Therefore the stress-strain relationship of the reinforcing steel is described by a polygon (with up to 30 points, which allows a very close representation of the real behavior). This model which consists of a parabola and a trilinear continuation takes into account the influence of confinement by stirrups on the strength σ, and corresponding strain ε' the descending branch of the stress-strain relationship (defined σ_1/ε_2 and σ_3/ε_3) and on the residual strength σ_4.

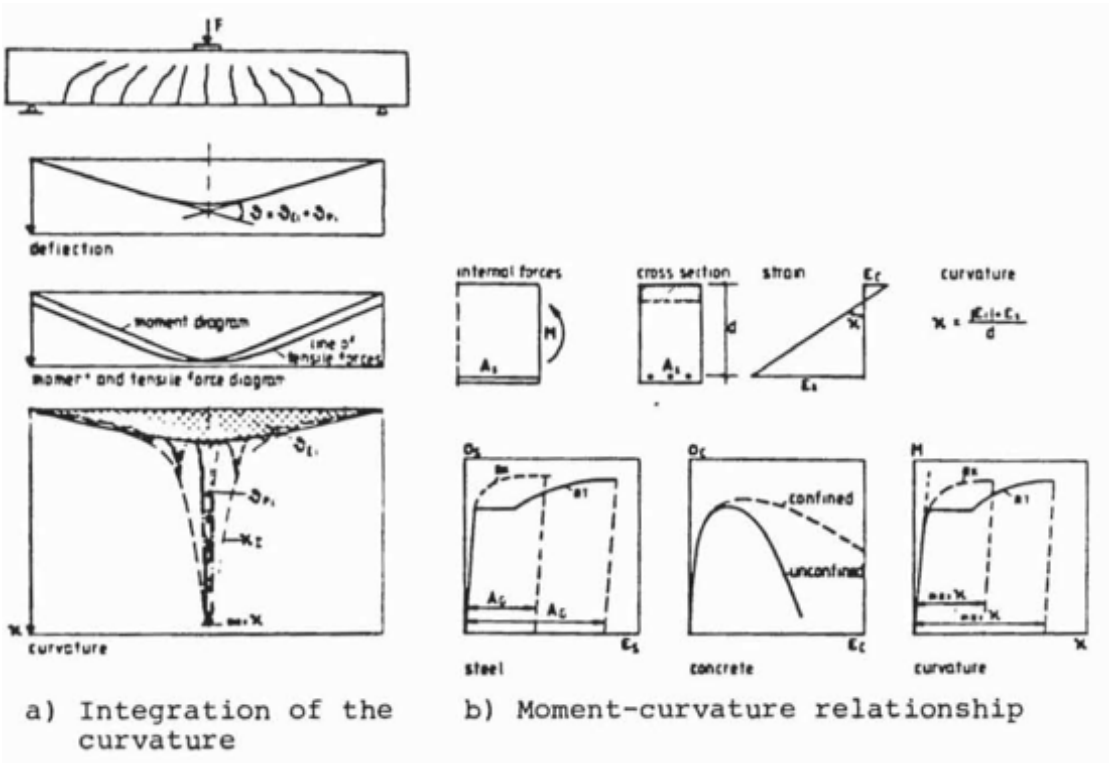

Figure 11 – Distribution of the Concrete cracks and Moment-Curvature Graphs

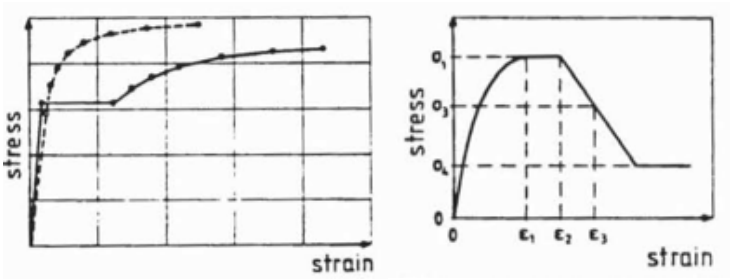

Figure 12 – Stress-Strain Relationship

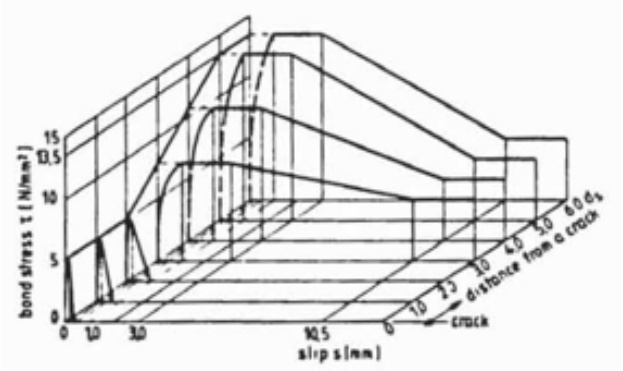

Figure 13 – Bond Stress-Cracks Graphs

At that point it is well established that the inelastic behavior of reinforced concrete (RC) sections leads to a redistribution of moments and forces, resulting in an increased load carrying capacity of the member and the indeterminate structure. As the applied load is increased, hinges start forming in succession at location where the hinge moment capacity is reached; with further increase in the applied load, these hinges forms converting the structure into a mechanism resulting in failure.

Rotation capacity refers to the yield capacity during bending and is measured in the maximum angular change that a plastic hinge can go through while keeping the maximum moment capacity. This means that when a plastic or elasto-plastic material reaches its yield stress it can deform further until the maximum rotation capacity is reached and failure occurs. For concrete members there are several methods of determining the rotational capacity, but they provide different results. According to Johansson (1997) on of the reasons may be because of the significant difference in steel properties used in reinforcement bars over the last decades.

The plastic hinges rotation, θ_p, of RC beams depends on a number of parameters including the definition of yielding and ultimate curvatures, section geometry, material properties, compression and tension reinforcement ratios, transverse reinforcement, cracking and tension stiffness, the stress-strain curve for reinforcing steel, bond-slip characteristics between the concrete and the reinforcing steel, support conditions and the magnitude and type of loading, axial force, width of the loading plate, influence of shear and the presence of column.

Form Eurocode 2, CEN (2004), the method of estimating the maximum allowed rotation capacity is acquired from diagram with regard to the the quality of concrete, reinforcement class and the ration between the compressed zone x and the effective depth, as sees in Below.

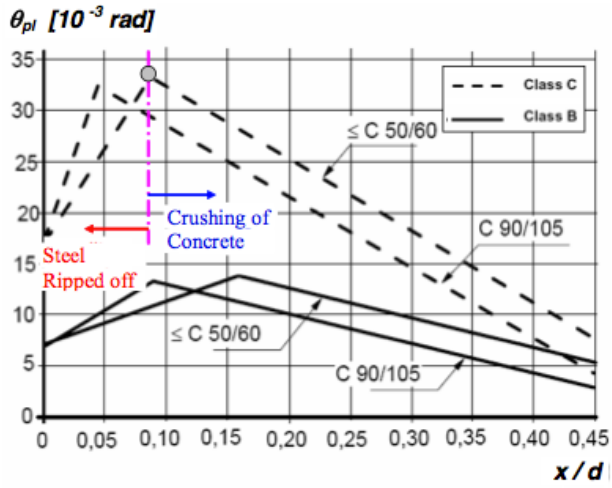

Figure 14 – Plastic Rotation Capacity

The lines in the figure 14 are based on a share slenderness λ=3,0, where λ is given by:

$$\lambda = \frac{l_0}{d}$$

where l_0 is the length between the point of zero moment and the plastic hinge and d is the effective depth of the reinforcement.

If λ has values other than 3,0, the rotation capacity should be multiplied with a factor:

$$k_\lambda = \sqrt{\frac{\lambda}{3}}$$

in the following manner:

$$\theta_{rd} = k_\lambda * \theta_{pl}$$

Chapter

5

F.E.M. Models and Relative discussion of Analysis

1. Introduction

In this chapter the author analyzes the beams modeling process with Midas Gen Software, describing all single steps that leads up to the construction of the F.E.M. Models and the relatives discussion of the results obtained by those kind of analysis. As known, the fulfillment of F.E.M. Analysis was obtained by the use of Midas Gen Software, a general-purpose structural analysis and optimal design system.

Before starting to describe the construction of the model, it is important to explain the Finite Element Modeling properties. As known, engineering analysis of mechanical systems, have been addressed by deriving differential equation relating the variables of through basic physical principals such as equilibrium, conservation of energy, conservation of masses, the law of thermodynamics, Maxwell's equations and Newton's laws of motion. However, once formulated, solving the resulting mathematical models is often impossible, especially when the resulting models are non-linear partial differential equations. Only very simple problems of regular geometry such as rectangular or a circle with the simplest boundary conditions were tractable.

The Finite Element Method (F.E.M.) is the dominant discretization technique in structural mechanics. The basic concept in the physical interpretation of the FEM is the subdivision of the mathematical model into disjoint (non-overlapping) components of simple geometry called finite elements or elements for short. The response of each element is expressed in terms of a finite number of degrees of freedom characterized as the value of an unknown function, or functions, at a set of nodal points. The response of the mathematical model is then considered, to be approximated by that of the discrete model obtained by connecting or assembling the collection of all elements.

In general, a typical finite element analysis on a software system required the following information:

- Nodal point spatial locations (geometry);
- Elements connecting the nodal points;
- Mass properties;
- Boundary conditions or restraints;
- Loading or forcing function details;
- Analysis options.

Because FEM is a discretization method, the number of degrees of freedom of a FEM model is necessarily finite. They are collected in a column vector called [u]. This vector is generally called the DOF vector or state vector. Considering now the FEM Solution Process, procedures could be listed as:

- Divide structure into pieces (elements with nodes) (discretization/meshing);
- Connect the elements at the nodes to form an approximate system of equation for the whole structure (forming element matrices);
- Solve the system of equations involving unknown quantities at the nodes (displacements);
- Calculate desired quantities (strains and stresses) at selected elements.

So below, the author is going to explain in detail, all single step necessary to obtain the final models and the relative results of their analysis.

2. F.E.M. Model Construction

The author will now describe all steps characterizing the construction of the F.E.M. Model with Midas Gen Software. First of all, it is needed to explain what kinds of elements are considered for the analysis.

As presented into the previous chapters, the goal of this work is to analyze the behavior of columns structural elements subjected to blast loading. Especially, considering a surface explosion, the first elements involved are the external columns located at the ground and at the first floors. These elements are involved by the blast wave, caused by the explosion of the weapon, and consequently the fragments generated by the crash of the blast wave against the structure. Blast loads calculation and its properties were just explain into the chapter 3, presenting at the end, the relative charts and tables, for each case of study.

So in this case column elements, could be modeled as beams, linked with the rest of the structures by external constraints. As shown below, the beam model could be simplified as:

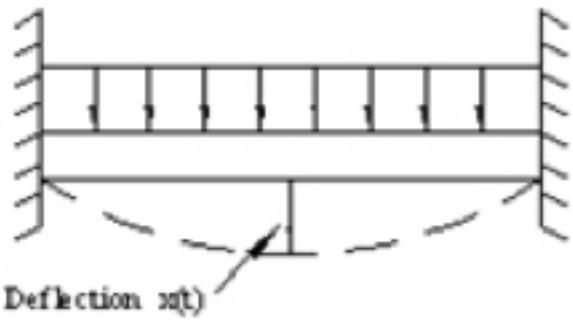

Figure 1 – Semplification of Model

subjected to a distributed load, representing the blast load involving the structure, and tied to the others elements with specific constraints:

- The base of the beam is tied with joint constraint, that impede all rotations and translations;
- The upper limit is characterized, by the obstacle of all rotations and only 2 translations, setting free the “z” translation. Indeed, structural columns are subjected to compression axial loads, calculated by the structural loads analysis.

As just presented into chapter 3, the aim of this analysis is to evaluate the behavior of columns with three different height (3 [m], 4 [m], 5 [m]).

2.1MIDAS GEN Models

For analyze the problem with the software Midas Gen, we decided to create single columns models. In this section the author will describe each single step occurs for the creation of the model and it consequently analysis.

Midas Gen is a F.E.M. software, and following we propose a complete image of the interface of the software.

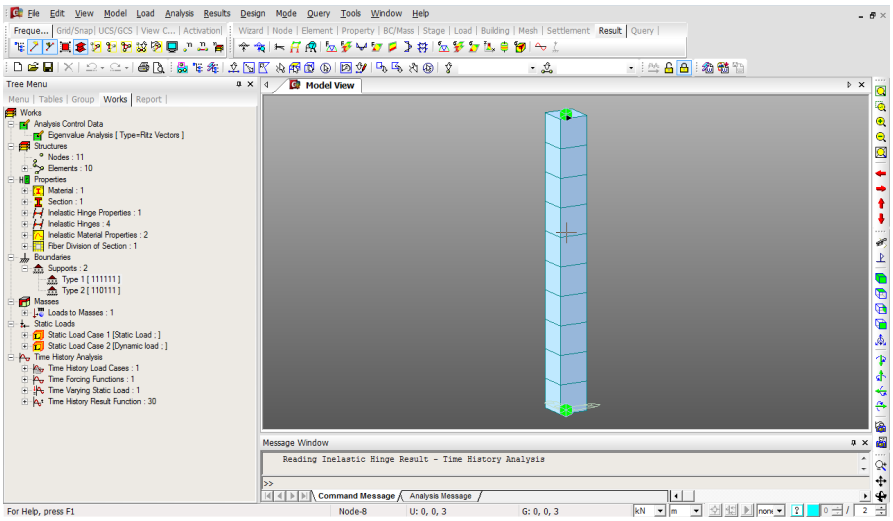

Figure 2 – Midas Gen

Describing all the step occurs for the construction of the model, first of all we need to explain that had been considered columns located at the ground or at the maximum at the first floor

Generally, considering for economical reason it is often used as approach of structural design of buildings, restraint that get free all rotation at the bottom of the columns. In this particular case, for security reasons, it was reasonable considering all bottom restraints as fixed. The top of the columns, connected to the upper floor of the buildings, has been tied to the rest of the structure with restraint that gets free only the displacement on z-direction, as shown in the next picture:

Next important step for the creation of a F.E.M. is the materials assignment, considering for that specific case of study concrete C30/37.

As explained, the columns section is a square section 50x50 cm dimensions, considering three different height: 3m, 4m and 5m.

For the analysis of a blast load event it is needed to consider an inelastic behavior of the

section and the materials, so we must had to create a fiber section in Midas Gen. This fiber section was created importing the section dimension into the software and imposing materials properties (for concrete and reinforcing steel bar) with the goal to create an inelastic behavior.

As shown into the following picture we decided to consider the Kent & Park Model for the concrete behavior, and the Menegotto-Pinto Model for reinforcement.

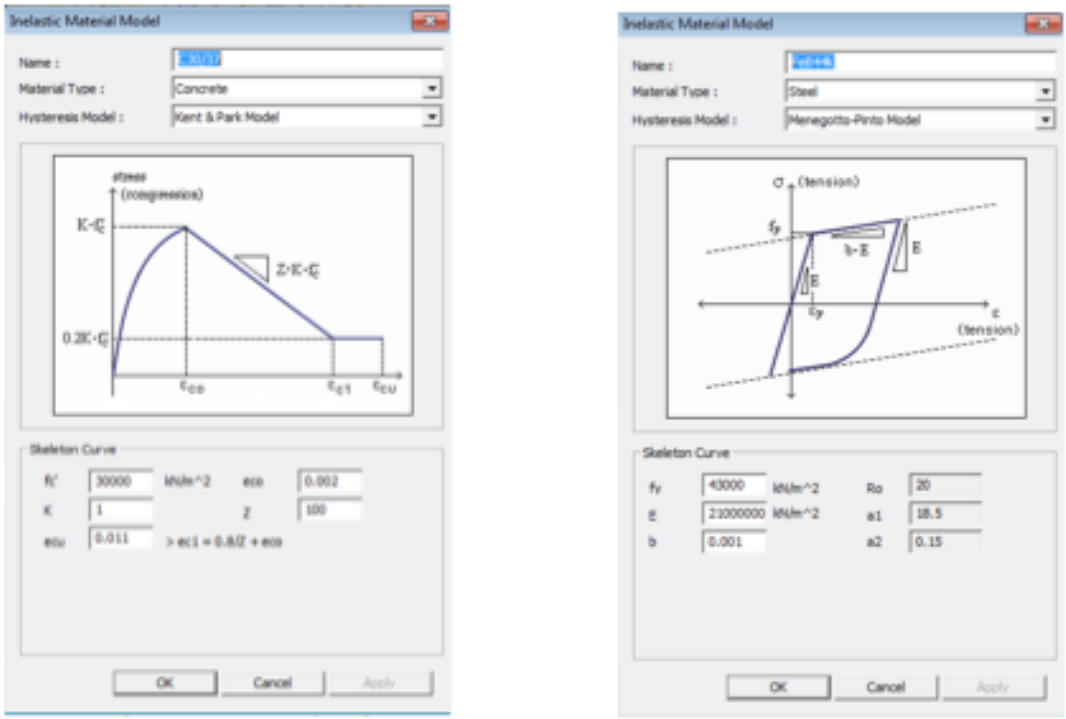

Figure 3 – Inelastic Material Properties

After this step it was possible to generate the real section of the columns adding the relative inelastic properties for each material, characterizing the elements.

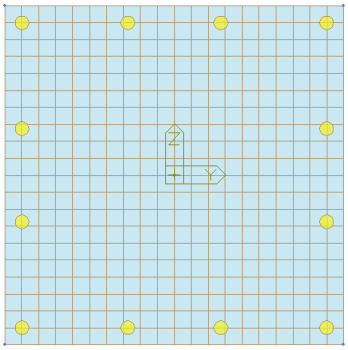

Figure 4 - Columns Section

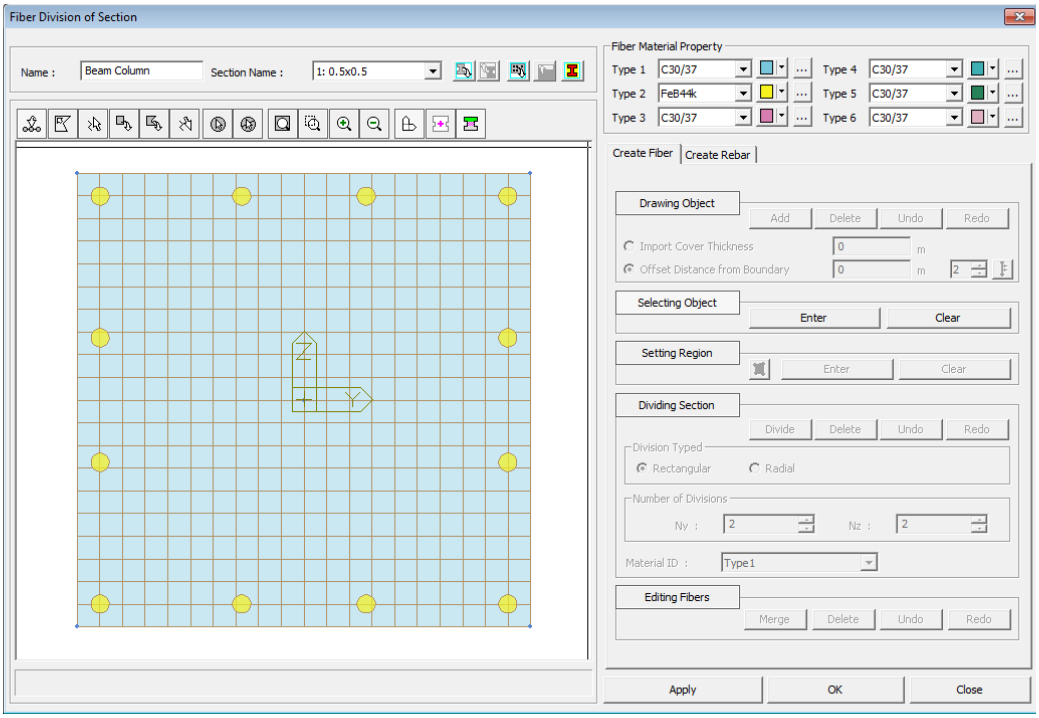

Figure 5 – Fiber Section Construction

So considering an inelastic behavior of section, next important step was the localization of plastic hinges, that considering our analysis of joints restraints, we know for sure that the first plastic hinges must be form at the edge of the columns (at the top and the bottom) and after that continuing to increase the load, function of blast loading phenomena, the third plastic hinge must be occurring in the middle of the column.

Indeed after the formation of the two external plastic hinges, the element become as a simple supported beam, with a uniform distributed load along its span. Because of that, the third plastic hinge will be generate at the maximum point of deflection, and so in the middle of the element.

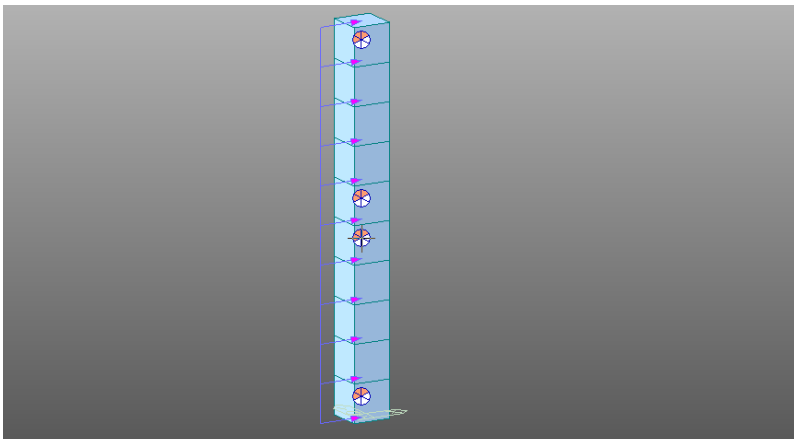

Figure 6 – Plastic Hinges

So considered all this steps, it was important to impose the loading occurring on the structure, using the load function calculated for a blast load event, as shown into the chapter 3.

First of all it is important to explain that, analyzing ground floor columns, was needed to apply an axial load on the top of the structural elements, just to simulate the dead and super-dead loads generated by the top structure of the considered building.

After that was possible to analyze the blast load that, as explain before must be considered as a uniform distributed load along the span of the column, so meshing the element and dividing it into 10 smaller elements, the load was applied as a joint distributed load, as well shown in the following picture.

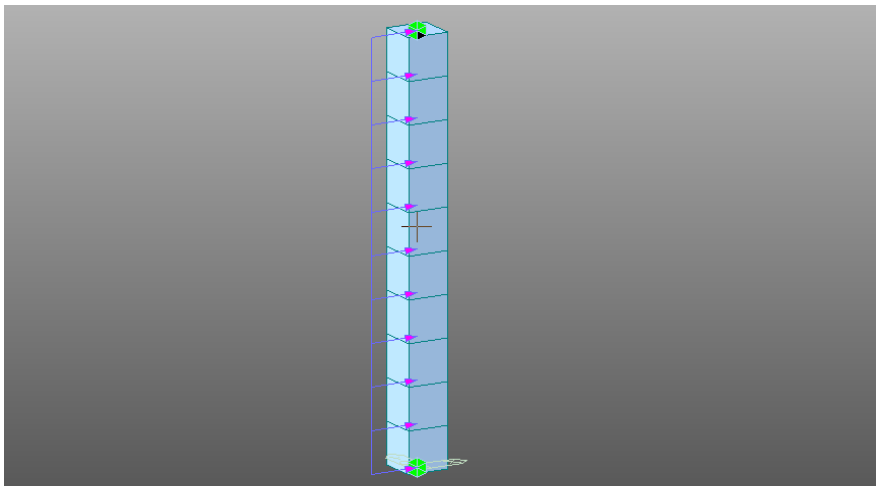

Figure 7 – Loads

This unitary static load becomes dynamics, creating a time-history load function, just importing from excel the load function tables obtain at the end of the long process for the calculation of blast load function graphs.

The Time-History load function was created in Midas Gen as a non-linear function, using a direct integration analysis method, as shown with the next picture.

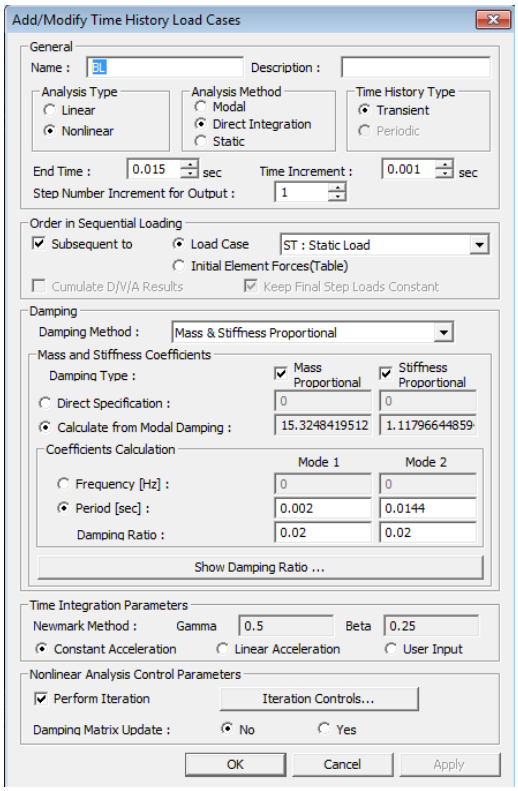

Figure 8 – Time History

Without considering the free vibration period, to be better clear the vibration occurring after the blast load events ends, the time-history load function could be the simple one shown in the picture.

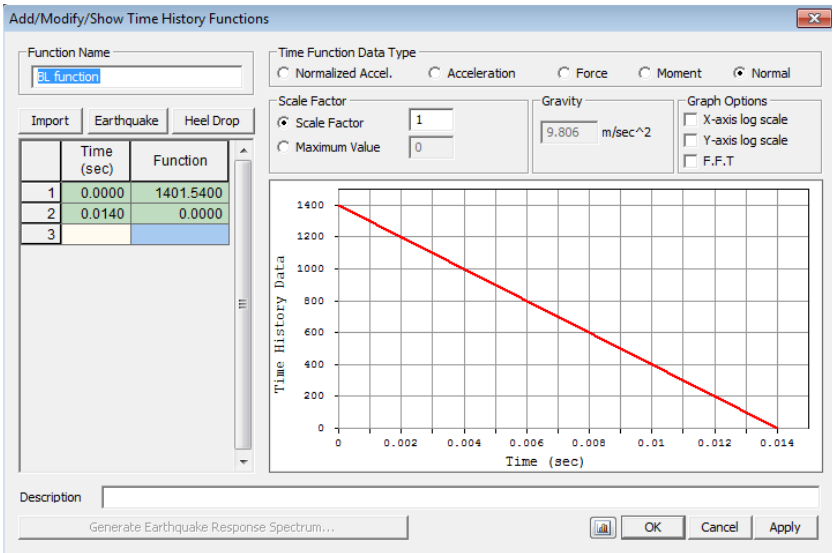

Figure 9 – Time-History Load Function

For complete the application of loads phase, it was needed to connect the static distributed load applied to the elements, with the dynamic function imposed during the construction process just explained, as shown in the following picture.

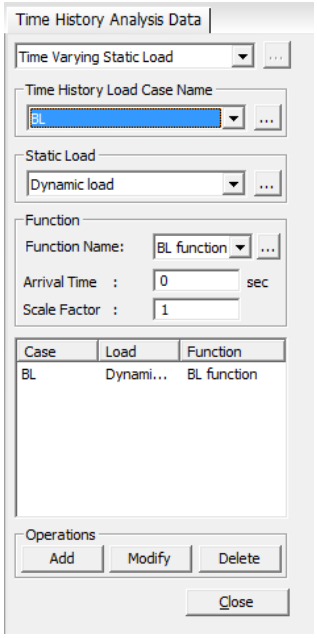

Figure 10 – Time-History Analysis Data

Last step for the creation of the model, before starting the relative analysis, was to choose the method used by the software for obtain the needed results. The method considered for this kind of blast analysis is the eigenvalue one.

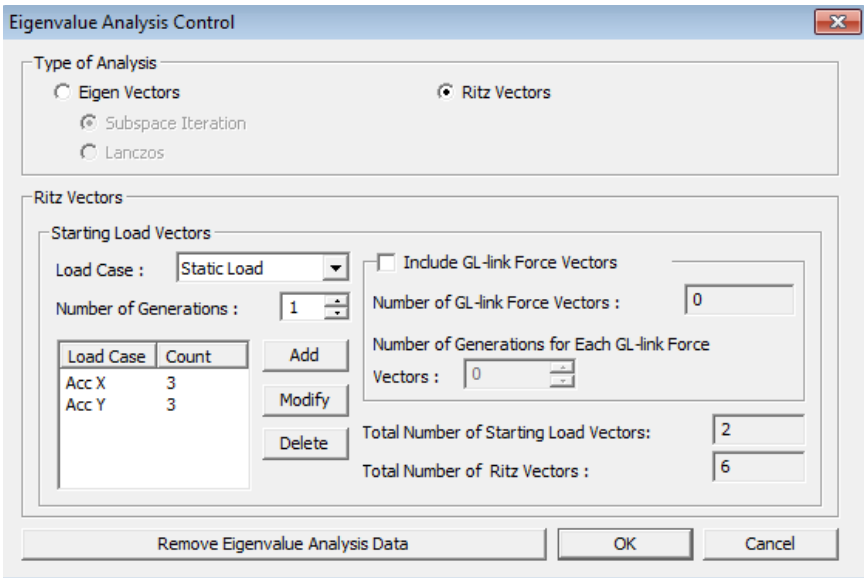

Figure 11 – Eigenvalue Analysis

2.2 Midas Gen Analysis Results

In this section the author will propose the results and some image from Midas Gen analysis results.

Considering each case, the most important thing to consider for the reply of the element subjected to a blast load, is the study of the deflection and so the displacement in the point of maximum deflection.

For the case of study, considering that after the formation of the plastic hinges on the top and the bottom of the columns, the element should be considered as a simple support beam with a distributed load along its span, the point of maximum deflection must be the middle of the columns.

For each case of study we can see from the picture proposed below, the entity of the deflection, depending on the length of the element and the load function applied.

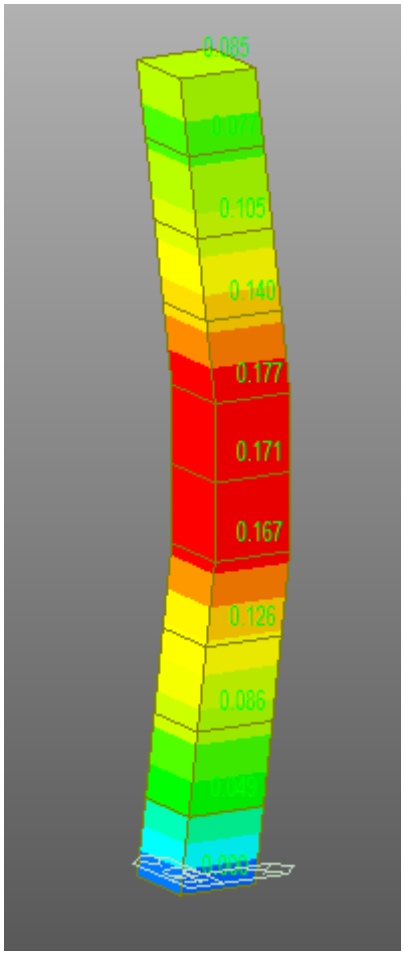

Figure 12 – Midas Gen Deflection

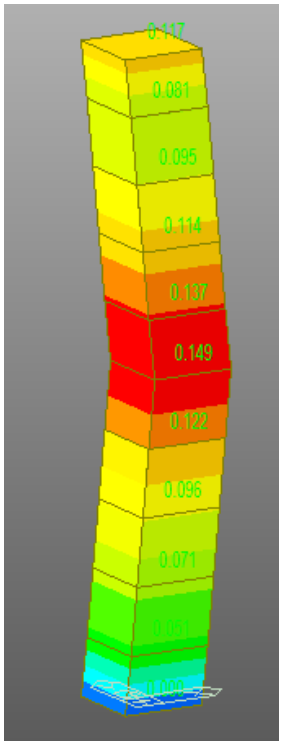

Figure 13 – Midas Gen Deflection

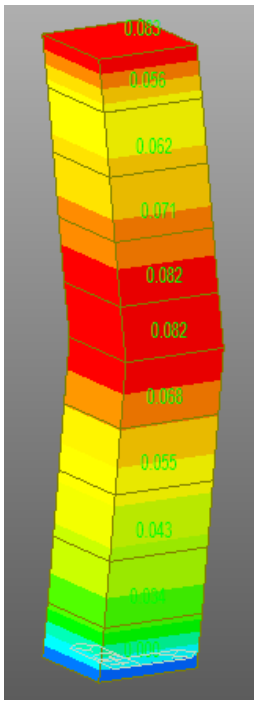

Figure 14 – Midas Gen Deflection

So analyzing all the cases modeled with software Midas Gen, we propose in the following some table resuming the displacement result obtain form the software output results:

- COLUMNS 5m Height

CASO 1							
Node	Load	DX (m)	DY (m)	DZ (m)	RX ([rad])	RY ([rad])	RZ ([rad])
1,00E+00	BL(all)	0.000000	0.000000	0.000000	0.000000	0.000000	0.000000
2,00E+00	BL(all)	0.000000	0.000000	-0.087038	0.000000	0.000000	0.000000
3,00E+00	BL(all)	0.015086	0.000000	-0.027870	0.000000	0.031610	0.000000
4,00E+00	BL(all)	0.030932	0.000000	-0.027870	0.000000	0.031697	0.000000
5,00E+00	BL(all)	0.046792	0.000000	-0.027870	0.000000	0.031655	0.000000
6,00E+00	BL(all)	0.062595	0.000000	-0.027870	0.000000	0.031501	0.000000
7,00E+00	BL(all)	0.078133	0.000000	-0.042092	0.000000	-0.010494	0.000000
8,00E+00	BL(all)	0.060639	0.000000	-0.060837	0.000000	-0.030483	0.000000
9,00E+00	BL(all)	0.045386	0.000000	-0.060837	0.000000	-0.030467	0.000000
1,00E+01	BL(all)	0.030167	0.000000	-0.060837	0.000000	-0.030386	0.000000
1,10E+01	BL(all)	0.014997	0.000000	-0.060837	0.000000	-0.030259	0.000000

Table 1 – Midas Gen Results – Case 1 (5m)

CASO 2							
Node	Load	DX (m)	DY (m)	DZ (m)	RX ([rad])	RY ([rad])	RZ ([rad])
1,00E+00	BL(all)	0.000000	0.000000	0.000000	0.000000	0.000000	0.000000
2,00E+00	BL(all)	0.000000	0.000000	-0.103762	0.000000	0.000000	0.000000
3,00E+00	BL(all)	0.066879	0.000000	-0.030189	0.000000	0.092558	0.000000
4,00E+00	BL(all)	0.113175	0.000000	-0.030189	0.000000	0.092670	0.000000
5,00E+00	BL(all)	0.159551	0.000000	-0.030189	0.000000	0.092756	0.000000
6,00E+00	BL(all)	0.205940	0.000000	-0.030189	0.000000	0.092729	0.000000
7,00E+00	BL(all)	0.205806	0.000000	-0.052341	0.000000	-0.000723	0.000000
8,00E+00	BL(all)	0.205408	0.000000	-0.074083	0.000000	-0.092095	0.000000
9,00E+00	BL(all)	0.159334	0.000000	-0.074083	0.000000	-0.092140	0.000000
1,00E+01	BL(all)	0.113260	0.000000	-0.074083	0.000000	-0.092071	0.000000
1,10E+01	BL(all)	0.067263	0.000000	-0.074083	0.000000	-0.091988	0.000000

Table 2 – Midas Gen Results – Case 2 (5m)

CASO 3							
Node	Load	DX (m)	DY (m)	DZ (m)	RX ([rad])	RY ([rad])	RZ ([rad])
1,00E+00	BL(all)	0.000000	0.000000	0.000000	0.000000	0.000000	0.000000
2,00E+00	BL(all)	0.000000	0.000000	-0.149594	0.000000	0.000000	0.000000
3,00E+00	BL(all)	0.174726	0.000000	-0.052188	0.000000	0.155143	0.000000
4,00E+00	BL(all)	0.252274	0.000000	-0.052188	0.000000	0.154854	0.000000
5,00E+00	BL(all)	0.329594	0.000000	-0.052188	0.000000	0.154372	0.000000
6,00E+00	BL(all)	0.406646	0.000000	-0.052188	0.000000	0.153881	0.000000
7,00E+00	BL(all)	0.407787	0.000000	-0.076636	0.000000	0.000414	0.000000
8,00E+00	BL(all)	0.406671	0.000000	-0.100948	0.000000	-0.153562	0.000000
9,00E+00	BL(all)	0.329778	0.000000	-0.100948	0.000000	-0.154052	0.000000
1,00E+01	BL(all)	0.252618	0.000000	-0.100948	0.000000	-0.154536	0.000000
1,10E+01	BL(all)	0.175227	0.000000	-0.100948	0.000000	-0.154817	0.000000

Table 3 – Midas Gen Results – Case 3 (5m)

CASO 7							
Node	Load	DX (m)	DY (m)	DZ (m)	RX ([rad])	RY ([rad])	RZ ([rad])
1,00E+00	BL(all)	0.000000	0.000000	0.000000	0.000000	0.000000	0.000000
2,00E+00	BL(all)	0.000000	0.000000	-0.025645	0.000000	0.000000	0.000000
3,00E+00	BL(all)	0.016001	0.000000	-0.009294	0.000000	0.032028	0.000000
4,00E+00	BL(all)	0.032027	0.000000	-0.009294	0.000000	0.032094	0.000000
5,00E+00	BL(all)	0.048095	0.000000	-0.009294	0.000000	0.032147	0.000000
6,00E+00	BL(all)	0.064181	0.000000	-0.009294	0.000000	0.032106	0.000000
7,00E+00	BL(all)	0.080075	0.000000	-0.009006	0.000000	0.028452	0.000000
8,00E+00	BL(all)	0.065319	0.000000	-0.016770	0.000000	-0.032339	0.000000
9,00E+00	BL(all)	0.049086	0.000000	-0.016770	0.000000	-0.032544	0.000000
1,00E+01	BL(all)	0.032769	0.000000	-0.016770	0.000000	-0.032658	0.000000
1,10E+01	BL(all)	0.016425	0.000000	-0.016770	0.000000	-0.032745	0.000000

Table 4 – Midas Gen Results – Case 7 (5m)

CASO 9							
Node	Load	DX (m)	DY (m)	DZ (m)	RX ([rad])	RY ([rad])	RZ ([rad])
1,00E+00	BL(all)	0.000000	0.000000	0.000000	0.000000	0.000000	0.000000
2,00E+00	BL(all)	0.000000	0.000000	-0.154130	0.000000	0.000000	0.000000
3,00E+00	BL(all)	0.175317	0.000000	-0.043410	0.000000	0.176214	0.000000
4,00E+00	BL(all)	0.263465	0.000000	-0.043410	0.000000	0.176117	0.000000
5,00E+00	BL(all)	0.351455	0.000000	-0.043410	0.000000	0.175742	0.000000
6,00E+00	BL(all)	0.439214	0.000000	-0.043410	0.000000	0.175273	0.000000
7,00E+00	BL(all)	0.441305	0.000000	-0.074703	0.000000	-0.001000	0.000000
8,00E+00	BL(all)	0.438913	0.000000	-0.105771	0.000000	-0.175399	0.000000
9,00E+00	BL(all)	0.351080	0.000000	-0.105771	0.000000	-0.175907	0.000000
1,00E+01	BL(all)	0.262999	0.000000	-0.105771	0.000000	-0.176328	0.000000
1,10E+01	BL(all)	0.174734	0.000000	-0.105771	0.000000	-0.176505	0.000000

Table 5 – Midas Gen Results – Case 9 (5m)

CASO 10							
Node	Load	DX (m)	DY (m)	DZ (m)	RX ([rad])	RY ([rad])	RZ ([rad])
1,00E+00	BL(all)	0.000000	0.000000	0.000000	0.000000	0.000000	0.000000
2,00E+00	BL(all)	0.000000	0.000000	-0.156161	0.000000	0.000000	0.000000
3,00E+00	BL(all)	0.127934	0.000000	-0.045724	-0.000000	0.126442	0.000000
4,00E+00	BL(all)	0.191159	0.000000	-0.045724	-0.000000	0.126356	0.000000
5,00E+00	BL(all)	0.254295	0.000000	-0.045724	0.000000	0.126208	0.000000
6,00E+00	BL(all)	0.317371	0.000000	-0.045724	0.000000	0.126000	0.000000
7,00E+00	BL(all)	0.317863	0.000000	-0.069194	0.000000	0.000586	0.000000
8,00E+00	BL(all)	0.317366	0.000000	-0.092198	0.000000	-0.123837	0.000000
9,00E+00	BL(all)	0.255377	-0.000000	-0.092198	0.000000	-0.124167	0.000000
1,00E+01	BL(all)	0.193198	-0.000000	-0.092198	0.000000	-0.124488	0.000000
1,10E+01	BL(all)	0.130877	-0.000000	-0.092198	0.000000	-0.124636	0.000000

Table 6 – Midas Gen Results – Case 10 (5m)

- COLUMNS 4m Height

CASO 1							
Node	Load	DX (m)	DY (m)	DZ (m)	RX ([rad])	RY ([rad])	RZ ([rad])
1,00E+00	BL(all)	0.000000	0.000000	0.000000	0.000000	0.000000	0.000000
2,00E+00	BL(all)	0.000000	0.000000	-0.116858	0.000000	0.000000	0.000000
3,00E+00	BL(all)	0.028735	-0.000004	-0.042281	0.000006	0.071695	0.000000
4,00E+00	BL(all)	0.057400	-0.000005	-0.042281	0.000005	0.071534	0.000000
5,00E+00	BL(all)	0.085979	-0.000006	-0.042281	-0.000005	0.071273	0.000000
6,00E+00	BL(all)	0.114425	-0.000007	-0.042281	-0.000005	0.070968	0.000000
7,00E+00	BL(all)	0.142645	-0.000008	-0.042282	-0.000005	0.070060	0.000000
8,00E+00	BL(all)	0.114355	-0.000007	-0.075657	-0.000006	-0.071077	0.000000
9,00E+00	BL(all)	0.085891	-0.000006	-0.075657	-0.000005	-0.071286	0.000000
1,00E+01	BL(all)	0.057327	-0.000005	-0.075657	-0.000004	-0.071499	0.000000
1,10E+01	BL(all)	0.028675	-0.000003	-0.075657	-0.000005	-0.071608	0.000000

Table 7 – Midas Gen Results – Case 1 (4m)

CASO 2							
Node	Load	DX (m)	DY (m)	DZ (m)	RX ([rad])	RY ([rad])	RZ ([rad])
1,00E+00	BL(all)	0.000000	0.000000	0.000000	0.000000	0.000000	0.000000
2,00E+00	BL(all)	0.000000	0.000000	-0.159304	0.000000	0.000000	0.000000
3,00E+00	BL(all)	0.060563	0.000000	-0.044196	0.000000	0.151848	0.000000
4,00E+00	BL(all)	0.121387	0.000000	-0.044196	0.000000	0.152239	0.000000
5,00E+00	BL(all)	0.182383	0.000000	-0.044196	0.000000	0.152452	0.000000
6,00E+00	BL(all)	0.243400	0.000000	-0.044196	0.000000	0.152356	0.000000
7,00E+00	BL(all)	0.243632	0.000000	-0.080171	0.000000	-0.000076	0.000000
8,00E+00	BL(all)	0.243342	0.000000	-0.116103	0.000000	-0.152334	0.000000
9,00E+00	BL(all)	0.182334	0.000000	-0.116103	0.000000	-0.152428	0.000000
1,00E+01	BL(all)	0.121347	0.000000	-0.116103	0.000000	-0.152210	0.000000
1,10E+01	BL(all)	0.060536	0.000000	-0.116103	0.000000	-0.151817	0.000000

Table 8 – Midas Gen Results – Case 2 (4m)

CASO 3							
Node	Load	DX (m)	DY (m)	DZ (m)	RX ([rad])	RY ([rad])	RZ ([rad])
1,00E+00	BL(all)	0.000000	0.000000	0.000000	0.000000	0.000000	0.000000
2,00E+00	BL(all)	0.000000	0.000000	-0.144610	0.000000	0.000000	0.000000
3,00E+00	BL(all)	0.093256	0.000000	-0.043552	-0.000000	0.196199	0.000000
4,00E+00	BL(all)	0.171767	0.000000	-0.043552	-0.000000	0.196102	0.000000
5,00E+00	BL(all)	0.250176	0.000000	-0.043552	0.000000	0.195780	0.000000
6,00E+00	BL(all)	0.328413	0.000000	-0.043552	0.000000	0.195330	0.000000
7,00E+00	BL(all)	0.331641	0.000000	-0.072178	0.000000	-0.000563	0.000000
8,00E+00	BL(all)	0.328175	0.000000	-0.100545	0.000000	-0.193463	0.000000
9,00E+00	BL(all)	0.250690	-0.000000	-0.100545	0.000000	-0.193885	0.000000
1,00E+01	BL(all)	0.173047	-0.000000	-0.100545	0.000000	-0.194180	0.000000
1,10E+01	BL(all)	0.095311	-0.000000	-0.100545	0.000000	-0.194264	0.000000

Table 9 – Midas Gen Results – Case 3 (4m)

CASO 7							
Node	Load	DX (m)	DY (m)	DZ (m)	RX ([rad])	RY ([rad])	RZ ([rad])
1,00E+00	BL(all)	0.000000	0.000000	0.000000	0.000000	0.000000	0.000000
2,00E+00	BL(all)	0.000000	0.000000	-0.043355	0.000000	0.000000	0.000000
3,00E+00	BL(all)	0.009389	0.000000	-0.015321	0.000000	0.023483	0.000000
4,00E+00	BL(all)	0.018775	0.000000	-0.015321	0.000000	0.023566	0.000000
5,00E+00	BL(all)	0.028233	0.000000	-0.015321	0.000000	0.023707	0.000000
6,00E+00	BL(all)	0.037750	0.000000	-0.015321	0.000000	0.023791	0.000000
7,00E+00	BL(all)	0.047241	0.000000	-0.015347	0.000000	0.023515	0.000000
8,00E+00	BL(all)	0.037767	0.000000	-0.027310	0.000000	-0.023749	0.000000
9,00E+00	BL(all)	0.028258	0.000000	-0.027310	0.000000	-0.023702	0.000000
1,00E+01	BL(all)	0.018793	0.000000	-0.027310	0.000000	-0.023581	0.000000
1,10E+01	BL(all)	0.009399	0.000000	-0.027310	0.000000	-0.023498	0.000000

Table 10 – Midas Gen Results – Case 7 (4m)

CASO 9							
Node	Load	DX (m)	DY (m)	DZ (m)	RX ([rad])	RY ([rad])	RZ ([rad])
1,00E+00	BL(all)	0.000000	0.000000	0.000000	0.000000	0.000000	0.000000
2,00E+00	BL(all)	0.000000	0.000000	-0.083721	0.000000	0.000000	0.000000
3,00E+00	BL(all)	0.092002	0.000000	-0.024967	0.000000	0.189258	0.000000
4,00E+00	BL(all)	0.167797	0.000000	-0.024967	0.000000	0.189348	0.000000
5,00E+00	BL(all)	0.243540	0.000000	-0.024967	0.000000	0.189082	0.000000
6,00E+00	BL(all)	0.319094	0.000000	-0.024967	0.000000	0.188627	0.000000
7,00E+00	BL(all)	0.324950	0.000000	-0.042568	0.000000	-0.000422	0.000000
8,00E+00	BL(all)	0.319430	0.000000	-0.059997	0.000000	-0.187553	0.000000
9,00E+00	BL(all)	0.244293	0.000000	-0.059997	0.000000	-0.187960	0.000000
1,00E+01	BL(all)	0.169028	0.000000	-0.059997	0.000000	-0.188163	0.000000
1,10E+01	BL(all)	0.093710	0.000000	-0.059997	0.000000	-0.188055	0.000000

Table 11 – Midas Gen Results – Case 9 (4m)

CASO 10							
Node	Load	DX (m)	DY (m)	DZ (m)	RX ([rad])	RY ([rad])	RZ ([rad])
1,00E+00	BL(all)	0.000000	0.000000	0.000000	0.000000	0.000000	0.000000
2,00E+00	BL(all)	0.000000	0.000000	-0.056580	0.000000	0.000000	0.000000
3,00E+00	BL(all)	0.055936	0.000000	-0.017525	0.000000	0.147963	0.000000
4,00E+00	BL(all)	0.115167	0.000000	-0.017525	0.000000	0.147963	0.000000
5,00E+00	BL(all)	0.174344	0.000000	-0.017525	0.000000	0.147740	0.000000
6,00E+00	BL(all)	0.233386	0.000000	-0.017525	0.000000	0.147356	0.000000
7,00E+00	BL(all)	0.234686	0.000000	-0.029761	0.000000	0.001208	0.000000
8,00E+00	BL(all)	0.231156	0.000000	-0.043571	0.000000	-0.146795	0.000000
9,00E+00	BL(all)	0.172342	0.000000	-0.043571	0.000000	-0.147135	0.000000
1,00E+01	BL(all)	0.113417	0.000000	-0.043571	0.000000	-0.147287	0.000000
1,10E+01	BL(all)	0.054471	0.000000	-0.043571	0.000000	-0.147190	0.000000

Table 12 – Midas Gen Results – Case 10 (4m)

- COLUMNS 3m Height

CASO 1							
Node	Load	DX (m)	DY (m)	DZ (m)	RX ([rad])	RY ([rad])	RZ ([rad])
1,00E+00	BL(all)	0.000000	0.000000	0.000000	0.000000	0.000000	0.000000
2,00E+00	BL(all)	0.000000	0.000000	-0.083021	0.000000	0.000000	0.000000
3,00E+00	BL(all)	0.015384	0.000000	-0.029865	0.000000	0.051240	0.000000
4,00E+00	BL(all)	0.030774	0.000000	-0.029865	0.000000	0.051173	0.000000
5,00E+00	BL(all)	0.046111	0.000000	-0.029865	0.000000	0.051027	0.000000
6,00E+00	BL(all)	0.061389	0.000000	-0.029865	0.000000	0.050884	0.000000
7,00E+00	BL(all)	0.076606	0.000000	-0.029882	0.000000	0.050526	0.000000
8,00E+00	BL(all)	0.061356	0.000000	-0.053960	0.000000	-0.050976	0.000000
9,00E+00	BL(all)	0.046048	0.000000	-0.053960	0.000000	-0.051061	0.000000
1,00E+01	BL(all)	0.030716	0.000000	-0.053960	0.000000	-0.051134	0.000000
1,10E+01	BL(all)	0.015353	0.000000	-0.053960	0.000000	-0.051160	0.000000

Table 13 – Midas Gen Results – Case 1 (3m)

CASO 2							
Node	Load	DX (m)	DY (m)	DZ (m)	RX ([rad])	RY ([rad])	RZ ([rad])
1,00E+00	BL(all)	0.000000	0.000000	0.000000	0.000000	0.000000	0.000000
2,00E+00	BL(all)	0.000000	0.000000	-0.070976	0.000000	0.000000	0.000000
3,00E+00	BL(all)	0.037003	0.000000	-0.020085	0.000000	0.123301	0.000000
4,00E+00	BL(all)	0.074028	0.000000	-0.020085	0.000000	0.123318	0.000000
5,00E+00	BL(all)	0.111032	0.000000	-0.020085	0.000000	0.123208	0.000000
6,00E+00	BL(all)	0.147980	0.000000	-0.020085	0.000000	0.123004	0.000000
7,00E+00	BL(all)	0.157870	0.000000	-0.051691	0.000000	-0.100192	0.000000
8,00E+00	BL(all)	0.126608	0.000000	-0.051169	0.000000	-0.105178	0.000000
9,00E+00	BL(all)	0.095009	0.000000	-0.051169	0.000000	-0.105384	0.000000
1,00E+01	BL(all)	0.063352	0.000000	-0.051169	0.000000	-0.105507	0.000000
1,10E+01	BL(all)	0.031671	0.000000	-0.051169	0.000000	-0.105517	0.000000

Table 14 – Midas Gen Results – Case 2 (3m)

CASO 3							
Node	Load	DX (m)	DY (m)	DZ (m)	RX ([rad])	RY ([rad])	RZ ([rad])
1,00E+00	BL(all)	0.000000	0.000000	0.000000	0.000000	0.000000	0.000000
2,00E+00	BL(all)	0.000000	0.000000	-0.082856	0.000000	0.000000	0.000000
3,00E+00	BL(all)	0.048891	0.000000	-0.025387	0.000000	0.163036	0.000000
4,00E+00	BL(all)	0.097854	0.000000	-0.025387	0.000000	0.163071	0.000000
5,00E+00	BL(all)	0.146790	0.000000	-0.025387	0.000000	0.162918	0.000000
6,00E+00	BL(all)	0.195644	0.000000	-0.025387	0.000000	0.162633	0.000000
7,00E+00	BL(all)	0.242494	0.000000	-0.038754	0.000000	0.041299	0.000000
8,00E+00	BL(all)	0.195911	0.000000	-0.057811	0.000000	-0.163056	0.000000
9,00E+00	BL(all)	0.146939	0.000000	-0.057811	0.000000	-0.163243	0.000000
1,00E+01	BL(all)	0.097924	0.000000	-0.057811	0.000000	-0.163294	0.000000
1,10E+01	BL(all)	0.048916	0.000000	-0.057811	0.000000	-0.163189	0.000000

Table 15 – Midas Gen Results – Case 3 (3m)

CASO 9							
Node	Load	DX (m)	DY (m)	DZ (m)	RX ([rad])	RY ([rad])	RZ ([rad])
1,00E+00	BL(all)	0.000000	0.000000	0.000000	0.000000	0.000000	0.000000
2,00E+00	BL(all)	0.000000	0.000000	-0.183583	0.000000	0.000000	0.000000
3,00E+00	BL(all)	0.061649	-0.000004	-0.039819	0.000007	0.205469	0.000000
4,00E+00	BL(all)	0.123340	-0.000005	-0.039819	0.000008	0.205500	0.000000
5,00E+00	BL(all)	0.185003	-0.000007	-0.039819	0.000008	0.205352	0.000000
6,00E+00	BL(all)	0.246591	-0.000009	-0.039819	-0.000008	0.205072	0.000000
7,00E+00	BL(all)	0.249079	-0.000008	-0.075924	-0.000011	-0.006047	0.000000
8,00E+00	BL(all)	0.249641	-0.000007	-0.112890	-0.000014	-0.205683	0.000000
9,00E+00	BL(all)	0.187868	0.000005	-0.112890	-0.000015	-0.205999	0.000000
1,00E+01	BL(all)	0.126005	-0.000005	-0.112890	-0.000015	-0.206195	0.000000
1,10E+01	BL(all)	0.064101	0.000008	-0.112890	-0.000022	-0.206228	0.000000

Table 16 – Midas Gen Results – Case 9 (3m)

CASO 10							
Node	Load	DX (m)	DY (m)	DZ (m)	RX ([rad])	RY ([rad])	RZ ([rad])
1,00E+00	BL(all)	0.000000	0.000000	0.000000	0.000000	0.000000	0.000000
2,00E+00	BL(all)	0.000000	0.000000	-0.094464	0.000000	0.000000	0.000000
3,00E+00	BL(all)	0.039134	0.000000	-0.030969	0.000000	0.130355	0.000000
4,00E+00	BL(all)	0.078263	0.000000	-0.030969	0.000000	0.130301	0.000000
5,00E+00	BL(all)	0.117354	0.000000	-0.030969	0.000000	0.130115	0.000000
6,00E+00	BL(all)	0.156363	0.000000	-0.030969	0.000000	0.129825	0.000000
7,00E+00	BL(all)	0.194630	0.000000	-0.030152	0.000000	0.122714	0.000000
8,00E+00	BL(all)	0.156907	0.000000	-0.063397	0.000000	-0.130298	0.000000
9,00E+00	BL(all)	0.117756	0.000000	-0.063397	0.000000	-0.130582	0.000000
1,00E+01	BL(all)	0.078526	0.000000	-0.063397	0.000000	-0.130756	0.000000
1,10E+01	BL(all)	0.039262	0.000000	-0.063397	0.000000	-0.130794	0.000000

Table 17 – Midas Gen Results – Case 10 (3m)

Another important aspect that must be considered for the analysis of the results, is the stress level inside the section, and because of considering this single aspect, the author noted that looking the general behavior of the columns, after the applied blast load, could be simplified as followed:

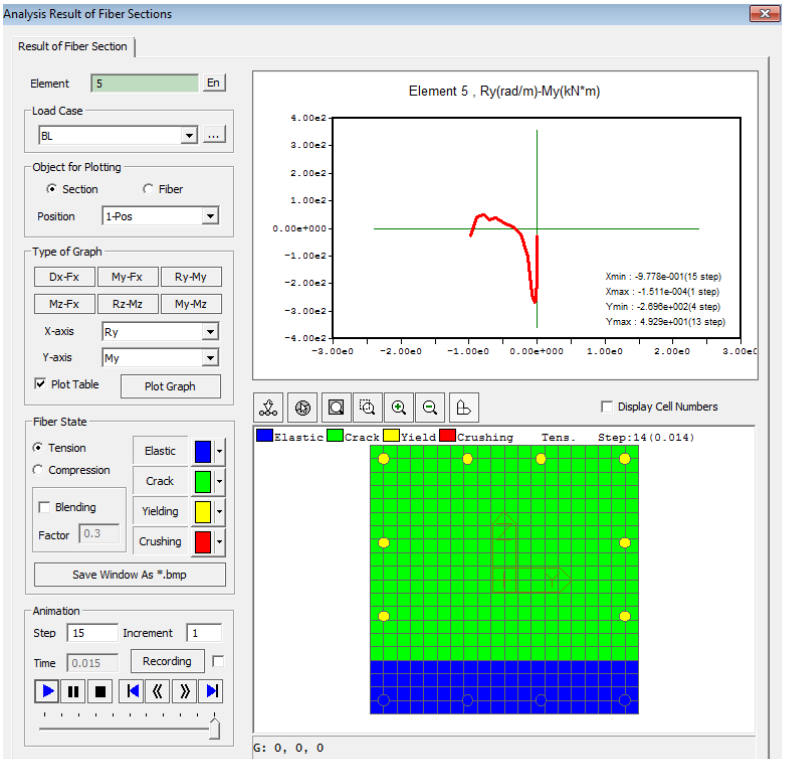

Figure 15 – Midas Gen Stress Level on Section

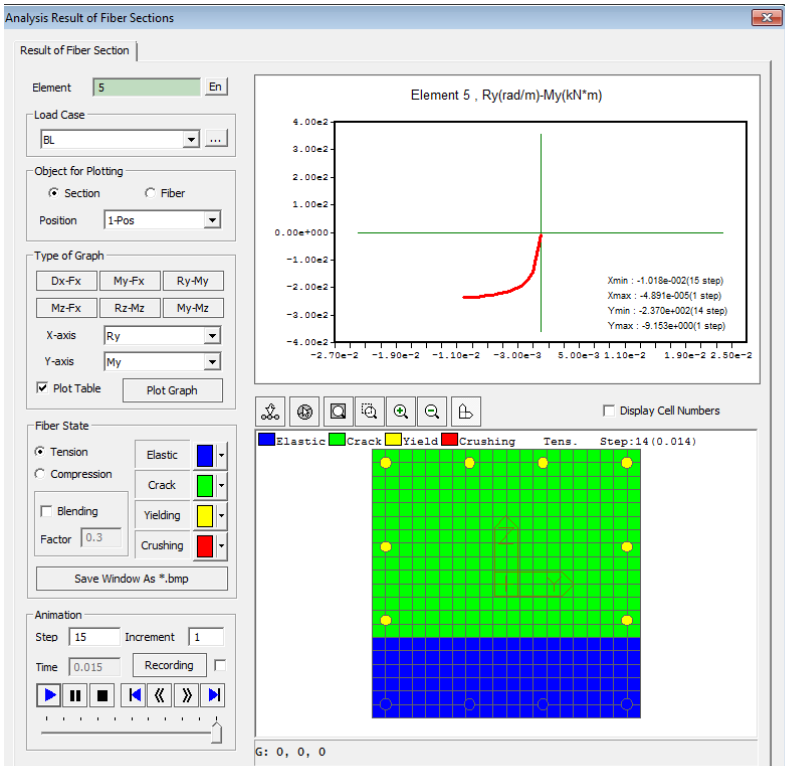

Figure 16 – Midas Gen Stress Level on Section

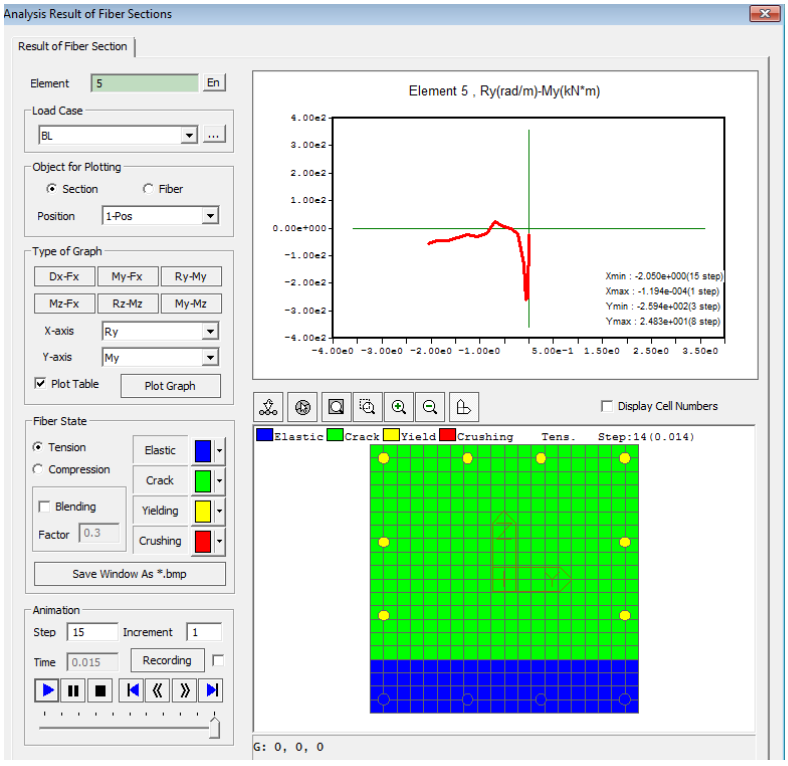

Figure 17 – Midas Gen Stress Level on Section

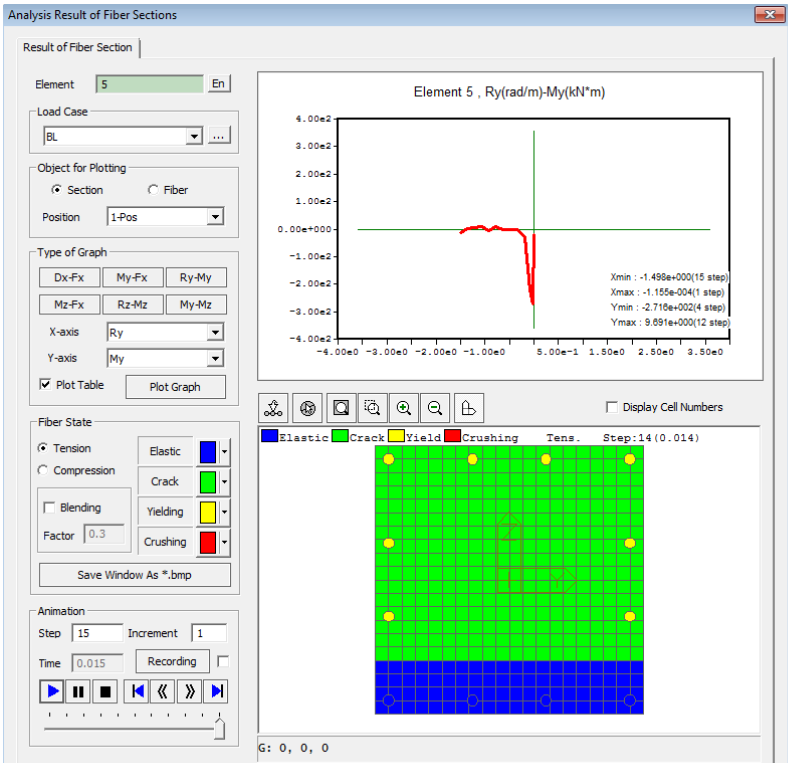

Figure 18 – Midas Gen Stress Level on Section

As it is possible to notice, after the blast load event, the columns presents yielding phenomena into the reinforcing steel bars and most part of the concrete section.

In general this phenomena should be explain considering the power of the detonation event. Indeed looking the results obtain, it is possible to see that for higher load occurring after detonation, the phenomena of cracking increase, causing the general yielding of the material for the most part of the section. For sure the phenomena of the cracking it is also generated by the crash of rubbles generate during the explosion event.

Chapter

6

Dynamics of Structures

And

SDOF Method Approach

1. Introduction

The state of tension relate to a structure could be evaluated with the static approach just in case of a very slow evolution of the loads involving the target, compared to the dynamics response of the structure. Indeed, the static calculation, comparing the load time t_r (defined as the necessary time for loads to reach their maximum values) and the period of the structure T_1 (relate to the maximum period of the structure considering the free vibration state), it is referred to the relationship occurring between this two parameters, when:

$$t_r \gg T_1$$

In reverse, the dynamic approach is necessary for the analysis of the structures, considering that, generally the effects of the motion causes an increase of the strain properties and deformations. From dynamics approach derived the introduction of dynamic coefficients, defined as the ratio between the dynamic and its related static effects.

The dynamic loads on structures are generally described by the intensity values, its distribution and the time variability. Sometimes append that the loads frequencies are too different from the self-structure frequencies, and generally in these cases the dynamic load could be considered as an equivalent static load, except some particularly cases of seismic or wind actions.

In general considering structures subjected to dynamic action, the degree of damage resulting from an explosion can be graphically determined from a pressure impulse diagram, where the impulse is defined as the integral of the side-on over pressure vs time diagram over the duration of the positive specific impulse.

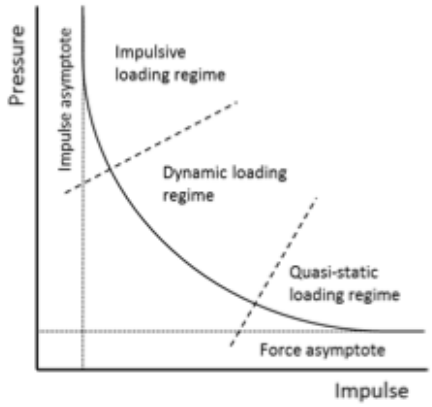

Figure 1 – Types of Loading

In this diagram, pressure-impulse lines are drawn which represent an equivalent level of damage for varying combinations of pressure and impulse.

2. Dynamic Models for Blast Analysis

The objective of a structural blast response analysis is to determine the deflection-time and the force-time histories on a structural component and its supports, which result from the application of an explosion impulse, as well as to establish whether the maximum values obtained are acceptable. There are two basics methods:

- Single Degree of Freedom (SDOF) Method;
- Multi Degree of Freedom (MDOF) Method.

Unlike the MDOF method, the SDOF method does not require the use of sophisticated software, and for simple structures it is easier to apply. A limitation in its application is that there is no commercially available software to support its use, which creates a disadvantage in quality assurance terms. The main problem with the SDOF method is that it is only feasible to apply to structures, which can be characteristics by a single stiffness (load-deflection) curve and the loading applied as a single time varying quantity.

Designing a structure and its supports so that it can deform plastically, without breaking, leads to great economies and increased explosion capacity. Although the application of the SDOF method to structures working in a ductile response regime has limitations as describes above, in practice most loading conditions (including drag loading) are largely confined to one direction, and many equipment can be idealized as suitable simple structures.

In general, because the variability of applied loads is a particular feature of equipment loadings, the SDOF method has a very big advantage over the MDOF method in that it can be used for a large number of different load scenarios.

Considering a dynamics analysis of beams and columns subjected to blast loads, the “Single Degree of Freedom” is the principle method used. It could be divided into two main SDOF approaches:

- Modal Method;
- Equivalent SDOF Method.

2.1 Approaches for The Equivalent SDOF Method

The Equivalent SDOF method was first presented fully in the USACE 1957 manual "Design of Structures to Resist the Effects of Atomic Weapons". This was a 9th volume manual, of which two volumes covered the Equivalent SDOF method, Volume 5, EM1110-345-415 "Principals of Dynamic Analysis and Design" and Volume 6, EM1110-345-416 "Structural Elements Subjected to Dynamic Loads". The firm of Amman and Whitney (A&W) were credited with much of the basic analytical work and the Massachusetts Institute of Technology (MIT) for further study and development of design material, and for the compilation, both under contract to the USACE. References cited included a 1949 MIT report on structural elements under impulsive loads, and a 1952 A&W interim design manual for protective construction.

The solution of any dynamic structural system is based on the use of two equations, Newton's Equation of motion, defining dynamic equilibrium of forces, and the principle of Conservation of Energy, stated as:

Work Done = Kinetic Energy + Strain Energy

Three approaches were presented for analyzing a basic dynamic system:

- Fictitious Maximum Work Done, where the Work Done Ratio (WDR) is the ratio of the actual maximum work done to the fictitious work calculated from the loading impulse. This is a SDOF equivalent to the Impulse Method, and ideal for systems with pure plastic resistance, although also suitable for elastic-plastic systems.
- Dynamic Load Factor (DLF), applied to elastic systems, which is the same as the Equivalent Static Load Method, used for elastic systems.
- Deflection Ratio (DR), defined as the ratio of the maximum deflection to the elastic deflection, also known as the ductility ratio. This can be solved either by rigorous analytical integration of the differential equations, or by numerical methods, which is equivalent to the approach by Newmark.

Considering the approach relate to the "Dynamic Load Factor", it is possible to say that is a special case of the displacement calculation used for the Deflection Ratio. Thus, there were two basic methods, using either the energy equation or the equation of motion to derive a solution. Although both were used in the document, sensitivity studies of percentage

increment ratios for a variety of factors and simplifications indicated that there was no real increase in accuracy in using the energy method.

Both methods could be used to calculate dimensionless charts using simplified loading and resistance functions. However, dimensional analysis showed that, for three dimensionless ratios presented on a single chart, only four independent variables could be used to define the loading and resistance. If two were used to define an elastic-plastic resistance, then the loading definition was limited to two variables, one for amplitude and one for time. This limits charts to loadings like a triangular pulse, a rectangular pulse and a step load with a finite rise time. However even this required solutions from up to eight different differential equations to find the peak deflection, so in practice the rigorous solution was limited to pre-solved simplified charts for preliminary design.

For the three loading types, charts were provided of DLF and peak time for elastic resistance, of WDR and peak time for plastic resistance, and DR, WDR and peak time for elastic-plastic resistance. Unlike the Newmark, the DR ratio extended down to 0.1, with elastic deflections shown with deflection ratios less than 1, for a triangular load. However it should be noted that the simplified loading curves only included positive phases, so the simplified charts do not model critical elastic rebound deflection from blast loading that includes a negative loading phase.

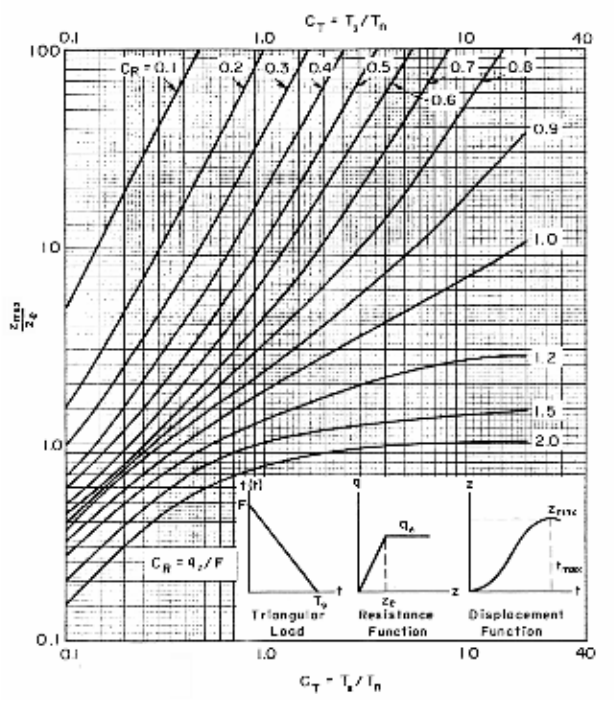

Figure 2 – SDOF Equivalent Method

The Linear Acceleration Extrapolation Method is more accurate, but required iteration to find the deflection in the elastic range. The Acceleration Impulse Extrapolation Method is less accurate for the same time step, but required no iterations. These methods are potentially more flexible than charts based on rigorous analysis, as simplification of loading or resistance functions is not required.

For the present case of study, this simplified approach was considered for a double check of analysis results. So considering the 10 cases which had been studied into this work, just doing simple hand calculation we obtain the following expose results.

First of all it is needed to consider material properties for concrete and reinforcement steel bar and also section properties of the columns analyzed:

MATERIALS					
Concrete	C30/37		Steel	B450C	
E_c	33	[Gpa]	E_s	210	[GPa]
f_{cc}	30	[N/mm^2]	f_y	430	[N/mm^2]
γ_c	1,2		f_u	540	[N/mm^2]
ρ	2400	[kg/m^3]	f_{yd}	391,3	[N/mm^2]
f_{cd}	15,63	[N/mm^2]			

Table 1 – Material Properties

SECTION PROPERTIES					
Column			Rebar		
Height	0,5	[m]	Φ	20	[mm]
Width	0,5	[m]	rebar n°	12	
Length 1	5	[m]	c	25	[mm]
Length 2	4	[m]			
Length 3	3	[m]			

Table 2 – Section Properties

To this followed the general sectional calculation, useful for determining the parameters referred this simplified approach:

Next step is the analysis of the impulse

Blast Load Parameters						
CASO 1	P_r	560617	[Pa]	t_d	0,014	[sec]
CASO 2	P_r	1104256	[Pa]	t_d	0,012	[sec]
CASO 3	P_r	1626375	[Pa]	t_d	0,011	[sec]
CASO 4	P_r	53883	[Pa]	t_d	0,021	[sec]
CASO 5	P_r	84549	[Pa]	t_d	0,023	[sec]
CASO 6	P_r	117125	[Pa]	t_d	0,024	[sec]
CASO 7	P_r	294555	[Pa]	t_d	0,013	[sec]
CASO 8	P_r	40493	[Pa]	t_d	0,019	[sec]
CASO 9	P_r	2207068	[Pa]	t_d	0,008	[sec]
CASO 10	P_r	2049343	[Pa]	t_d	0,006	[sec]

Table 3 – Blast Pressure and Time Values

Impulse Intensity values			
CASO 1	I_k	3924,32	[Pa-sec]
CASO 2	I_k	6625,54	[Pa-sec]
CASO 3	I_k	8945,06	[Pa-sec]
CASO 4	I_k	565,77	[Pa-sec]
CASO 5	I_k	972,31	[Pa-sec]
CASO 6	I_k	1405,50	[Pa-sec]
CASO 7	I_k	1914,61	[Pa-sec]
CASO 8	I_k	384,68	[Pa-sec]
CASO 9	I_k	8828,27	[Pa-sec]
CASO 10	I_k	6148,03	[Pa-sec]

Table 4 – Impulse Values

Blast Load				
	h=5m	h=4m	h=3m	
CASO 1	1401,54	1121,23	840,93	[kN]
CASO 2	2760,64	2208,51	1656,38	[kN]
CASO 3	4065,94	3252,75	2439,56	[kN]
CASO 4	134,71	107,77	80,82	[kN]
CASO 5	211,37	169,10	126,82	[kN]
CASO 6	292,81	234,25	175,69	[kN]
CASO 7	736,39	589,11	441,83	[kN]
CASO 8	101,23	80,99	60,74	[kN]
CASO 9	5517,67	4414,14	3310,60	[kN]
CASO 10	5123,36	4098,69	3074,01	[kN]

Table 5 – Blast Loads

SDOF ratio Parameters						
	R_u/F (h=5m)	R_u/F (h=4m)	R_u/F (h=3m)	t_d/T_N (h=5m)	t_d/T_N (h=4m)	t_d/T_N (h=3m)
CASO 1	0,63	0,99	1,76	0,97	1,27	1,31
CASO 2	0,32	0,50	0,89	0,83	1,09	1,12
CASO 3	0,22	0,34	0,61	0,76	1,00	1,03
CASO 4	6,58	10,28	18,28	1,46	1,91	1,96
CASO 5	4,19	6,55	11,65	1,60	2,09	2,15
CASO 6	3,03	4,73	8,41	1,67	2,18	2,24
CASO 7	1,20	1,88	3,34	0,90	1,18	1,21
CASO 8	8,76	13,68	24,33	1,32	1,73	1,78
CASO 9	0,16	0,25	0,45	0,56	0,73	0,75
CASO 10	0,17	0,27	0,48	0,42	0,55	0,56
				DYNAMIC CASE $0,1 < t_d/T_N < 10$		

Table 6 – SDOF Ratio Parameters

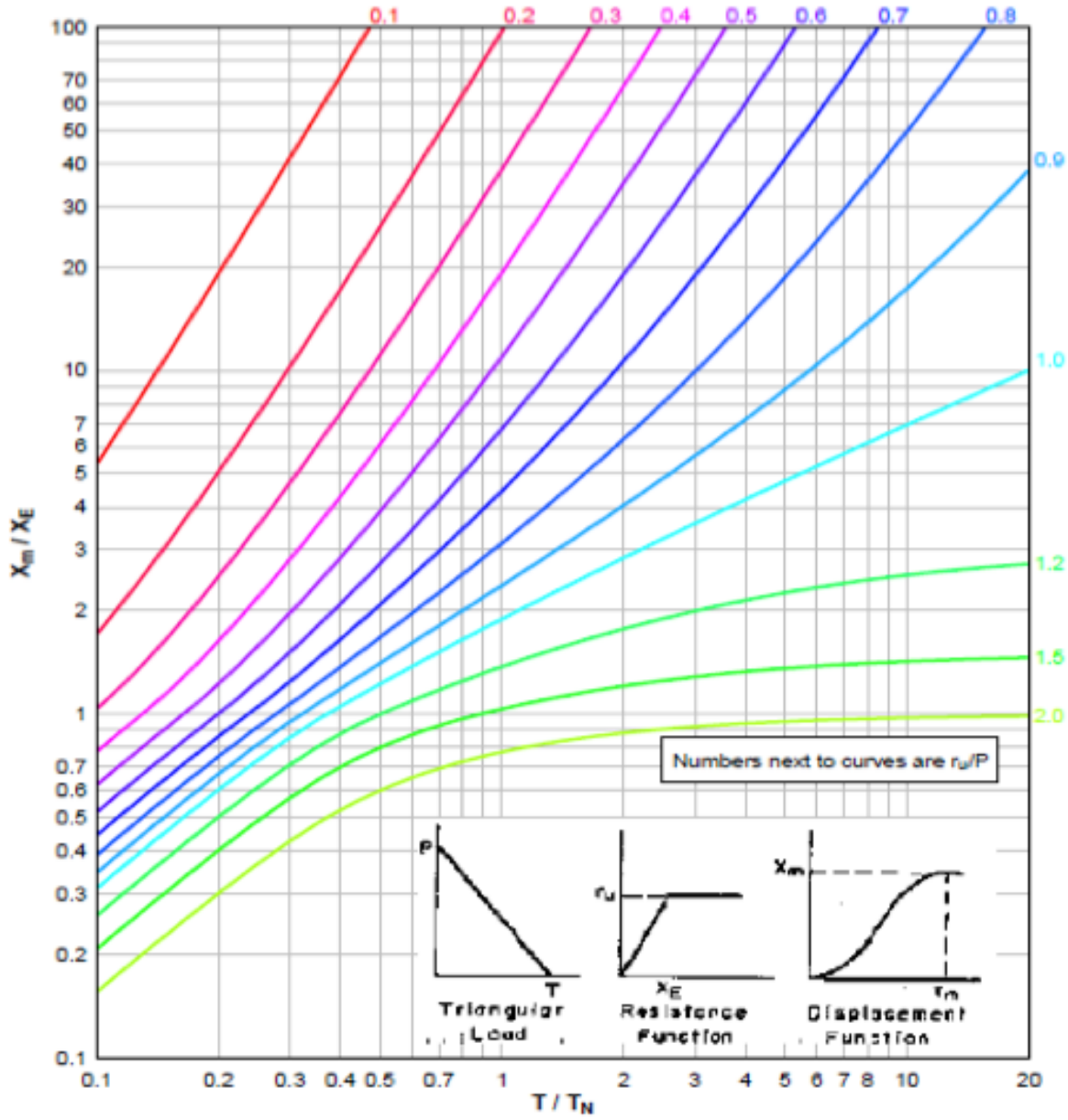

Figure 3 – SDOF Equivalent Method

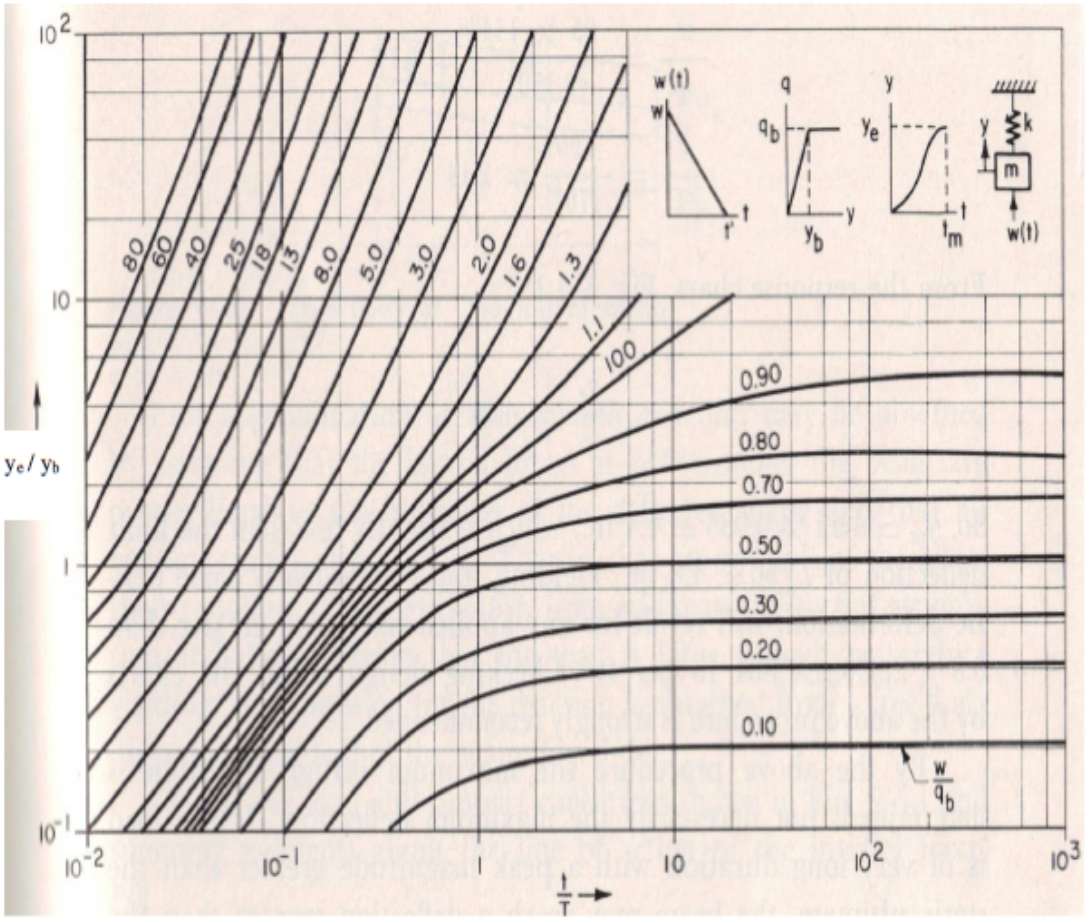

Figure 4 – SDOF Equivalent Method

Blast Displacement						
	X_m/X_e (h=5m)	X_m/X_e (h=4m)	X_m/X_e (h=3m)	X_m (h=5m)	X_m (h=4m)	X_m (h=3m)
CASO 1	5,50	2,40	0,95	0,072	0,020	0,004
CASO 2	19,00	12,00	3,00	0,249	0,101	0,014
CASO 3	37,00	25,00	6,30	0,485	0,210	0,030
CASO 4				0,000	0,000	0,000
CASO 5				0,000	0,000	0,000
CASO 6				0,000	0,000	0,000
CASO 7	1,50	0,87		0,020	0,007	0,000
CASO 8				0,000	0,000	0,000
CASO 9	38,00	27,00	9,00	0,498	0,227	0,043
CASO 10	25,00	14,00	5,30	0,328	0,118	0,025

Table 7 – Blast Displacement

Permanent displacement				
	X_p (h=5m)	X_p (h=4m)	X_p (h=3m)	
CASO 1	0,079	0,12	0,05	[m]
CASO 2	0,236	0,21	0,12	[m]
CASO 3	0,432	0,305	0,25	[m]
CASO 4				[m]
CASO 5				[m]
CASO 6				[m]
CASO 7	0,07	0,063		[m]
CASO 8				[m]
CASO 9	0,485	0,29	0,22	[m]
CASO 10	0,315	0,21	0,2	[m]

Table 8 – Permanent Blast Displacement

In general looking the results proposed into this table it is possible to see that the displacement value in orange colours are related to deflection over the allowable limit, and so the plastic deformation conduct the element for sure to the collapse.

In general having a look on the results proposed by the F.E.M. analysis with the software Midas Gen, it is possible to confirm that most of the elements for the cases underline with a green colour, presents deformation under the allowable limit, conducting at the end of the loading process to limitated cracking phenomena, just generated by the impact against the element of rubble coming from other near elements, cause the load applied does not result so big for generate the rilevant cracking phenomena that could be generate the consequently collapse of the single element.

2.2 The Principles of the Equivalent SDOF Method

The distributed masses of the given structure are lumped together into a number of concentrated masses. The strain energy is assumed to be stored in a number of weightless springs which do not have to behave elastically. Similarly the distributed load is replaced by a number of concentrated loads acting on the concentrated mass and varying with time.

The reduction of a given distributed structure to an equivalent dynamic system involves the principle of dynamic similarity, which is the requirement that the work done, strain energy and kinetic energy of the equivalent system must be identical with the respective property of the given structure. The simplest dynamic system consists of a single concentrated mass supported by a single spring acting in one direction and subjected to a single concentrated load in that direction, i.e. a system with a single degree of freedom (SDOF).

2.3 Numerical Analysis with the SDOF Method

The behavior of structures due to blast loading is conveniently represented with single degree of freedom (SDOF) models. These simplifying models try to evaluate a structure using only one physical degree of freedom, the horizontal deflection. Advantages that still indicate the use of these state of practice or common practice models include the quick evaluation for assessment of structures (within larger scenarios), intuitive transition from static to dynamic models, use of static experimental data and available data collected for these models.

The SDOF model which can be interpreted as an idealized assumption, can be classified in three parts: material assumptions, loading assumptions and geometry assumptions. Within these three groups a complete SDOF model may be considered to consist of the initial condition, the pressure force term or loading function, the resistance force term or resistance function, effective mass, load-mass factors or dynamic design factors, and the failure model. If two-dimensional visualization is included the pressure-impulse shape is considered to be a part of the model. The loading consists of the pressure–time history and an effective area expression. The resistance may depend on the deflection and velocity locally in time, or in a functional way on the complete deflection- and velocity-time history.

Besides the mass and loading data and their parameterization the SDOF model depends on the functional form and the parameters of the resistance function. Often the best parameters are determined from static experiments and used together with several kinds of factors to

determine a dynamic SDOF model. However, also dynamic data are available. It is often only used to determine failure criteria and factors that modify the static response behavior. So it is desirable to develop procedures that determine ideal dynamic parameters of dynamic SDOF models and structural resistance functions.

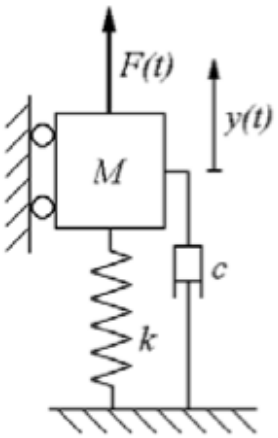

Figure 5 – SDOF Approach

A SDOF system is one in which the position of the system at any instant can be defined in terms of a single coordinate. Since the spring is assumed massless, the motion of the mass, resulting from the application of a time-varying force, can be determined by isolating the mass, and then applying the external forces. Neglecting the damping force, the external forces are the applied force F(t) and the spring force ky (for a linear spring). The gravity force does not appear in the figure, which implies that the displacement y is measured from the neutral position. Having isolated mass, the equation of motion may be rewritten by simply applying the elementary formula F=Ma. F is the net sum of the forces acting on the mass, and the positive direction of the force is the same as that for displacement or acceleration. Thus, the equation of motion for the damped system is:

$$m\ddot{y}(t) + c\dot{y}(t) - ky(t) = F(t)$$

The differential equation may be solved to determine the variation of displacement with time once the loading function, the initial conditions and the other parameters are known.

Considering the equation of motion, the generic condition at the start, are:

$$y(t = 0) = y_0$$

$$\dot{y}(t = 0) = \dot{y_0}$$

Introducing the value of natural pulse, natural period and the critical damping, it is possible to obtain the new equation of motion for the SDOF method:

$$\omega_n = \sqrt{\frac{k}{m}}$$

$$T_n = \frac{2\pi}{\omega_n}$$

$$\xi = \frac{c}{2\sqrt{km}}$$

$$\ddot{y}(t) + 2\xi\omega_n\dot{y}(t) + \omega_n^2 y(t) = \frac{F(t)}{m}$$

If the duration of the overpressure t_d is shorter than the natural period T_n, the blast effect could be represented by the impulsive load, without the use of a time-history function. In this case, the dynamic analysis with the SDOF method, conducts to the generation of the following system of equations:

$$\ddot{y}(t) + 2\xi\omega_n\dot{y}(t) + \omega_n^2 y(t) = 0$$

$$y(t=0) = y_0$$

$$\dot{y}(t=0) = \frac{i}{m}$$

The equation of motion and the relative initial condition proposed above, are referred to a system with an indefinitely elastic behavior. While the hypothesis that the structure, under the blast loading, remains in an elastic field, it is not economic for the project design of the construction. So it is important, also using the simplified design models, to consider the plastic behavior, using a bilinear strength function:

$$F = k_e x \qquad when \qquad x \leq x_{lim}$$

$$F = k_e x_{lim} + k_y(x - x_{lim}) \qquad when \qquad x > x_{lim}$$

Where x_{lim} represents the critical displacement. Beyond it, the behavior of the structure change, using k_e (for the elastic field) and k_y (for the plastic field) as the new value of stiffness. To evaluate the stiffness after the critical displacement, same authors suggest to

calculate the k_y as the 20% of the k_e. In this case the bilinear strength function, is represented by the following graphs:

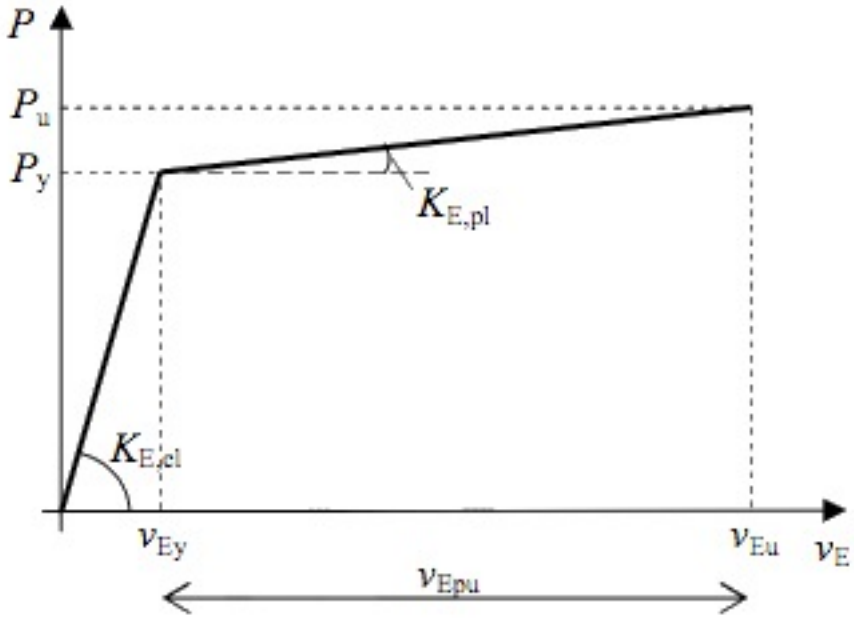

Figure 6 – Bilinear Strenght function

As an alternative, it is possible to consider k_y=0, assuming a strength function as elastic-completely plastic, held by the following equations:

$$F = k_e x \qquad when \qquad x \leq x_{lim}$$

$$F = F_{lim} = k_e x_{lim} \qquad when \qquad x > x_{lim}$$

In this case, the graphs representing the strength function, it must be as followed.

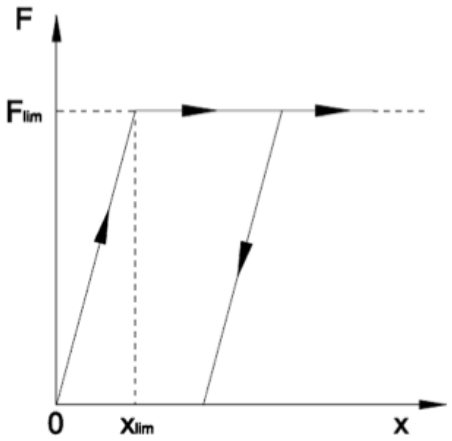

Figure 7 – Force-Displacement Graph

Considering what explained before, in term of SDOF Method analysis, it is possible now to propose another type of double check comparing this result to the one obtain by using of F.E.M. software Midas Gen:

Impulse Intensity values			
CASO 1	I_k	3924,32	[Pa-sec]
CASO 2	I_k	6625,54	[Pa-sec]
CASO 3	I_k	8945,06	[Pa-sec]
CASO 4	I_k	565,77	[Pa-sec]
CASO 5	I_k	972,31	[Pa-sec]
CASO 6	I_k	1405,50	[Pa-sec]
CASO 7	I_k	1914,61	[Pa-sec]
CASO 8	I_k	384,68	[Pa-sec]
CASO 9	I_k	8828,27	[Pa-sec]
CASO 10	I_k	6148,03	[Pa-sec]

Table 9 – Impulse Intensity Values

Blast Load Parameters						
CASO 1	P_r	560617	[Pa]	t_d	0,014	[sec]
CASO 2	P_r	1104256	[Pa]	t_d	0,012	[sec]
CASO 3	P_r	1626375	[Pa]	t_d	0,011	[sec]
CASO 4	P_r	53883	[Pa]	t_d	0,021	[sec]
CASO 5	P_r	84549	[Pa]	t_d	0,023	[sec]
CASO 6	P_r	117125	[Pa]	t_d	0,024	[sec]
CASO 7	P_r	294555	[Pa]	t_d	0,013	[sec]
CASO 8	P_r	40493	[Pa]	t_d	0,019	[sec]
CASO 9	P_r	2207068	[Pa]	t_d	0,008	[sec]
CASO 10	P_r	2049343	[Pa]	t_d	0,006	[sec]

Table 7 – Blast Loads Parameters

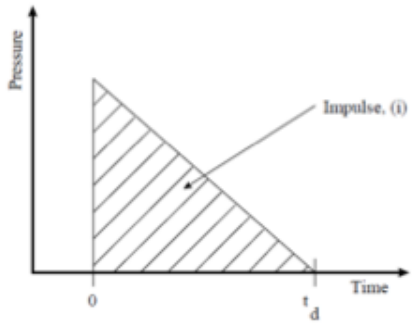

Figure 8 – Pressure-Time Graphs

DISPLACEMENTS [m] - Column h = 5 [m]										
	CASO 1	CASO 2	CASO 3	CASO 4	CASO 5	CASO 6	CASO 7	CASO 8	CASO 9	CASO 10
uel,I	0,01875128	0,0316583	0,04274152	0,00270338	0,00464593	0,00671579	0,00914842	0,0018381	0,04218346	0,02937666
uel,II	0,0367605	0,06206376	0,0837916	0,00529978	0,00910801	0,01316582	0,01793481	0,00360347	0,08269758	0,05759078
upl	0,04148712	0,11825695	0,21555168	0,00086232	0,00254681	0,00532165	0,00987516	0,00039865	0,20995976	0,10182548
uep	0,05079002	0,25755986	0,41485459	0,01016522	0,01184972	0,01462456	0,06917807	0,00970156	0,45926266	0,31112839

DISPLACEMENTS [m] - Column h = 4 [m]										
	CASO 1	CASO 2	CASO 3	CASO 4	CASO 5	CASO 6	CASO 7	CASO 8	CASO 9	CASO 10
uel,I	0,01200082	0,02026131	0,02735457	0,00173017	0,0029734	0,00429811	0,00585499	0,00117639	0,02699742	0,01880106
uel,II	0,02352672	0,03972081	0,05362662	0,00339186	0,00582913	0,00842613	0,01147828	0,00230622	0,05292645	0,0368581
upl	0,02655175	0,07568445	0,13795307	0,00055188	0,00162996	0,00340586	0,0063201	0,00025514	0,13437424	0,06516831
uep	0,10250562	0,19163831	0,29390693	0,00650574	0,00758382	0,00935972	0,05227396	0,006209	0,2803281	0,23112217

DISPLACEMENTS [m] - Column h = 3 [m]										
	CASO 1	CASO 2	CASO 3	CASO 4	CASO 5	CASO 6	CASO 7	CASO 8	CASO 9	CASO 10
uel,I	0,00675046	0,01139699	0,01538695	0,00097322	0,00167254	0,00241769	0,00329343	0,00066172	0,01518605	0,0105756
uel,II	0,01323378	0,02234295	0,03016497	0,00190792	0,00327888	0,0047397	0,00645653	0,00129725	0,02977113	0,02073268
upl	0,01493536	0,0425725	0,0775986	0,00031043	0,00091685	0,00191579	0,00355506	0,00014351	0,07558551	0,03665717
uep	0,04828441	0,10592155	0,27094765	0,00365948	0,0042659	0,00526484	0,0069041	0,00349256	0,21893456	0,19000622

Table 8 – Blast Final Displacement

Chapter 7

Conclusions

Modelling of reinforced concrete structures under accidental load cases, such as explosion, impact or fires, requires precise state of the art approaches to describe the structure under regular and accidental loading conditions. Different approaches are applicable for the description of reinforced concrete under static and dynamic loading such as single degree of freedom (SDOF) or finite element methods (FEM). These approaches may differ in their level of description and complexity but need to be able to describe the nonlinear behaviour of reinforced concrete structures accurately.

For an accurate description of dynamic problems these methods should be capable of describing the structural behaviour within the dynamic but also in the static domain as preload may influence the results.

In general Single degree of freedom (SDOF) models have been widely used for predicting dynamic response of concrete structures subjected to blast loading. The popularity of the SDOF method in blast-resistant design lies in its simplicity and cost-effective approach that requires limited input data and less computational effort. SDOF model gives reasonable good results if the response mode shape is representative of the real behavior. Accuracy of the dynamic response calculations significantly depends on whether the adopted resistance function resembles the actual hysteretic behavior of the structure.

At the end it is possible to accurately simplify the displacements of structural columns for different material behaviours with an SDOF-model by using certain transformation factors. Because the column's initial deflection for a highly impulsive load differs a lot from static deflection shape the simplification is initially poor, but by the time the deflection reaches its maximum value the deflection shapes are very similar and the results converge well.

For design purpose it is of interest to compare the undamped SDOF-model with the FE-analysis. When the moment from the SDOF-model was compared to the FE-analysis it was easy to understand the difference between the F.E. Model compare to Hand Calculation with the use of SDOF equivalent models. Indeed the results can be considered better accurate with a FE-analysis.

When comparing the displacements from the SDOF-model to the FE Models it is possible to understand that the differences between the two results it is minimum, and it depend on how much is sophisticate the way to calculate.

Considering this specific case of study, it is possible to say that the response of the single element, column, studied using the F.E. Analysis it is easily compared to the results obtain by simple hand calculation using normative approach and using more specific approach as the

SDOF Method. Looking the results proposed on Chapter 5, obtain by modeling the elements with the help of the Midas Gen Software and the one proposed on Chapter 6, relate to hand calculation and SDOF Method, it is possible to conclude that the displacement are really closed and that, using different method it is possible to obtain very similar results.

Indeed, comparing displacement obtain by the F.E. Analysis with the other specific analysis, it is possible to notice that the different are included on a range of millimeters values. In general we noticed that for the worst case like as the one relate to columns 5m height, the displacement obtain by the F.E. differ from the others result for 0.01mm at maximum.

In general, as explain in this work, the objective was to analyze columns elements subjected to different situation of blast event, caused by terroristic attack, and verify their replay for different case of loading.

So in general, we saw, in relation to the slenderness, the columns 5m height were the ones that suffer more the blast load event, presenting at the end of the analysis, yielding of the steel reinforcements and big cracks of the concrete. Plastic behavior it is relevant for that kind of columns, in reverse to the one 3m height that are more resistant, as slenderness ratio is more little.

It is also important don't forget that usually the cracking on concrete and the generation of yields on the steel reinforcement it is caused by the rubbles that crash against the structures cause by the explosion event, phenomena generally ignored during the structural elements design in case of blast occurance.

References

Books

- Carta G, Stochino F. "Theoretical models to predict the flexural failure of reinforced concrete beams under blast loads". Engineering Structures, Volume 49, April 2013, Pages 306–315 (2013)
- dx.doi.org/10.1016/j.engstruct.2012.11.008 Acito M. Stochino F. Tattoni S "Structural response and reliability analysis of rc beam subjected to explosive loading".
- International Conference: PROTECT 2011 "Protection & Strengthening of Structures under Extreme Loading" – Lugano 08/30 –09/01 2011 - Applied Mechanics and Materials Vol. 82 (2011) pp 434-439 doi:10.4028/www.scientific.net/AMM.82.434
- Tattoni S–Stochino F.(2012): "Azioni esplosive sulle strutture in c.a." 19° Congresso CTE, Bologna 11/8-10 2012-Pag. 407-417, ISBN: 978-88-903647-9-2
- Acito M. Stochino F. Tattoni S., "Analisi della sicurezza di travi in c.a. soggette ad azioni da esplosione". Giornate AICAP 2011 – Le prospettive di sviluppo delle opere in calcestruzzo strutturale nel terzo millennio, Padova 05/19-21 2011 – Pag. 3-11.
- Stochino F. Tattoni S., "Incremento prestazionale per edifici in c.a. resistenti ad esplosione e relativa valutazione economica". Giornate AICAP 2011 – Le prospettive di sviluppo delle opere in calcestruzzo strutturale nel terzo millennio, Padova 05/19-21 2011 – Pag. 375-380.
- G. C. Mays, P. D. Smith, (1995), "Blast Effect on Buildings"- second edition, Thomas Telford Publications, London ISBN: 978-0-7277-3521-8. B. Genova, M. Genova, M.Silvestrini, (2010), "Sicurezza degli edifici nei riguardi dei fenomeni esplosivi",UTET Scienze Tecniche, ISBN: 978-88-598-0415-4.
- Magnusson J, Hallgren M. High performance concrete beams subjected to shock waves from air blast. Report n. FOA-R--00-01586-311--SE, Defence Research Establishment (FOA), Tumba, Sweden; 2000.
- Magnusson J, Hallgren M. High performance concrete beams subjected to shock waves from air blast, Part 2. Report n. FOI-R--1116--SE, Swedish Defence Research Agency (FOI), Tumba, Sweden; 2003.
- Magnusson J, Hallgren M. Reinforced high strength concrete beams subjected to air blast loading. In: Jones N, Brebbia CA, editors. Structures under shock and impact VIII. Southampton : WIT Press; 2004, p. 53-62.

- Magnusson J, Hallgren M, Ansell A. Air-blast-loaded, high-strength concrete beams. Part I: Experimental investigation. Mag Concr Res 2010; 62: 127-136.
- Magnusson J, Hallgren M, Ansell A. Air-blast-loaded, high-strength concrete beams. Part II: Numerical non-linear analysis. Mag Concr Res 2010; 62: 235-242.
- Zhu F. & Lu G. A Review of Blast and Impact of Metallic and Sandwich Structures, Electronic J Struct Eng, 7 Special Issue: Loading on Structures (2007) , 92-101
- Lee E.H. and Symonds P.S. Large Plastic Deformation of Beam Under Transverse Impact. J. Appl. Mech. Vol.19, No.3, 1952. 308-314.
- Conroy M.F. and Providence R.I. Plastic – Rigid Analysis of Long Beams under Transverse Impact. Journal of Applied Mechanics- ASME – vol. 19 – 1952. 465-470
- Symonds P.S. and Providence R.I. Dynamic Load Characteristic in Plastic Bendings of Beams. Journal of Applied Mechanics- ASME – vol.20 1953. 475-481
- Martin J.B. and Symonds P.S. Mode Approximations for impulsively-loaded rigid plastic- structures" – Journal of Engineering Mechanics – ASCE 1966 EM.43-46
- Prager W. An introduction to plasticity. Addison Wesley Press, Reading, Mass. 1959.
- Vashi, K.M., 1966. Effect of shear deformation in a beam impulsively loaded on a central portion, Master's thesis, Division of Engineering, Brown University, USA.
- Symonds P.S. Plastic shear deformations in dynamic load problems. In: Heyman J, Leckie FA, editors. Engineering Plasticity. Cambridge: Cambridge University Press; 1968 p.674-64
- Symonds, P.S.; Jones, N. Impulsive loading of fully clamped beams with finite plastic deflections and strain-rate sensitivity. International Journal of Mechanical Sciences vol. 14 issue 1 January, 1972. p. 49-69
- Nonaka T. Some interaction effects in a problem of plastic beam dynamics. Parts 1–3. ASME J Appl Mech 1967;34:623–43.
- Nonaka T. Shear and bending response of a rigid-plastic beam to blast-type loading. Ing-Arch 1977;46:35–52.
- Menkes S.B., Opat H.J. Broken beams Experimental Mechanics, 13 (1973), pp. 480–486